Thesis for the degree of Doctor of Philosophy

Multiport Antenna Systems for Space-Time Wireless Communications

Nima Jamaly

CHALMERS

Communication Systems Group
Department of Signals and Systems
Chalmers University of Technology
Gothenburg, Sweden 2013

Multiport Antenna Systems for Space-Time Wireless Communications

Nima Jamaly

This thesis has been prepared using LaTeX.

ISBN 978-91-7385-800-7
School of Electrical Engineering
Chalmers University of Technology
Ny Serie No. 3481
ISSN 0346-718X

Department of Signals and Systems
Chalmers University of Technology
SE-412 96 Gothenburg, Sweden

Phone: +46 (0)31 772 1000
Fax: +46 (0)31 772 1748
E-mail: jamaly@chalmers.se

Printed by Chalmers Reproservice
Gothenburg, Sweden, March 2013

To my beloved parents and brother

Foreword

As an indispensable part of modern wireless communication systems, multiport antennas play a crucial role in overall performance. Characterisation, design and measurement of multiport antennas establish the main part of this thesis. The multidisciplinary nature of multiport antennas makes them the subject of many research groups worldwide, resulting in inconsistent nomenclature. In this thesis, much effort is expended to look upon this realm of engineering in a unifying way with the foremost stress on the microwave and electromagnetic aspects.

In the first step we clearly distinguish between the power loss in the terminations, which is caused by coupling, and other types of dissipation in the antenna structure. This distinction is of huge aid in enabling us to compactly formulate multiport matching efficiencies in the presence of any arbitrary number of cascaded networks. The concept of mean matching efficiency is illustrated, and its application in quick estimation of diversity gain is underlined.

Furthermore, we present the electromagnetic characteristics of an ideal dual-port dual-polarised isotropic reference antenna. This achievement serves our purpose best to safely normalise the received signals' covariance matrix in correlated nonuniform Rayleigh fading environments. A salient feature of the latter formulation is that it bestows the opportunity to distinctly highlight the effects of terminating impedances and radiation efficiencies on the covariance matrix.

The notion of richness threshold as a further performance gauge is introduced. This metric indicates relatively how much bulk of the diversity gain is achieved through pattern diversity, and how much of it is obtained by element separation. Indeed, to ensure that a multiport antenna design performs well also in a non-rich multipath scenario, one needs to refer to its richness threshold. Moreover, we show numerically that a Butler network, which seems to be ineffectual in a rich multipath environment, is in contrast considerably beneficial in multipath environments of finite richness.

The important role of predictor antenna systems in overall performance of modern moving relays is already known. As a discipline of its own, an analysis of predictor antenna systems for the foregoing application is presented. We describe the interesting choice of lossless single-mode antennas for prediction purposes. Subsequently, a simulation tool is developed, whereby one can quantify the ultimate performance gain achievable by removing the effects of coupling. Besides, formulas are presented to allow calculation of these performance gains also in the presence of a cascaded network.

The remainder of the thesis concentrates on measurements of multiport antennas in a reverberation chamber. We stress that the main concern in a reverberation chamber is

the number of independent samples available in a desired frequency range. This issue has a direct impact on accuracy of the measurements carried out in these chambers. By an empirical investigation, one can show that, compared to the diversity gain, measurements of radiation efficiency and spatial correlations require far fewer independent samples. Based on this fact, we devise two compact formulas for dual-port diversity gain calculation, as a function of the forgoing performance metrics. The accuracy of these formulas is demonstrated by a comparative study. Moreover, we propose the choice of reverberation chamber for a quick measurement of the pattern overlap matrix. To the best of our knowledge, this is the fastest way to measure the aforementioned metric.

Finally, we dedicate a short part to designing multiport antennas for future mobile communication systems. Contrary to conventional wisdom, the shape and configuration of the radiation elements are not the entire concern in the design phase. Rather, interaction between the multiple antennas and the near-field user is of an equal significance. By a number of simulations and measurements, we illustrate that our proposed compact design stands out as a brilliant choice.

Keywords: Beamforming, Cascaded Networks, Correlated Multipath, Covariance Matrix, Multiport Antennas, Multiport Effective Area, Multiport Effective Length, Multiport Matching Efficiency, Non-rich Multipath, Pattern Overlap Matrix, Predictor Antenna System, Richness Threshold, Spatial Correlation, Uncorrelated Multipath.

Acknowlegments

This thesis has developed during the last few years partly in Communication Systems Group and Antenna Group at Chalmers University of Technology, and partially in ARAM laboratory at University of California Los Angeles. Before anything, I would like to express my gratitude to my respectable supervisors who have been abundantly helpful during these years.

Prof. Anders Derneryd, the legend of microstrip antennas, has been the main supervisor for this thesis. I owe you a great experience and many ideas on antenna research and analysis. To me you are a true gentleman of excellent characters, to whom I have developed a profound respect. Prof. Tommy Svensson, my co-supervisor, is deeply appreciated for taking this thesis in charge at a critical time. It has been a pleasure to work under your leadership in Artist4G project. An honourable mention goes to Prof. Yahya Rahmat-Samii for his invaluable scientific assistance. It has been a magnificent experience to do research under your guidance. Your favours and constant supports will never be forgotten. Prof. Per-Simon Kildal and Prof. Jan Carlsson are sincerely acknowledged for their patience, constructive discussions, and kind support during the early stage of this thesis.

Let me also avail myself of this opportunity to appreciate Prof. Mats Viberg, Chalmers' first vice president. The current thesis would have never seen the light of day without your able support and encouragement. Words are insufficient in describing my sense of gratitude to you. Prof. Mikael Persson has been responsible as the examiner for this work. Thank you for your time and kind help. I would like to gratefully acknowledge the head of the department, Prof. Arne Svensson, and the director of graduate studies, Prof. Martin Fabian for their never-failing support. A special mention goes to Prof. Erik Ström, the head of our division, for his kindness and brilliant leadership. The accomplishment of this thesis depended also on encouragement and guidelines of Profs. W. Wiesbeck, U. Westergren, A. Kishk, S. Popov, and A. Alavi, as well as Dr. S. Farjami and Dr. A. Bassari. Warm thanks to all of you.

The Department of Signals and Systems, Chalmers University of Technology, should be acknowledged as the main sponsor of the research carried out in the frame of this thesis. This research work has also been partly supported by Swedish Governmental Agency for Innovation Systems (VINNOVA) within the VINN Excellence Centre Chase at Chalmers.

My special thanks to all staff of S2, in particular my dears L. Börjesson, A. Kinnander, A. Lindbom, C. Johansson, and N. Adler. I also wish to express my gratitude to all former and current members of Communication Systems Group, Antenna Group, and ARAM laboratory staff in UCLA. My sincere gratefulness to all of you for creating an

unforgettable period in my life. My further acknowledgement goes to my respectable Iranian friends at Chalmers. From the bottom of my heart I thank you for your kind friendship and invaluable and consistent support. You will be forever deep within my heart. I am also in debt to my dears, N. Mohammad-Gholizadeh, A. Taeb, H. Ghaemi, B. Klein, and A. Garcia Romero, who have always been more than a friend to me. Cheers to you all! Last but not least, this thesis is dedicated to my most beloved ones, the light of my life, my respectable parents, Manijeh and Masih, and brother, Mani. I do love you and your love has always been my sole source of inspiration.

List of Appended Papers

Paper A
N. Jamaly and A. Derneryd, "Efficiency Characterisation of Multiport Antennas," in *IET Journal of Electronics Letters*, vol. 48, no. 4, pp. 196-198, February 2012

Paper B
N. Jamaly, A. Derneryd and Y. Rahmat-Samii, "A Revisit to Spatial Correlation in Terms of Input Network Parameters," in *IEEE Antennas and Wireless Propagation Letters*, vol. 11, pp. 1342-1345, October 2012

Paper C
N. Jamaly, A. Derneryd and Y. Rahmat-Samii, "Spatial Diversity Performance of Multiport Antennas in the Presence of a Butler Network," Submitted to *IEEE Transactions on Antennas and Propagation*, November 2012

Paper D
N. Jamaly, A. Derneryd and T. Svensson, "Analysis of Predictor Antenna System for Wireless Moving Relays," Submitted to *IEEE Transactions on Antennas and Propagation*, February 2013

Paper E
N. Jamaly, P.-S. Kildal and J. Carlsson, "Compact Formulas for Diversity Gain of Two-port Antennas," *IEEE Antennas and Wireless Propagation Letters*, vol. 9, pp. 970-973, October 2010

Paper F
N. Jamaly and A. Derneryd, "Fast Measurement of Antenna Pattern Overlap Matrix in Reverberation Chamber," in *IET Journal of Electronics Letters*, vol. 49, no. 5, pp. 318-319, February 2013

Paper G
Y. B. Karandikar, D. Nyberg, N. Jamaly and P.-S. Kildal, "Mode Counting in Rectangular, Cylindrical and Spherical Cavities with Application to Wireless Measurements in Reverberation Chambers," *IEEE Transactions on Electromagnetic Compatibility*, vol. 5, pp. 1044-1046, November 2009

Paper H

A. A. Al-Hadi, N. Jamaly, K. Haneda and C. Icheln, "Comparative Study of Two- to Eight-element Mobile Antenna Designs for LTE 3500 MHz Band," Submitted to *IEEE Transactions on Antennas and Propagation*, March 2013

List of Additional Related Papers

- C. Gomez-Calero, N. Jamaly, R. Martinez and L. Haro Ariet, "Comparison of Different MIMO Antenna Arrays and User's Effect on their Performances," Submitted to *Microwave and Optical Technology Letters*, January 2013

- N. Jamaly, A. Derneryd and T. Svensson, "Analysis of Antenna Pattern Overlap Matrix in Correlated Nonuniform Multipath Environments," in *Proceedings of the Seventh European Conference on Antennas and Propagation*, April 2013

- N. Jamaly and A. Derneryd, "Multiport Matching Efficiency in Antenna Systems with Cascaded Networks," *15th International Symposium on Antenna Technology and Applied Electromagnetics*, June 2012

- N. Jamaly and A. Derneryd ,"Coupling Effects on Richness Threshold of Multiport Antennas in Multipath Environments," *15th International Symposium on Antenna Technology and Applied Electromagnetics*, June 2012

- N. Jamaly, M. T. Iftikhar and Y. Rahmat-Samii, "Performance Evaluation of Diversity Antennas in Multipath Environments of Finite Richness," in *Proceedings of the Sixth European Conference on Antennas and Propagation*, March 2012

- N. Jamaly, "Spatial Characterisation of Multi-element Antennas," *Technical Report, Chalmers University of Technology*, ISSN 1403-266X (available online), March 2011

- P.-S. Kildal, N. Jamaly and J. Carlsson, "Performance of Different Theoretical Small Antennas in Isotropic 3-D and Horizontal 2-D Multipath Environments with Application to OTA Testing," *IEEE International Symposium on Antennas and Propagation*, July 2010

- N. Jamaly, H. Zhu, P.-S. Kildal and J. Carlsson, , "Performance of Directive Multi-Element antennas versus Multi-Beam Arrays in MIMO Communication Systems," in *Proceedings of the Fourth European Conference on Antennas and Propagation*,

April 2010

- A. A. H. Azremi, J. Toivanen, T. Laitinen, O. Vainikainen, X. Chen, N. Jamaly, J. Carlsson, P.-S. Kildal and S. Pivnenko, "On Diversity Performance of Two-Element Coupling Element-Based Antenna Structure for Mobile Terminal," in *Proceedings of the Fourth European Conference on Antennas and Propagation*, April 2010

- N. Jamaly, J. Carlsson and P.-S. Kildal, "Multipath Emulator for Simulation of Wireless Terminals' Performance," *Gigahertz Symposium, Lund University*, March 2010

- X. Chen, N. Jamaly, J. Carlsson, J. Yang, P.-S. Kildal and A. Hussain, "Comparison of Diversity Gains of Wideband Antennas Measured in Anechoic and Reverberation Chambers," *Gigahertz Symposium, Lund University*, March 2010

- J. Carlsson, K. Karlsson, N. Jamaly and P.-S. Kildal, "Analysis and Optimisation of Multiport Antennas by using Circuit Simulation and Embedded Element Patterns from Full-Wave Simulation," COST2100/ASSIST *Workshop on Multiple Antenna Systems on Small Terminals*, May 2009

- C. Gomez-Calero, N. Jamaly, L. Gonzalez and R. Martinez, "Effect of Mutual Coupling and Human Body on MIMO Performances," in *Proceedings of the Third European Conference on Antennas and Propagation*, March 2009

- N. Jamaly, C. Gomez-Calero, P.-S. Kildal, J. Carlsson and A. Wolfgang, "Study of Excitation on Beam Ports versus Element Ports in Performance Evaluation of Diversity and MIMO Arrays," in *Proceedings of the Third European Conference on Antennas and Propagation*, March 2009

Contents

Acronyms

2G	Second Generation
3G	Third Generation
4G	Fourth Generation
ADG	Apparent Diversity Gain
AoA	Angle of Arrival
BS	Base Station
CDF	Cumulative Distribution Function
EDG	Effective Diversity Gain
EDGE	Enhanced Data Rates for GSM Evolution
EM	Electromagnetic
FDMA	Frequency Division Multiple Access
GPRS	General Packet Radio Service
GSM	Global System for Mobile
HSPA	High Speed Packet Access
LTE	Long Term Evolution
MED	Mean Effective Directivity
MEG	Mean Effective Gain
MIMO	Multiple Input and Multiple Output
MRC	Maximum Ratio Combining
PCA	Principal Component Analysis
PDF	Probability Density Function
PEC	Perfect Electric Conductor
RF	Radio Frequency
SC	Selection Combining
SNIR	Signal-to-Noise plus Interference Ratio
SNR	Signal-to-Noise Ratio
ST	Space-Time
TDMA	Time Division Multiple Access
UE	User Equipment
WCDMA	Wideband Code Division Multiple Access
XPR	Cross Polarization Ratio

Part I

An Introduction to

Multiport Antenna Systems

Chapter 1

Introduction

The ever increasing demand for wireless data transfer is a major withstanding challenge for wireless communication community to evolve the present communication systems and devise rigorous solutions for future standards. A simple look at the schematics of the modern wireless communication systems reveals that their differences with a conventional system are likely limited to three main parts. That is, Space-Time (ST) coding/interleaving, prefiltering, and finally multiport radiation terminals. The latter is the main concern of the current thesis. In what follows and throughout this thesis we are going to carefully study the performance evaluation of multiport antenna systems and to investigate the different gauges whereby they are characterised. As an introduction to the present thesis, this chapter starts with a brief review of the history of personal mobile communication systems. Later, the important role of multiport antennas in the modern communication systems is highlighted. The overall organisation of the book is described to provide an outlook of the ensuing materials. We will eventually finalise this chapter with a short review of the notations which are consistently used in this thesis.

1.1 A Brief History of Wireless Communications

In earlier days, the analogue wireless communication was carried out through a central antenna system. But, due to limited frequency spectrum availability, the number of users whom the system could support was limited. A fundamental step towards increasing the capacity and the coverage of a wireless system was taken with the advent of cellular communication systems. In these systems, instead of a central antenna, multiple antennas were deployed and connected through a core network. Each of these antennas has been referred to as Base Station (BS). By virtue of these systems, different User Equipments (UEs) could communicate with different BSs using the same radio resources such as frequency and time. The concept of reusing the same resource for different UEs within a certain area brought the crucial issue of interference into picture whose treatment added to the complexity of the communication systems.

The further demand for system capacity required a more efficient communication scheme. Thus, the digital communications substituted for its analogue counterpart. In contrast to analogue systems which required considerable resources for each user, the digital communication rendered more flexibility allowing multiple users to share the same

channel. Among the second generation (2G) wireless communication systems, perhaps the most widespread one is the GSM system. Rolled out in the beginning of 90's, the GSM system is built on Time Division Multiple Access (TDMA) in combination with Frequency Division Multiple Access (FDMA). In this system, different frequency channels are subdivided into a number of time frames consisting of several time slots. Each user is dedicated a part of a frame rendering a constant throughput up to 9.6 kbps. This indeed implicitly means, when there is not sufficient number of users, part of the channel remains unused. To communicate between the UE and the BS, data networking is applied, which is possible through two ways. In the first approach known as circuit switching, there is a dedicated link between the receiver and the sender. In contrast to circuit switching, the users' information bits can be grouped into different packets which can be sent over undedicated links. This is referred to as packet switching. Based on this technique, GSM was further evolved with General Packet Radio Service (GPRS) wherein a mobile user was allocated more time slots within a frame. This made the overall performance of the system more efficient, increasing the data rate to 140 kbps. Subsequently, by using intelligent coding and modulation formats as well as link adaptation, the capacity of the system could increase up to 348 kbps within the frame of Enhanced Data Rates for GSM Evolution (EDGE).

To further quench the thirst of high data rate, at the turn of the millennium, communication engineers added a new dimension to the radio resources. This led to implementation of the third generation (3G) cellular systems, known as Wideband Code Division Multiple Access (WCDMA). These systems provided a data rate of up to 3 Mbps for the indoor users. In particular, an appreciable efficiency enhancement for 3G systems occurred by virtue of the High Speed Packet Access (HSPA) rendering a data rate of 5.7 Mbps uplink and 14 Mbps downlink [1]. The 3G system's evolution in turn has given birth to HSPA Evolution and Long Term Evolution (LTE) which is a fully packet-oriented system. In development of these two systems, engineers added an additional resource, namely the space domain, to use spatial signatures of multipath propagation mechanism to their advantage. Both HSPA Evolution and LTE systems which are the predecessor of the fourth generation (4G) cellular systems are currently being deployed around the world.

Among different aforementioned systems, HSPA Evolution and LTE systems require multiport antenna technologies at both link ends. This necessity comes in conjunction with some sophisticated algorithms using Multiple-Input and Multiple-Output (MIMO) transmission schemes. The latter technology, as an indispensable part of modern wireless communication systems, will undeniably remain as a keystone for the 4G mobile systems too [2].

1.2 Multiport Antenna Technologies

Usage of multiple antennas in multipath environments has long been of concern for advantages it renders. Most likely the very first benefit of multi-element antennas was recognised in 1920s and 1930s. During this time, it was observed that fluctuations in the received signal powers in a multipath environment, referred to as *fading*, were statistically independent at different antenna elements. Recall that when the power of a signal drops significantly, it is said to be *in fade* resulting in a loss of connection. To

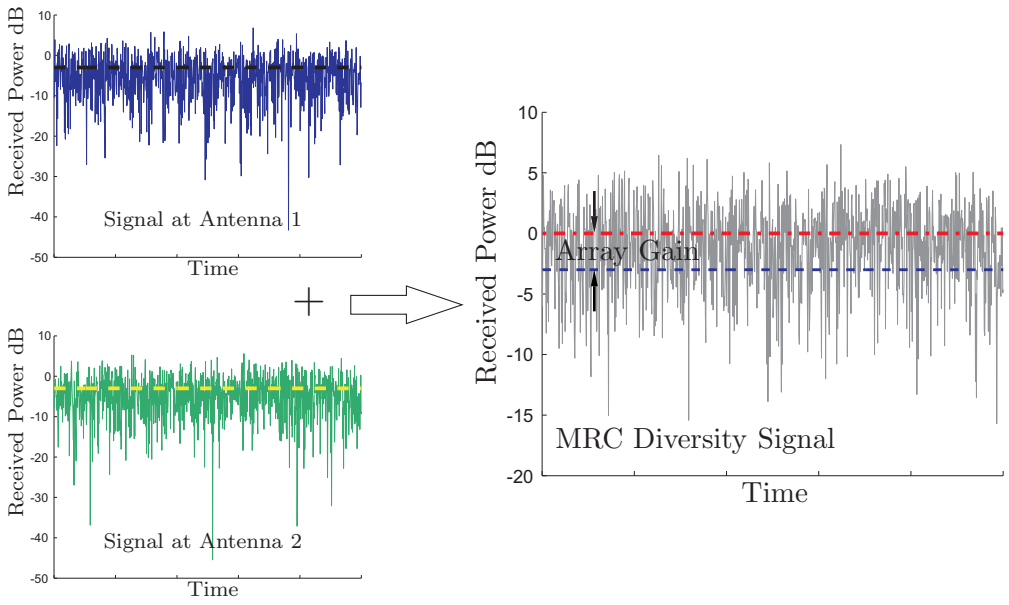

Figure 1.1: Received signals at ports of two antennas in a Rayleigh fading environment and their MRC combined diversity signal. The average values are plotted in dash. The red dash-dot line is the mean value of the combined signal.

combat fading, engineers recommended selecting the antenna with the strongest signal at each time instant. This was the advent of selection combining receiver diversity antenna systems. By the late 1960s, coherent combining schemes like Maximum Ratio Combining (MRC) and equal gain combining schemes were developed [2, 3, 4, 5]. The foregoing linear combination schemes bestowed an extra gain, called *array gain*. In general, array gain is referred to an enhancement in average received signal-to-noise ratio (SNR) at the receiver as a result of coherent combining of the available signals. To illustrate the concept, in Fig. 1.1 we show the random received signals versus time at the ports of two identical radiation elements in a uniform Rayleigh fading environment. These received signals are statistically independent. The MRC diversity signal based on these two signals is also plotted. As evident from the figure, the fading properties of the combined signal are far better than its two ingredients. Shown is also the array gain by virtue of this coherent combining scheme [6].

With further development of the multiport antenna concept, in late 80's and early 90's, the coherent combining was extended to cover transmitter antenna diversity, beamforming, and more significantly spatial multiplexing. The latter facilitated multiple data streams being transmitted in parallel while taking advantage of the space domain in addition to frequency and time domains [7]. This achievement revealed a remarkable advantage of multiport antennas in increasing the throughput of a wireless communication system, which is perhaps the primary reason for their worldwide popularity [7]. Let us spend a few moments briefly elaborating the spatial multiplexing. In its simplest form, a bit stream to be transmitted can be demultiplexed into two half-rate substreams, and transmitted through different antennas simultaneously. Under a suitable channel condition, the spatial signatures of these signals at the receiver terminal are separable. Hence, the receiver having knowledge of the channel can differentiate between these two co-channel

signals and extract the corresponding substreams accordingly [6]. In addition to spatial multiplexing, the multiport antenna technology provides a further critical advantage. For instance, as mentioned earlier, the frequency reuse in wireless channel is the main source of interference. When multiport antennas are used, the difference between the spatial signatures of signals with the same frequency makes it possible to reduce the interference between them too [6].

The concepts and the principles upon which the multiport antennas are designed and developed have been known for many years [8]-[14]. However, until quite recently, never has there been an essential need to realise a number of radiation elements on a small compact chassis. The presence of radiation elements in the nearby vicinity results in high signal correlation and mutual coupling [15]-[19]. The latter, not only reduces the overall quality performance of the communication system significantly, but also has impressive adverse effects on the battery reservoir of the mobile terminal. This has turned out to be a long-standing challenge in personal wireless communication industries. These crucial concerns remain beside the detuning and gain imbalance of the radiation elements which occur upon implementation of such a multiport system [20, Chapter 10].

Bear in mind that the multiport antennas specially on the user side should retain their efficient performance in different propagation circumstances. For instance, depending on the distribution of the incoming electromagnetic (EM) waves and their angle of arrival (AoA), polarisation, Doppler frequencies and correlation, different propagation scenarios bestow different potential levels for diversity and spatial multiplexing gains. The latter issue is an additional challenge for antenna engineers. The literature is fairly rich in this respect and there are still ongoing researches in this area worldwide [20, Chapter 10], [21]. Therefore, a brief part in the current thesis is dedicated for an acceptable multiport antenna design which preserves its effective performance in different multipath scenarios.

To make certain that a design meets the necessary requirements of a system specification, the antenna engineers need certain robust criteria and performance metrics. These parameters play an essential role for antenna engineers and establish a considerable portion of this thesis. Besides, measurement of the multiport antennas which are particularly designed to work in multipath environments is a further concern for antenna engineers [22]-[23]. No doubt, the most reliable way to verify an antenna's performance is its measurement in a fail-safe multipath scenario. Thus, in the frame of our thesis we accommodate an important part for research and study on this matter too.

1.3 Organisation of the Thesis

To present a consistent description of the works carried out in the framework of this thesis, we have organised the current report into two main parts. The first part is subdivided into several chapters, whereas the second part consists of the research papers appended to this thesis.

The organisation of Part I is as follows. Chapter 2 is dedicated to throwing light upon different power metrics in the area of multiport antennas. In this chapter, we extend the prevalent definitions for the case of single-port antennas to their multiport counterparts. The terms which are going to be used in the later chapters are carefully described and treated here. In a unified manner, an introduction to the notion of multiport

matching efficiency is provided. The review of this part is useful for a more comfortable comprehension of the subsequent chapters.

The third chapter concentrates on the precise formulation of the received voltage signals at the ports of a multiport antenna. In this chapter we generalise the effective length of antennas to hold in cases of multiport antennas and refer to it as multiport effective length. The matrix algebra is used to treat the received signals upon presumption of an incoming EM wave. The latter bestows huge help in making our analysis easier. The effects of terminating impedances in a compact system are clarified here. We further provide a brief description about the received signal calculation in a multipath by virtue of the superposition principle. The mathematical modelling of the incoming EM waves in a Rayleigh fading multipath is treated here. Chapter 3 establishes a rigorous ground for the ensuing chapters and thus deserves a proper regard.

Perhaps the major source for deriving different performance metrics in the area of multiport diversity antennas is the received signals' covariance matrix. Chapter 4 is devoted to precise formulation and normalisation of the covariance matrix in different types of multipath environments. The bases of these formulations rely on foundations initiated in the two preceding chapters. Here, we distinctly outline the impacts of terminating impedances, total radiation efficiencies, and the properties of the multipath environments upon the covariance matrix. The concepts of mean effective directivity and gain are described to a point of satisfaction. We also briefly explain the classic yet important category of minimum scattering antennas at the end of this chapter.

The purpose of Chapter 5 is to provide formulas for evaluation of the covariance matrix in the presence of an arbitrary number of cascaded networks. This part may associate more with the area of microwave engineering yet provides a special insight for antenna engineers too. An algorithm is elaborated here which is highly useful for calculation of total S-matrix of a chain of arbitrary known networks. Interestingly, there would be no restriction on the number of ports and cascaded networks in the proposed algorithm. Hence, in this sense, it is quite a general approach. Thereafter, it is shown how one can calculate different performance metrics in the presence of a number of cascaded networks. Indeed, the materials provided in this chapter are essential for a major portion of the works conducted in this thesis and are thus of significance for our development.

Chapter 6 follows with a fair introduction of the simulation approach used in many of our appended papers. It subsequently concentrates on the evaluation of diversity gain based on different prevalent methods. The notion of richness threshold which we have coined in this thesis is addressed and an example is provided for better elucidation.

Finally, the overall goal of Chapter 7 is to provide a short description of the contributions made in this thesis. During this period, we have also published a number of papers as a complementary to the studies presented in the appended papers. A summary of the contributions in these supplementary papers is highlighted. In each part, we also briefly speak of the limitations inherent in our studies presented in different papers. At the end, some words are dedicated for potential works that can subsequently follow the research frame presented in this thesis.

The second part of this book comprises the research papers in their published or submitted format. Nevertheless the layout of them has been accordingly modified to go well with the rest of this book. A similar modification has been applied to their notations.

1.4 Notation Description

In the frame of different chapters in this thesis, we are involved with important derivations and formulations. Thus, before entering to the heart of the current report, it is worthwhile making the readers comfortable with the selected notations in the forthcoming analyses. Throughout this book, matrices are denoted by bold letters whereas column vectors by an overbar sign. In particular, the identity matrix is shown by $\mathbf{I}$ and a null matrix by $\mathbf{0}$. The transpose, conjugate, and Hermitian transpose are signified by the superscripts $\cdot^T$, asterisk, and the dagger sign, respectively. The intrinsic impedance of the medium is denoted by η. The operator $\Re$ returns the real part of its argument. 'tr' stands for the trace of a matrix, and 'diag' returns a diagonal matrix with the corresponding entries of its argument. The symbol $\mathbb{E}$ denotes the expectation over time or realisation. The Sans Serif font is exclusively used to denote the probability functions. Furthermore, the number of ports in a multiport system is shown by n. As an exception, in Chapter 4 on page 29, the subindex n was also used occasionally to denote the normalised metric. Covariance matrices are in general signified by $\mathbf{C}$. A vector with magnitude and direction is denoted by an over-vector sign, $\vec{\cdot}$, whereas the unit vector by a hat sign. For the sake of clarity in appearance, sometimes we use a dot between two matrices to show their product. It does not denote the scalar product between two vectors.

Chapter 2

Antenna Efficiency Description

Regardless of being a single-port or multiport antenna, no matter if it is used in line-of-sight or non-line-of-sight scenarios, the radiation efficiency of the antennas plays a significant role in overall performance of a wireless system. Although the terminologies associated with radiation efficiency in the conventional single-port antennas are well established in the literature, there is almost no unanimous definition for metrics addressing the radiation efficiencies of multiport antennas. Therefore, before entering to the heart of our analysis in this thesis, we should dedicate adequate time to throwing light upon certain terms on this discipline which are part of the game in the subsequent chapters. By this clarification, the ensuing parts of this thesis are understood more fluently. This chapter is initialised with a brief review of some definitions holding for the single-port antennas. These definitions are subsequently extended to stand for the cases of multiport antennas. By virtue of the introduced terminologies, we clearly describe some noteworthy radiation efficiencies to be used in multiport antennas. At first, for pedagogical reasons, we introduce these definitions by assuming a single active port in a multiport system, and derive some simple expressions for different definitions presented. Later, we elaborate how the matrix algebra can be utilised rendering some compact formulas for direct calculation of these useful efficiency metrics.

2.1 Some Definitions

Voltage sources can in general be described by their internal impedances as well as their maximum available power, P_{avs}. The *maximum available power* from a source is the maximum power that can be delivered to a conjugate matched load from a source of certain internal impedance. In case of a multiport excitation scheme, the sum of the P_{avs} at the corresponding ports is the associated maximum available power.

The *accepted power* by an antenna, denoted by P_{acc}, is defined as a part of the incident power at its port(s) which is available for radiation. In case of a single-port antenna, the accepted power is the incident power P_{inc} subtracted by the reflected power P_{rfl},

$$P_{\text{acc}} = P_{\text{inc}} - P_{\text{rfl}} \qquad (\text{Single-port Antennas}) \ . \tag{2.1}$$

In contrast, in multiport antennas, description of the accepted power by a radiation element might be slightly tricky due to the presence of coupling among different ports.

In this circumstance, we should note that the accepted power is not simply the incident power minus the reflected power at each port. Instead, one needs to also take into account the *coupled power* at other ports, which is dissipated on their terminations and therefore not available for radiation. For instance, consider the ith port in an n-port antenna system. The coupled power pertinent to its excitation, P^i_{cpl}, is

$$P^i_{\text{cpl}} = P^i_{\text{inc}} \sum_{j=1, j\neq i}^{n} |s_{ji}|^2 \qquad (\text{Multiport Antennas}) \ , \tag{2.2}$$

wherein s_{ji} is a specified entry of the antenna's scattering matrix denoted by $\mathbf{S}_{a\ (n\times n)}$. The superscript i indicates to which port the corresponding power belongs. It is well known that the reflected power at port i in term of the incident power at this port is

$$P^i_{\text{rfl}} = |s_{ii}|^2 \ P^i_{\text{inc}} \ . \tag{2.3}$$

Therefore, in light of (2.2), the accepted power when port i is excited, P^i_{acc}, becomes

$$P^i_{\text{acc}} = P^i_{\text{inc}} \left(1 - \sum_{j=1}^{n} |s_{ji}|^2 \right) \qquad (\text{Multiport Antennas}) \ . \tag{2.4}$$

Of course, the accepted power in (2.4) is a general definition which in the absence of coupling, *i.e.*, $s_{ji} = 0$ for all j except probably $j = i$, reduces to (2.1). In other words, in the absence of coupling, a multiport antenna can be thought of as a group of independent single-port antennas. Bear in mind that, upon presumption of a known incident power at the ports, the accepted power relies solely on the input network parameters. This is a salient feature of the accepted power which we will make use of later in this chapter.

In addition, in case of ohmic losses on the structure of the antenna or in its vicinity, a portion of the accepted power is dissipated which is commonly referred to as *loss power* denoted by P_{los}. Note that the loss power can be dependent not only on the lossy objects in the proximity of the radiation structure, but also on the terminating impedances of the other ports in the presence of coupling. In general, the ohmic losses are not handy to treat and depend on numerous factors in actual scenarios. Nevertheless, in the absence of external losses, and as long as the losses over the structure can be modelled by a loss resistance in series with the radiation resistance associated with each port[1], treatment of ohmic losses are far more convenient. Clearly, this excludes losses due to lossy dielectrics, interaction with chassis, or electric current leakage.

As it was stressed, the loss power is a portion of accepted power which is lost. The remainder of accepted power is the radiated power denoted by P_{rad}. That is, for ith port,

$$P^i_{\text{rad}} = P^i_{\text{acc}} - P^i_{\text{los}} \ . \tag{2.5}$$

To elaborate it a little more, P^i_{los} is the loss power when port i is excited and all other ports are terminated. Note that P^i_{los} does not include the power dissipated in the termination of other coupled radiation ports. Likewise, P^i_{rad} is the radiated power when port i is excited

[1] This corresponds to Thevenin circuit model. By reciprocity, for Norton equivalent circuits, the 'well-behaviour' losses are modelled by a shunt loss conductance.

while the other ports are terminated. In general, the radiated power can only be obtained by virtue of the (embedded element) far-field pattern of the antennas.[2] However, in case of a lossless structure and in the absence of nearby lossy objects, the radiated power equals the accepted power and is thus expressible by the input network parameters. This is of considerable help for antenna engineers in quick estimation of their designs' overall performance regardless of the antennas' far-field patterns.

2.2 Efficiency Characterisation of Antennas

One of the major performance metrics in the history of antennas is their radiation efficiency. In simple words, it indicates how effectively an antenna can convert the electric energy available at its port(s) to the EM radiation fields around it.

As a brief review, for single-port antennas, the radiation efficiency, e, is the ratio between the total radiated power P_{rad} and the accepted power P_{acc} at its port.[3] This efficiency contains information about losses over the structure of the antenna, P_{los}. That is, in cases of a lossless radiation structure, the radiation efficiency is unity. In a like fashion, the total radiation efficiency e_{tot} is the ratio between the total radiated power P_{rad} and the maximum available power from the source, P_{avs}. The total radiation efficiency in a single-port antenna not only contains information about its ohmic losses, but also provides information about how well the antenna is matched to the internal impedance of its source. As an important point, the ratio between the total radiation efficiency and the radiation efficiency is referred to as *matching efficiency*, e_{mch}. That is,

$$e_{\text{tot}} = e_{\text{mch}} \cdot e_{\text{rad}} \qquad (\text{Single-port Antennas}) \ . \tag{2.6}$$

Nevertheless, when it comes to multiport antennas, the concept of radiation efficiency has not been treated unanimously worldwide [24]. Thus, our main goal in this section is to clarify some noteworthy efficiency gauges in the area of multiport antenna systems.

2.2.1 Total Embedded Element Efficiency

In principle, for an antenna in the presence of other radiating elements, aside from losses in the non-ideal conductors, dielectrics, and lossy objects, absorption in the terminations of the neighbouring elements as well as reflection on its own port contribute to the reduction of its radiation performance. The *total embedded element efficiency* is indeed a measure implying the reduction in radiation performance caused by the aforementioned factors. In effect, the total embedded element efficiency for port i, e^i_{tot}, is the ratio between the radiated power and the maximum available power at this port while other present ports are passively terminated. In the absence of coupling in a multiport antenna system, the total embedded element radiation efficiencies reduce to the corresponding total radiation efficiencies defined for single-port antennas. In this particular case, each port can be regarded as an isolated port which is not affected by its neighbouring radiating elements.

[2] To see how, refer to Equation (2.13).

[3] Also refer to IEEE Standard Definitions of Terms for Antennas, IEEE Std 145-1993.

2.2.2 Embedded Element Efficiency

Similarly, the embedded element efficiency for port i is defined as the ratio between the radiated power and the accepted power when port i is excited and all other ports are terminated. This efficiency is denoted by e^i_{emb}. In the absence of coupling, an embedded element efficiency reduces to the corresponding *radiation efficiency*. Thus, it is a more general metric. Note that the embedded element efficiency only contains information about the losses over the antenna structure or in its vicinity.

2.2.3 Multiport Matching Efficiency

In simple words, *multiport matching efficiency* is the multiport version of the conventional matching efficiency used for single-port antennas. For a port, say, i in a multiport antenna system, the ratio between the accepted power and the maximum available power at this port is referred to as multiport matching efficiency. In the frame of the current thesis, we denote this useful efficiency metric by e^i_{mp}. The link between the three foregoing efficiency metrics is as follows:

$$e^i_{\text{tot}} = e^i_{\text{mp}} \cdot e^i_{\text{emb}} \qquad (\text{Multiport Antennas}) \ . \tag{2.7}$$

A detailed description of the multiport matching efficiency can be found in [Paper A], wherein the excitation scheme has also been included in the definition.

2.2.4 Decoupling Efficiency

As it can be seen from (2.4), the less the coupling among the nearby elements in a multiport antenna system, the more the accepted power, and thus the more the radiated power. The latter by all means enhances the total radiation efficiency. This fact has created a trend in engineers to reduce coupling in a multiport radiation system as much as possible in order to improve the overall performance. To measure engineers success in this respect a parameter has been coined called *decoupling efficiency* [25]. Indeed, the decoupling efficiency is a measure to quantify how well the behaviour of an embedded radiation element in a multiport antenna system can be characterised by its single-port (*i.e.*, isolated) properties.

The decoupling efficiency for a certain port i, denoted by e^i_{dcl}, is defined as the ratio between the accepted power and the incident power at the associated port when all other ports are passively terminated [25]. Based on this definition, the expression within the parentheses in (2.4) yields the decoupling efficiency at the port i. The main feature of the decoupling efficiency is that it can be simply achieved by the input network parameters. It does not depend on the terminating impedances. In this respect, it is quite unique. It is also worth noting that the multiport matching efficiency equals decoupling efficiency when the terminating impedances are matched to the characteristic impedances of the multiport system. As a final point, we should acknowledge that although the terminology used here is quite novel[4], the associated expression for the decoupling efficiency has long been known given by S. Stein [26, Equation (8)] in early 1960s.

[4] This terminology belongs to reference [25].

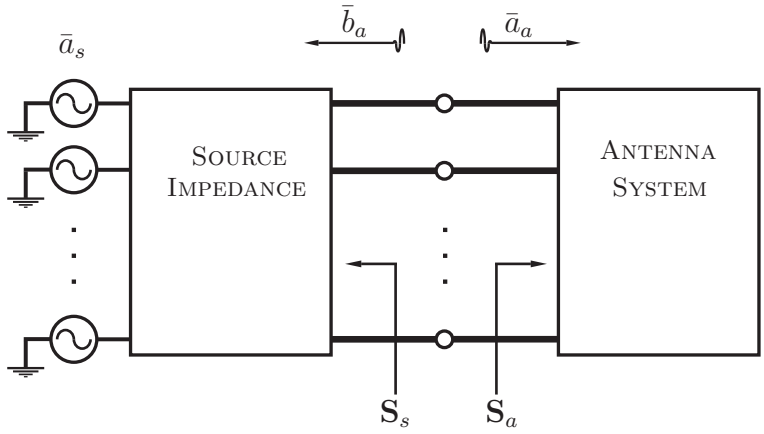

Figure 2.1: Circuit model of a multiport antenna connected to a set of sources.

2.2.5 Mean Matching Efficiency

The notion of *mean matching efficiency* has been introduced for narrowband diversity antennas in [Paper A]. It is quite useful for a quick estimation of diversity performance in a multiport antenna system with a fair amount of spatial correlation between different ports. Mean matching efficiency is indeed the geometric mean value of all multiport matching efficiencies in a lossless multiport antenna system. In order to extract the corresponding diversity gain, depending on the total effective number of elements, one only needs to use the product of mean matching efficiency and the maximum achievable diversity gain for either selection combining or maximum ratio combining schemes.[5] The maximum achievable diversity gains for the aforementioned combining schemes versus different numbers of ports are listed in [27, Table I].

2.3 Formulation of Efficiency Metrics

Mathematically, the most compact and comfortable way to simultaneously calculate efficiency metrics in multiport antenna systems is to use matrix algebra. To clearly illustrate it, Fig. 2.1 is of considerable help. In this figure, the incident waves at the ports of the antennas are given in a column vector $\bar{a}_a$ and the reflected waves in its counterpart $\bar{b}_a$. The length of these vectors are evidently n, the number of ports in the system. Further in this figure, the antenna structure is specified by its input ports' S-matrix, $\mathbf{S}_a$, while the sources are collectively characterised by $\mathbf{S}_s$. The vector $\bar{a}_s$ contains the source voltages for each excitation scheme. For the time being, let us limit ourselves to identical single-port excitation schemes. This means, in all port excitations, we use $a_\circ$ source voltage in volts at each port.

[5] To read more about spatial diversity combining schemes refer to [4, Chapter 7].

2.3.1 Maximum Available Power Formulation

Based on Fig. 2.1, the diagonal maximum available power matrix for the multiport system is [6]

$$\mathbf{P}_{\text{avs}} = P_{\text{s}}\ \text{diag}\left[\mathbf{T}_m{}^{\dagger}\left(\mathbf{I}-\mathbf{S}_s\mathbf{S}_s{}^{\dagger}\right)\mathbf{T}_m\right]\ , \tag{2.8}$$

where the 'diag' operator returns a diagonal matrix with the corresponding diagonal entries of its argument, and

$$\mathbf{T}_m = \left[(\mathbf{I}+\mathbf{S}_s)(\mathbf{I}-\mathbf{S}_s)^{-1}(\mathbf{I}-\mathbf{S}_s{}^{\dagger})+(\mathbf{I}+\mathbf{S}_s{}^{\dagger})\right]^{-1}\ . \tag{2.9}$$

The constant $P_{\text{s}} = 1/(2Z_{\circ})|a_{\circ}|^2$ in watts is the source power for the foregoing identical excitations. Of course, $Z_{\circ}$ is the characteristic impedance of the system.

2.3.2 Multiport Matching versus Decoupling Efficiencies

Having the maximum available power matrix in access by (2.8), we can compactly write the diagonal multiport matching efficiency matrix as

$$\mathbf{e}_{\text{mp}} \ = \ \text{diag}\left[\mathbf{T}_m{}^{\dagger}\left(\mathbf{I}-\mathbf{S}_s\mathbf{S}_s{}^{\dagger}\right)\mathbf{T}_m\right]^{-1}\cdot\text{diag}\left[\mathbf{T}_s{}^{\dagger}\left(\mathbf{I}-\mathbf{S}_a{}^{\dagger}\mathbf{S}_a\right)\mathbf{T}_s\right]\ , \tag{2.10}$$

in which

$$\mathbf{T}_s = \left[(\mathbf{I}+\mathbf{S}_s)(\mathbf{I}-\mathbf{S}_s)^{-1}(\mathbf{I}-\mathbf{S}_a)+(\mathbf{I}+\mathbf{S}_a)\right]^{-1}\ . \tag{2.11}$$

Similarly, the diagonal decoupling efficiency matrix, $\mathbf{e}_{\text{dcl}}$, can be simply given by

$$\mathbf{e}_{\text{dcl}} = \text{diag}\left[\mathbf{I}-\mathbf{S}_a\mathbf{S}_a^{\dagger}\right]\ , \tag{2.12}$$

which solely depends on the input network parameters of the multiport antenna system. If source impedances are matched to the characteristics impedances of the system, we have $\mathbf{S}_s = \mathbf{0}$ which eventually leads to the equivalence of the decoupling efficiency and multiport matching efficiency. This shows that the multiport matching efficiency inherently contains information provided by the decoupling efficiency.

2.3.3 Total Embedded Element Efficiency Formulation

In order to formulate the total embedded element radiation efficiency in a multiport antenna system, we first require the total radiated power. In this way, to find the total radiated power, we further need to define a terminated embedded pattern matrix. In the spherical coordinate system, the embedded far-field pattern matrix of an n-port antenna can be written in a $2\times n$ matrix, $\mathbf{G}_r$. The first row of this matrix is the vertical or θ-polarisation components of the embedded patterns, whereas the second row is associated with their horizontal or ψ-polarisation components. Let us assume that the foregoing matrix is measured or simulated while excited by the identical sources of $a_{\circ}$ volts with arbitrary source impedances. The embedded far-field pattern matrix is evidently a function of angular direction denoted by Ω. In this coordinate system, a solid angle can in turn be specified by the latitude θ and longitude ψ angles, *i.e.*, $\Omega(\theta,\psi)$.

[6] The details in derivation of these formulas are partly provided in [Paper C].

Now, we can achieve the total radiated power by virtue of the Poynting's vector [28, Section 8-5]. If the intrinsic impedance of the medium is denoted by η, the diagonal total radiated power[7] matrix becomes

$$\mathbf{P}_{\text{rad}} = \frac{1}{2\eta}\ \text{diag}\left[\oint_{4\pi} \mathbf{G}_r^T(\Omega)\cdot\mathbf{G}_r^*(\Omega)\ d\Omega\right]\ . \tag{2.13}$$

Using the maximum available power expression in (2.8) and the total radiated power in (2.13), we can find the total embedded element efficiencies in a diagonal matrix by

$$\mathbf{e}_{\text{tot}} = \frac{1}{2\eta}\ \mathbf{P}_{\text{avs}}^{-1}\cdot\text{diag}\left[\oint_{4\pi} \mathbf{G}_r^T(\Omega)\cdot\mathbf{G}_r^*(\Omega)\ d\Omega\right]\ . \tag{2.14}$$

We will make use of the above total embedded element efficiency matrix in the subsequent chapters. Pursuing the same way, one can also derive a compact expression for the embedded element efficiency matrix. Bear in mind that the following general relation holds between the three major aforementioned efficiencies:

$$\mathbf{e}_{\text{tot}} = \mathbf{e}_{\text{mp}}\cdot\mathbf{e}_{\text{emb}} \qquad (\text{Multiport Antennas})\ , \tag{2.15}$$

which in case of a single-port antenna reduces to (2.6).

2.4 Summary

This chapter has been dedicated to clarifying some important efficiency metrics in multiport antenna systems. The importance of this clarification resides on the fact that it is rare to find a unanimous definition or terminology on this issue among different research groups worldwide. We have evolved the radiation efficiency concept for multiport antennas by a brief review over those of more mature single-port antenna cases. We have shown how one can extend the available definitions for single-port antennas to hold for multiport antennas too. For this purpose, we required some interpretations of relevant power definitions in the multiport antenna systems. This concern has been carefully addressed. Later, we provide a compact expression for the aforementioned radiation metrics by virtue of the matrix algebra. The results presented here will be used in the subsequent chapters.

[7] It is better to refer to it as 'total average radiated power'. But, for simplicity, we drop the 'average'.

Chapter 3

Received Signals in Multiport Antenna Systems

The main concern of the current chapter is to derive some useful formulas rendering the received voltage signals at the ports of a multiport antenna system upon presumption of a known incident EM wave. Formulation of the received signal at the port of a single-port antenna has been well established in the literature [29]-[28]. Yet, things are somewhat different when it comes to a multiport antenna system in which each radiation element operates in the presence of some neighbouring radiators or parasitic elements. Indeed, in this situation, the coupling mechanism will cause an infinite chain of scattered and rescattered fields [30, page 425]. These radiated and scattered fields superimpose vectorially rendering the ultimate voltage signal at the corresponding element's port. The received signal under the aforementioned circumstance can be quite different from that obtained by the same antenna in the absence of nearby radiating structures. Therefore, complexity of the coupling mechanism inherent in the multiport antenna systems requires a delicate formulation in a generic sense. The latter is the main point of interest in this chapter. Different steps in derivation of the functions linking the incident EM waves to the corresponding antenna ports are elaborated to a point of satisfaction while details remain within our patience.

3.1 Effective Length of Multiport Antennas

The effective length of an antenna, regardless of the presence of nearby radiating elements, is a function relating an incident EM wave to the corresponding open-circuit induced voltage at the port of the antenna. Irrefutably, the effective length is intrinsically of vectorial nature. In a multiport antenna system, an incident EM wave can induce voltage at the open-circuit port of each radiating element. In this regard, associated to each port in this antenna system, there comes a certain effective length. The effective lengths of different radiation elements in a multiport antenna system can most conveniently be cast in a matrix, forming what can best be called *multiport effective length matrix*. The entries of multiport effective length matrix are complex components of polarisation vectors which are, in turn, functions of angular direction, $\Omega(\theta, \psi)$.

In order to obtain the multiport effective length matrix, we pursue a similar approach

to the one used for single-port antennas in [31]. Let us consider current-driven multiport antennas. In contrast to voltage-driven antennas like slot antennas, the current-driven antennas can be more comfortably modelled by their Thevenin equivalent circuit. An example of current-driven antennas is the wire antenna, which is frequently used in this thesis. Consider also a plane wave $\vec{E}_d(\Omega)$ created by an infinitesimal dipole of length l. For simplicity, the orientation of this infinitesimal antenna, $\hat{l}$, is orthogonal to its position vector, $\vec{r}_d$. The far-field radiation of this antenna when excited by an electric current, i_d, is well known:

$$\vec{E}_d(\vec{r}) = \frac{-j\eta}{2\lambda}\; i_d\; l\hat{l}\; \frac{\exp\left(+j\vec{k}\cdot(\vec{r}-\vec{r}_d)\right)}{|\vec{r}-\vec{r}_d|}\;. \tag{3.1}$$

In the above expression, λ is the wavelength and $\vec{k}$ is the wavenumber vector.[1] The electric current of this infinitesimal dipole induces voltages at different ports of a multiport antenna when they are open-circuited. Let us designate the open-circuit voltage at, say, the mth port by $v_{\circ_m}$. By reciprocity, the same current i_d applied to this port of the multiport antenna, while other ports remain open-circuited, induces the same open-circuit voltage at the port of the infinitesimal dipole. If we assume that the phase reference point of the multiport antenna is at the origin, *i.e.*, $\vec{r}=0$, this open-circuit voltage can be obtained by

$$v_{\circ_m} = -\int_{-\frac{l}{2}}^{\frac{l}{2}} \vec{E}_m(\vec{r}_d)\cdot l\hat{l}\; dl = -\frac{\exp(-j\vec{k}\cdot\vec{r}_d)}{|\vec{r}_d|}\; l\; \vec{G}_m(\hat{r}_d)\cdot\hat{l} \tag{3.2}$$

Finding $l\hat{l}$ from (3.1), and inserting the resultant into (3.2) yields

$$v_{\circ_m} = \frac{-2j\lambda}{\eta}\; \frac{1}{i_d}\; \vec{G}_m(\hat{r}_d)\cdot\vec{E}_d \tag{3.3}$$

which is tantamount to its counterpart in [31, Equation (4)]. We stress that the incident field $\vec{E}_d$ at $\vec{r}=0$ is a complex vector with amplitude, phase and polarisation at the phase reference point of the multiport antenna, when this multiport radiation structure is absent. To derive an expression for multiport effective length matrix, let us first elucidate the open-circuit pattern matrix.

3.2 Open-circuit Pattern Matrix

Let us concentrate further on what we obtained as the effective length of an antenna. In (3.3), the parameter $\vec{G}_m$ is the open-circuit embedded far-field pattern of the multiport antenna, when mth port is excited by the electric current i_d while all other ports are open-circuited. A division by i_d effectively removes the influence of electric current on $\vec{G}_m$. The outcome will have an ohmic nature which gives the embedded far-field pattern of the port when excited by 1 ampere electric current while all other ports are open-circuited. We refer to this normalised embedded pattern as the open-circuit embedded far-field pattern. Associated with each port, there is an open-circuit embedded far-field pattern. Similar to the embedded pattern matrix in Section 2.3.3, all open-circuit embedded patterns in

[1] For more information on wavenumber vector refer to [28, page 362].

a multiport structure can be cast in a matrix which establishes the building block of our further developments. To describe it a little more, for an n-port antenna system, the open-circuit embedded far-field pattern matrix is a $2 \times n$ matrix whose rows are the corresponding vertical θ-polarisation and horizontal ψ-polarisation components. We denote this important matrix by $\mathbf{G}$ and for the sake of simplicity refer to it as *open-circuit pattern matrix*. This matrix is a function of Ω. A straightforward comparison between the open-circuit pattern matrix and the multiport effective length matrix, $\mathbf{L}$, reveals the link between them as follows:

$$\mathbf{L} = \frac{2\lambda}{j\eta}\, \mathbf{G}^T \ . \tag{3.4}$$

The columns of $\mathbf{L}_{n\times 2}$ are the associated radiation elements' effective length vectors for θ and ψ polarisations in the spherical coordinate system, respectively.

3.3 Embedded Far-field Patterns

The open-circuit pattern matrix is the basis of the renowned embedded far-field pattern of a multiport antenna system. To distinguish between them, recall that the latter has already been denoted by $\mathbf{G}_r$. Should we look upon an n-port antenna system as a microwave network with input impedance matrix of $\mathbf{Z}$, the electric currents across different ports when excited by a set of sources, $\bar{v}_s$, is

$$\bar{i} = (\mathbf{Z} + \mathbf{Z}_s)^{-1} \bar{v}_s \ , \tag{3.5}$$

where $\mathbf{Z}_s$ is a diagonal matrix containing the complex source impedances connected to the ports. Associated with each excitation scheme there comes an embedded far-field pattern. In the modern wireless communication systems, the signals at the ports of a multiport system are normally regarded incoherently. This corresponds to a single-entry excitation vector, $\bar{v}_s$, in (3.5). One can stack all the current vectors corresponding to different single-entry excitations in a matrix signified by $\mathbf{i}$. For instance, if the identity matrix $\mathbf{I}_{n\times n}$ is collectively used as n sets of single-entry excitation vectors, the associated electric current matrix in amperes reads

$$\mathbf{i} = (\mathbf{Z} + \mathbf{Z}_s)^{-1} \ . \tag{3.6}$$

Consequently, the embedded far-field pattern matrix in volts becomes

$$\mathbf{G}_r = \mathbf{G} \cdot \mathbf{i} \ . \tag{3.7}$$

The embedded pattern which belongs to a single-entry excitation scheme can be distinctly referred to as the *embedded element far-field pattern*. This parameter plays a significant role in receive-mode diversity antenna systems.

From a practical point of view, in a multiport antenna system, measurements of embedded element patterns are more common. In this regard, finding a relation between the multiport effective length matrix and the embedded element pattern matrix is of interest. Given the foregoing parameter, we can simply derive the multiport effective length matrix through

$$\mathbf{L} = \frac{2\lambda}{j\eta}\, \mathbf{i}^{-1^T} \cdot \mathbf{G}_r{}^T \ . \tag{3.8}$$

In (3.8), we can interpret $\mathbf{i}$ as the electric current matrix at the antenna ports whereby the embedded far-field patterns in $\mathbf{G}_r$ have been either measured or simulated.

3.4 Received Voltage Signals

The received voltage signals are the signals at the ports of a receiver connected to a multiport antenna system.[2] These received voltages are dependent on the terminating impedances at the receiver ports. One can recast the complex impedances at these ports in a diagonal matrix, denoted by $\mathbf{Z}_r$. Now, by virtue of voltage division rule in the fundamental circuit theorem, the relation between the received voltages at the ports of the receiver, $\bar{v}_r$, and the open-circuit voltages available at the antenna ports, $\bar{v}_\circ$, becomes

$$\bar{v}_r = \mathbf{Z}_r \ (\mathbf{Z} + \mathbf{Z}_r)^{-1} \ \bar{v}_\circ \ . \tag{3.9}$$

An incident EM field from an angular direction Ω can be written as

$$\vec{E}(\Omega) = E_\theta(\Omega) \ \hat{\theta} + E_\psi(\Omega) \ \hat{\psi} \tag{3.10}$$

in volts per meters. This can also be rewritten in a column vector form, $\bar{E}_{2\times 1}$, whose entries are E_θ and E_ψ. Considering the relation between the open-circuit voltage vector $\bar{v}_\circ$ and the incident wave, $\bar{E}$, we can recast the received voltage vector as

$$\bar{v}_r = \mathbf{Z}_r \ (\mathbf{Z} + \mathbf{Z}_r)^{-1} \ \mathbf{L}(\Omega) \cdot \bar{E}(\Omega) \ . \tag{3.11}$$

It is worthwhile expressing the received voltage $\bar{v}_r$ in terms of the available embedded patterns. Assume that the embedded element pattern matrix, $\mathbf{G}_r$, is achieved by the electric currents across ports in (3.6). Let us denote the source impedances, whereby $\mathbf{G}_r$ is obtained, by a diagonal matrix, $\mathbf{Z}_s$. If the same multiport antenna system is connected to a receiver with $\mathbf{Z}_r$ input impedances, using the equivalence in (3.8), we can find the received voltage vector by[3]

$$\bar{v}_r = \frac{2\lambda}{j\eta} \ \mathbf{Z}_r \ (\mathbf{Z} + \mathbf{Z}_r)^{-1} (\mathbf{Z} + \mathbf{Z}_s) \ \mathbf{G}_r^T(\Omega) \cdot \bar{E}(\Omega) \ . \tag{3.12}$$

In case the source impedances by which the embedded element pattern matrix is evaluated are the same as the corresponding receiver impedances, *i.e.*, $\mathbf{Z}_s = \mathbf{Z}_r$, the expression in (3.12) can be further simplified as

$$\bar{v}_r = \frac{2\lambda}{j\eta} \ \mathbf{Z}_r \ \mathbf{G}_r^T(\Omega) \cdot \bar{E}(\Omega) \ . \tag{3.13}$$

[2] In the simplest case, the multiport antenna is directly connected to the receiver. Thus, signals at the antenna ports and the receiver ports are the same. Nevertheless, as we will see in Chapter 5, in the presence of a cascaded network the signals at these two sets of ports are different.

[3] Compare this expression with its single-port counterpart in [27, Equations (3.13) & (3.14)].

3.5 Average Received Power

In practice, measurement of voltage signals at the receiver ports are to some extent troublesome since they require the phase information too. In contrast, measurement of the corresponding average received power, P_{rec}, at each port is far easier. Therefore, it is worth finding a function rendering the average received power upon presumption of a sinusoidal incident EM wave from an arbitrary direction. Let us start with the simplest case in which the source impedances whereby the embedded element pattern matrix is measured and the receiver impedances are all the same and of resistive nature. Thais means, $\mathbf{Z}_s = \mathbf{Z}_r = Z_\circ \mathbf{I}$. Under this constraint, the received voltage is given by the expression in (3.13). In this case, for the received power matrix we have

$$\mathbf{P}_{\text{rec}} = \frac{1}{2Z_\circ} \text{ diag } [\bar{v}_r \cdot \bar{v}_r^\dagger] \ , \tag{3.14}$$

where, like before, 'diag' assembles a diagonal matrix with the corresponding diagonal entries of its argument. Of course, the entries of $\mathbf{P}_{\text{rec}}$ are the corresponding received average power at each port. Inserting $\bar{v}_r$ from (3.13) yields the received average power matrix as

$$\mathbf{P}_{\text{rec}} = \frac{2Z_\circ \lambda^2}{\eta^2} \text{ diag } \left[\mathbf{G}_r^T \cdot \bar{E} \cdot \bar{E}^\dagger \cdot \mathbf{G}_r^*\right] \ . \tag{3.15}$$

Referring back to (3.6), the electric current vector used for calculation of $\mathbf{G}_r$ is obtained by assumption of identical voltage sources with similar maximum available powers, P_{avs}.[4] It follows that

$$\mathbf{P}_{\text{rec}} = \frac{\lambda^2}{4\eta^2 \ P_{\text{avs}}} \text{ diag } \left[\mathbf{G}_r^T \cdot \bar{E} \cdot \bar{E}^\dagger \cdot \mathbf{G}_r^*\right] \tag{3.16}$$

in which we used [27, Equation (3.1)] for P_{avs}. The above expression should be compared with its counterpart in [27, Equation (3.6)] which holds for an arbitrary single-port antenna.

It is also instructive to know the received average power in terms of the multiport effective length matrix. Using (3.6) and (3.8) and after some manipulations, we arrive at

$$\mathbf{P}_{\text{rec}} = \frac{Z_\circ}{2} \text{ diag } \left[(\mathbf{Z} + \mathbf{Z}_\circ)^{-1} \ \mathbf{L} \cdot \bar{E} \cdot \bar{E}^\dagger \cdot \mathbf{L}^\dagger \ (\mathbf{Z} + \mathbf{Z}_\circ)^{-1^\dagger}\right] \tag{3.17}$$

wherein $\mathbf{Z}_\circ = Z_\circ \mathbf{I}$. Note that in equations (3.15)-(3.17) presented for the average received power, we dropped the arguments for the sake of conciseness in appearance. The advantage in using (3.17) compared to (3.16) shall soon be clarified.

Furthermore, it is also valuable to derive an expression of the received power for the general case of arbitrary complex terminations, $\mathbf{Z}_r$. Pursuing the same path as we followed to arrive at (3.15) leads to

$$\mathbf{P}_{\text{rec}} = \frac{2\lambda^2}{\eta^2} \ (\Re[\mathbf{Z}_r])^{-1} \text{ diag } \left[\mathbf{Z}_r \ \mathbf{G}_r^T \cdot \bar{E} \cdot \bar{E}^\dagger \cdot \mathbf{G}_r^* \ \mathbf{Z}_r\right] \ . \tag{3.18}$$

Or, alternatively in terms of the associated multiport effective length matrix,

$$\mathbf{P}_{\text{rec}} = \frac{1}{2} (\Re[\mathbf{Z}_r])^{-1} \text{ diag } \left[\mathbf{Z}_r \ (\mathbf{Z} + \mathbf{Z}_r)^{-1} \ \mathbf{L} \cdot \bar{E} \cdot \bar{E}^\dagger \cdot \mathbf{L}^\dagger \ (\mathbf{Z} + \mathbf{Z}_r)^{-1^\dagger} \ \mathbf{Z}_r{}^\dagger\right] \ . \tag{3.19}$$

[4] To read more about the maximum available power refer to Section 2.3.1 on page 14.

3.6 Multiport Effective Area

When it comes to receiving antennas' analysis, it is convenient to recall the notion of *effective area* of an antenna, A_e. Within the frame of multiport radiation terminals, an extended version of the foregoing quantity seems useful, which can best be called *multiport effective area*. In general, we can associate an *embedded effective area* to each port of a multiport antenna. Under matched polarisation constraint, it is defined as the ratio between the average power delivered to the load to the average power density of the incident EM wave.[5] By this definition, it should be evident that the terminating impedances at different ports affect this quantity. That is the reason why in case of a single-mode antenna, it is defined based on the conjugate matched terminations [28].[6]

However, from a practical standpoint, the concept of conjugate matched in a multiport antenna system is admittedly complex and cumbersome for implementation [32], [33]. Hence, we presumably narrow the definition of multiport effective area to the cases of matched terminating impedances.[7] Having this definition in mind, let us derive an expression for the multiport effective area matrix. For simplicity and to comply with the matched polarisation constraint, let us also assume a unipolarised incoming EM wave, *e.g.*, we have only a θ-polarised wave. In addition, the antennas have the same polarisation. Under this condition, the relation provided in (3.16) is useful. By virtue of the Poynting's vector, we can denote the average power density of the incoming wave from Ω direction in watts per square meters by

$$\mathcal{P}_i(\Omega) = \frac{1}{2\eta}|E_\theta(\Omega)|^2. \tag{3.20}$$

Using (3.17), the average received power becomes

$$\mathbf{P}_{\text{rec}} = \frac{\lambda^2}{2\eta\ P_{\text{avs}}}\ \mathcal{P}_i(\Omega)\ \text{diag}\left[\mathbf{G}_r^T(\Omega)\cdot\mathbf{G}_r^*(\Omega)\right]\ , \tag{3.21}$$

whence the multiport effective area comes to be

$$\mathbf{A}_e(\Omega) = \frac{\lambda^2}{2\eta\ P_{\text{avs}}}\ \text{diag}\left[\mathbf{G}_r^T(\Omega)\cdot\mathbf{G}_r^*(\Omega)\right]\ . \tag{3.22}$$

It is worthwhile finding $\mathbf{A}_e$ in terms of the embedded directivities. To do so, we can use the materials provided in Section 2.3.3, in particular the expression for the total embedded element radiation efficiency matrix (2.14). Subsequently, we can recast the embedded element pattern matrix in terms of the corresponding directivity matrix, $\mathbf{D}_r$. Recall that based on its definition[8], the directivity matrix is subject to

$$\text{diag}\left[\oint_{4\pi}\mathbf{D}_r^T(\Omega)\cdot\mathbf{D}_r^*(\Omega)\ d\Omega\right] = 4\pi\ \mathbf{I}_{n\times n}\ . \tag{3.23}$$

[5] To be precise, there is no unanimous definition for the effective area of an antenna in the literature. For instance, see [28, page 834] and [30, page 81].

[6] In [30], this particular assumption is made for what is called 'maximum effective area'.

[7] By matched terminating impedance we mean $Z_\circ$ terminating impedance, as used earlier.

[8] For instance, refer to the definition provided in [28, page 610] which is associated with single-port antennas. See also [30, Equation (2-16)].

In this way, we arrive at

$$\mathbf{A}_e(\Omega) = \frac{\lambda^2}{4\pi}\ \mathbf{e}_{\text{tot}} \cdot \text{diag}\left[\mathbf{D}_r^T(\Omega) \cdot \mathbf{D}_r^*(\Omega)\right]\ . \tag{3.24}$$

It is worth noting that $\mathbf{e}_{\text{tot}}$ in (3.24) owes its presence to the way we defined the multiport effective area. Had we defined it for multiport conjugate matched terminations, with no ohmic loss present, the aforementioned factor in (3.24) would disappear and a similar expression to its single-port counterpart in [30, Equation 2-110] would emerge. As a final point, using (3.17), we can further recast the multiport effective area matrix in terms of the corresponding multiport effective length matrix as

$$\mathbf{A}_e(\Omega) = \eta\ \mathbf{Z}_\circ \cdot \text{diag}\left[(\mathbf{Z}+\mathbf{Z}_\circ)^{-1}\ \mathbf{L}(\Omega) \cdot \mathbf{L}^\dagger(\Omega)\ (\mathbf{Z}+\mathbf{Z}_\circ)^{-1^\dagger}\right]\ . \tag{3.25}$$

In general, it is always advantageous to characterise the multiport antennas by their multiport effective length or open-circuit pattern compared to the embedded element pattern. The reason is that the former two parameters are independent of the terminating impedances and the maximum available power of the source by which the embedded patterns are simulated or measured. But, using the embedded element pattern requires the aforementioned extra information. Thus, formulations based on the multiport effective length or alternatively open-circuit pattern is apparently more useful. This is why the expression in (3.17) is preferable compared to that of (3.16).

3.7 Antennas in Multipath Environments

The beauty of electromagnetics comes from the fact that it is governed by a set of linear equations. This allows the concept of superposition to be applied. Therefore, in case we have multiple incoming EM waves incident on the multiport antenna structure, the received voltage signal is achieved by their superposition. In this particular case, in the presence of K number of incoming EM waves, the received voltage vector in (3.11) becomes

$$\bar{v}_r = \mathbf{Z}_r\ (\mathbf{Z}+\mathbf{Z}_r)^{-1}\ \sum_{k=1}^{K} \mathbf{L}(\Omega_k) \cdot \bar{E}(\Omega_k)\ . \tag{3.26}$$

In a rich multipath environment[9], where the probability of incoming waves from Ω direction is given by $\mathsf{P}(\Omega)d\Omega$, the expression in (3.26) can be rewritten as

$$\bar{v}_r = \mathbf{Z}_r\ (\mathbf{Z}+\mathbf{Z}_r)^{-1}\ \oint_{4\pi} \mathbf{L}(\Omega) \cdot \bar{E}(\Omega)\ \mathsf{P}(\Omega)\ d\Omega\ , \tag{3.27}$$

in which P is the probability density function of AoA for the incoming waves.[10] This is commonly considered as a characteristic of a multipath environment. Different models for the foregoing parameter have been proposed resembling a typical real multipath environment.

[9] For definition of a rich multipath environment refer to Chapter 6 on page 55.

[10] It is better to write $\mathsf{P}_{\theta,\psi}$. Even so, we preferably stick to P for simplicity.

3.8 EM Waves in Multipath Environments

As it is clear from (3.27), in multipath environments the received signals at the ports of a multiport antenna depend not only on the antenna's embedded radiation properties, but also on the characteristics of the incoming EM waves. Up to now, we have studied only the effects of radiation properties of the antennas upon the associated received signals. Yet, for a fair investigation, we also require a brief description and characterisation of the incoming EM waves, which are the main concerns of the following subsections.

3.8.1 Angle of Arrival Distribution

In its general treatment, distributions of AoA for two orthogonal polarisations, say vertical (*i.e.*, θ) and horizontal (*i.e.*, ψ) ones, are considered independently. In addition to that, AoA density functions for the azimuth plane, P_θ, as well as the elevation plane, P_ψ, may also be independent. That means,

$$\mathsf{P}(\Omega) = \mathsf{P}_\theta(\Omega)\ \mathsf{P}_\psi(\Omega)\ . \tag{3.28}$$

In a generic sense, from the random orientation of the terminal in the azimuth plane, the distribution of AoA for both polarisations can be presumably modelled by a uniform distribution [34], [35]. Yet, for the elevation plane, there is no unanimous agreement on the best model and it highly depends on the properties of the associated multipath area [34], [35].

Consider the latitude θ and longitude ψ coordinates of AoA. Typically, the probability density function for ψ can be uniform upon the range $[0, 2\pi]$. To address our concern about θ, let us first define its domain within $[0, \pi]$, *i.e.*, $\theta = \pi/2$ represents the azimuth plane. Several models have been introduced in the literature to fit the measured data best, among which the following models are more common: Gaussian [34], truncated Gaussian [36], uniform [22], truncated uniform [37], double exponential [35], Laplacian [35], rectangular [38], and finally sinusoidal density functions [38]. If we presume that the two random variables, θ and ψ, are independent, the joint probability density function of them complies with a certain format. Should we consider a uniform probability density for one of the angles, say $\mathsf{P}_\psi(\Omega) = 1/2\pi$, some probability density functions for θ can be written as:

- Uniform

$$\mathsf{P}_\theta(\Omega) = \mathrm{C}\ \sin(\theta) \qquad\qquad \theta \in [0\ ,\ \pi] \tag{3.29}$$

- Gaussian

$$\mathsf{P}_\theta(\Omega) = \mathrm{C}\ \exp\left(-\frac{(\theta-\theta_m)^2}{2\sigma^2}\right)\ \sin(\theta) \qquad \theta \in [0\ ,\ \pi] \tag{3.30}$$

- Double exponential

$$\mathsf{P}_\theta(\Omega) = \begin{cases} \mathrm{C}\ \exp\left(-\frac{\sqrt{2}|\theta-\theta_m|}{\sigma^-}\right)\ \sin(\theta) & \theta \in [\theta_m\ ,\ \pi] \\ \mathrm{C}\ \exp\left(-\frac{\sqrt{2}|\theta-\theta_m|}{\sigma^+}\right)\ \sin(\theta) & \theta \in [0\ ,\ \theta_m] \end{cases} \tag{3.31}$$

which are the most common distributions in the literature. In the above equations, θ_m stands for the angle of arrival in which the number of incident waves is the highest. Parameters σ, σ^- and σ^+ indicate the spread of the distributions around θ_m. The constant C, which is different for different cases, is determined through the general restriction on probability density functions, which reads

$$\oint_{4\pi} \mathsf{P}(\Omega)\ d\Omega = 1\ .$$

There is no hindrance in expanding the given equations to the corresponding truncated ones. For that purpose, only the domain of θ has to be revised and accordingly the associated constants. Besides this, note that the Laplacian probability density function is a particular case of double-exponential density function in which σ^+ and σ^- are equal.

It is worth injecting a point of caution here about the joint density function of θ and ψ angles. Bear in mind that the conditional density functions of θ given ψ, and ψ given θ are subject to *Borel's paradox* and shall be paid ultimate care for cases in which the distributions in azimuth and elevation planes are both nonuniform [39, Problem 4.6.1]. It is also rewarding to note that concentrating solely on the distribution of AoA in an environment is obviously lacking inasmuch as it does not take into account the orientation of the radiation terminal having presumably a nonuniform gain pattern. Therefore, for any single orientation of the terminal an independent characterisation must be made, which gives rise to a new different set of gauges.[11] The latter has created a trend for engineers to seek a reference environment. In general, for a viewer on the coordinates of the multiport antenna, the AoA distribution for different orientations of it could *on average* be fairly represented by a uniform function.

3.8.2 Field Distribution of the Incoming EM Waves

In addition to AoA distribution, as long as the characteristics of the incoming EM waves are concerned, there shall be polarisation as well as amplitude and phase description. In an uncorrelated multipath environment[12], cross polarisation ratio (XPR) denoted by χ is defined as the ratio between the averaged received powers by an isotropic $\theta-$polarised ideal antenna and that of a $\psi-$polarised one [34]. For small moving multiport antennas, since the antenna can have any arbitrary orientation in space, the same kind of reasoning given for an average AoA distribution can be applied equally well here too. Hence, the notion of balanced polarisation has been coined to indicate incoming waves of arbitrary polarisations, *e.g.*, $\chi = 0$ dB. The two aforementioned features of an uncorrelated multipath environment, *i.e.*, uniform density function of AoA and balanced polarisation, establish the main characteristics of a reference environment referred to as *isotropic* environment. This particular environment achieves a practical appeal mostly due to the fact that it can be almost precisely emulated in a fine reverberation chamber.

To address our curiosity about the nature of the coming EM waves, *e.g.*, distribution of their amplitudes and phases, we refer to certain mechanisms whereby the EM propagating

[11] In the subsequent chapters we find more about these gauges.

[12] For the definition of uncorrelated multipath environment refer to Section 3.8.3 on the next page.

waves interact with the surrounding objects. In a multipath environment, waves can redirect towards the receiver antenna by *reflection* through large smooth objects or by *scattering* through small objects or rough surfaces. Moreover, the replicas of the incoming waves can also reach the receiver antennas through *diffraction* around the sharp edges or by *transmission* through the objects. For convenience in further analyses, let us resort to simplified statistical models. It is important to remember that in the frame of this thesis, we restrict ourselves to the small-scale fading.[13]

Recall that in a multipath environment, the incident electric fields could presumably be random variables of independent identical distributions. Regardless of the precise forms of their distribution functions, based on the central limit theorem, the superposition of all these incoming waves eventually yields complex Gaussian random signals at different ports [39]. Many experimental results show that the amplitudes of the received voltage signals across all ports comply with Rayleigh distribution [3, Section 1.1]. Therefore, for empirical reasons alone, having complex Gaussian random signals across the ports of antennas in multipath environments is justified. It is a question of interest to know how many random incoming waves are required for convergence in received signals' distributions. Yet, somewhat too formal in the frame of this thesis.[14] To solely focus on the effects of antenna systems upon the overall performance, and for the sake of convenience in analysis, we presume that the random incoming EM waves in both θ and ψ polarisations are zero-mean complex Gaussian random variables.

3.8.3 Polarisation Matrix

To mathematically model the time-average incoming EM waves of certain characteristics in a multipath, we use the *polarisation matrix* [40]. For random incoming EM waves from Ω and Ω' angular directions, the polarisation matrix $\mathbf{\Gamma}$ in watts per square meters is defined as

$$\mathbf{\Gamma}(\Omega, \Omega') = \frac{1}{2\eta}\, \mathbb{E}[\bar{E}(\Omega) \cdot \bar{E}^{\dagger}(\Omega')] \ . \tag{3.32}$$

in which $\mathbb{E}$ operates upon different time samples or realisations. In other words,

$$\mathbf{\Gamma}(\Omega, \Omega') = \begin{bmatrix} \Gamma_{\theta\theta}(\Omega, \Omega') & \Gamma_{\theta\psi}(\Omega, \Omega') \\ \Gamma_{\psi\theta}(\Omega, \Omega') & \Gamma_{\psi\psi}(\Omega, \Omega') \end{bmatrix} \ , \tag{3.33}$$

wherein

$$\Gamma_{\theta\psi}(\Omega, \Omega') = \frac{1}{2\eta}\, \mathbb{E}[E_{\theta}(\Omega) E_{\psi}(\Omega')] \ , \tag{3.34}$$

as defined in [40]. If the incoming EM waves from different AoAs are uncorrelated and the EM waves of different polarisation from the same AoAs are also uncorrelated, the off-diagonal entries in $\mathbf{\Gamma}$ vanish. The resultant can further be recast as

$$\mathbf{\Gamma}(\Omega) = \Gamma_{\psi\psi}(\Omega) \begin{bmatrix} \chi(\Omega) & 0 \\ 0 & 1 \end{bmatrix} \tag{3.35}$$

[13] It is also known as fast fading, microscopic fading, and narrowband fading. For more information on this subject, refer to [6, Section 2.2.2] or [4, Section 3.2].

[14] The interested reader is referred to [39, Chapter 7]. For definition of convergence in distribution, refer to Definition 1(d) in [39, Section 7.2].

with $\Gamma_{\psi\psi}(\Omega)$ being the power density per steradic square of the incoming waves in $\psi-$polarisation. The parameter χ in (3.35) is the XPR as defined in Section 3.8.2, which signifies the amount of polarisation imbalance of the incoming EM waves [34]. That is,

$$\chi(\Omega) = \frac{\Gamma_{\theta\theta}(\Omega)}{\Gamma_{\psi\psi}(\Omega)} \ . \tag{3.36}$$

A multipath environment whose polarisation matrix regardless of AoA is diagonal is called an *uncorrelated* multipath environment. In other words, in an uncorrelated multipath environment, the EM incoming waves are spatially uncorrelated and those of the same AoA but different polarisations are also uncorrelated. Bear in mind that the isotropic environment, as defined in the preceding section, is an uncorrelated environment of uniform AoA distribution and balanced polarisation. In contrast, in a correlated multipath environment, the polarisation matrix is in general a non-diagonal matrix being normally a function of angular direction.

3.9 Summary

In this chapter, we have dealt with certain important parameters which play crucial roles in the upcoming chapters. The notion of multiport effective length of the antennas have been introduced and linked to the more known parameters like embedded far-field patterns and open-circuit patterns. We have shown the effects of terminating impedances on the received signals in a compact multiport antenna system. Some precise expressions for the average received power in these systems have also been presented. This leads to the notion of multiport effective area of a radiation system. Tantamount to its single-port counterpart, we derive a general relation between the multiport effective lengths and areas in a multiport antenna system. Some words have been dedicated on how we could model the incoming EM waves in a multipath scenario. In particular, we have talked about the AoA distributions and the distribution of the incoming EM waves. To mathematically model the potential link between the incoming waves of different AoAs and polarisations, we use the concept of polarisation matrix with a slight modification to its original form. The latter parameter helps us to clearly distinguish between three types of multipath environments as correlated, uncorrelated, and isotropic. The results presented here are important for the rest of this thesis.

Chapter 4

Performance Metrics in Multipath Environments

It is quite well known that the performance of a wireless communication system, *e.g.*, link quality, depends to a considerable extent upon the received SNR. The SNR in turn before anything relies on the gain of the antennas involved which plays a crucial role in the link budget. The antenna gain meant here is not considered towards a single direction in which the received power is precisely governed by Frii's formula [30]. Rather, it concerns an area in space from which the random incoming waves are more probable. The engineers' tendency to quantify antennas' receiving capability in a multipath environment has led to a significant performance metric called *mean effective gain* (MEG). Besides MEG, another major performance metric in a multiport antenna system is the *spatial correlation*. Interestingly, the original source of both foregoing performance metrics is the covariance matrix of the received signals in multipath environments. The main goal in this chapter is to discuss and provide some precise expressions for the covariance matrix with a proper normalisation. Many of the essential features of this discussion are used in [Paper B]. The formulas enable us to distinctly reveal the influence of terminating impedances, radiation efficiencies, and shapes of the embedded far-field patterns upon the covariance matrix. This can be used to extend the definitions of MEGs and mean effective directivities (MEDs) to hold also in correlated multipath environments.

4.1 Ideal Isotropic Reference Antennas

Before entering to the heart of our derivation, we first need to precisely describe the type of the antenna used for normalisation purposes known as the reference antenna. In [34], the author opted for two hypothetical ideal isotropic antennas with vertical and horizontal polarisations. The same kind of antenna does more than suffice here too. In other words, we choose an ideal dual-port dual-polarised isotropic antenna as the reference antenna in the frame of our analysis. In this section, we first elaborate the electromagnetic specifications of such an ideal reference antenna and subsequently derive some compact expressions for the received power at its ports in different types of multipath environments.

4.1.1 Electromagnetic Properties of Reference Antenna

The ultimate goal for using an ideal reference antenna is to find the maximum available power in a multipath scenario. For this purpose, the terminating impedances at the ports of this dual-polarised dual-port antenna should be conjugate matched to its input impedances. For the sake of simplicity, let us presumably assume that the input impedance matrix of this ideal reference antenna is the same as the characteristic impedance matrix of the system. That is,

$$\mathbf{Z}_{\text{ref}} = \mathbf{Z}_{\circ} \ .$$

Furthermore, let us associate each port to a certain polarisation. Under these constraints and with some straightforward manipulations, it follows that the multiport effective length matrix of this ideal dual-polarised reference antenna is

$$\mathbf{L}_{\text{ref}}(\Omega) = -j\lambda \sqrt{\frac{Z_{\circ}}{\eta\pi}} \cdot \mathbf{I}_{2\times 2} \ , \tag{4.1}$$

with λ being the operational wavelength and η the intrinsic impedance of the medium. The reference antenna with the above characteristics when matched terminated *i.e.*, $\mathbf{Z}_r = \mathbf{Z}_{\circ}$, realises the maximum available power in a multipath environment.

4.1.2 Average Received Power by Reference Antenna

Considering the expressions for received average power in Section 3.5 and referring to Section 3.8.3, we are able to provide an expression for the total received power at the ports of our ideal reference antenna. Let us pursue our goal under presumption of first uncorrelated and then more general cases of correlated multipath environments.

Uncorrelated Multipath Environments

Since the terminating impedances of our reference antenna are the characteristic impedance of the system, we can use Equation (3.17). Here, the average received power can be obtained by averaging over all possible incoming waves in each scenario. This is done by virtue of the expectation operator as defined in Section 3.8.3. Recall that in uncorrelated multipath environments, as it is the case here, the polarisation matrix, $\mathbf{\Gamma}$, is a diagonal matrix.[1] Under presumption of zero-mean complex Gaussian random variables and by virtue of $\mathbf{\Gamma}$, we can show that the total average received power at the ports of our reference antenna P_{ref} is

$$P_{\text{ref}} = \frac{\lambda^2}{4\pi} \ \text{tr} \left[\oint_{4\pi} \mathbf{\Gamma}(\Omega) \ \mathsf{P}(\Omega) \ d\Omega \right] \ , \tag{4.2}$$

wherein 'tr' stands for the trace of its argument. As an interesting choice, if in an uncorrelated multipath environment the polarisation matrix is independent of AoA, the expression for total average received power simplifies to

$$P_{\text{ref}} = \frac{\lambda^2}{4\pi} \Gamma_{\psi\psi} \ (1+\chi) \ . \tag{4.3}$$

[1] In this case, an expression for $\mathbf{\Gamma}$ has been provided in (3.35).

Remember that in (4.3), χ stands for XPR and $\Gamma_{\psi\psi}$ is the power density of the incoming EM waves of horizontal polarisation. Also, note that χ in (4.3) is a constant independent of AoA. In an isotropic environment, which is a particular case of uncorrelated environments, the total average received power by this ideal reference antenna can be obtained by plugging $\chi = 1$ into (4.3).

Correlated Multipath Environments

In the preceding section, we restricted ourselves to uncorrelated multipath environments in which the incoming EM waves are spatially uncorrelated both in polarisation and in AoA. Conversely, in a general multipath circumstance, neither of the aforementioned condition holds. Thus, it is necessary for us to provide an expression covering the cases in which we have correlated multipath environments.

To that end, there are two concerns. The first one is associated with the probability density function. Note that, in this general condition, the incoming waves from different AoAs in space can be correlated. Thus, the probability density function of the incoming waves depends on a pair of random variables, say Ω' and Ω, rather than a single variable. This is described by joint probability density function, denoted by $\mathsf{P}(\Omega', \Omega)$, and is very much in harmony with what has been presented for uncorrelated multipath case. To elaborate more, in an uncorrelated multipath environment, the incoming waves from Ω and Ω' are independent. Thus, for the corresponding density function we have $\mathsf{P}(\Omega, \Omega')\delta(\Omega' - \Omega)$.[2] For simplicity, the latter expression has been already shown by a single argument, *i.e.*, $\mathsf{P}(\Omega)$.

In the current framework, we are further concerned with the non-diagonal nature of the polarisation matrix in correlated multipath environments. In this general circumstance, the total received power cannot be the sum of the average received powers at both ports. This is because the signals at the ports of our reference antenna are correlated. To conquer this issue, we need to use the Frobenius norm of the resultant average received power matrix. Considering all the aforementioned points, we can obtain the total average received power in correlated multipath environments by

$$P_{\text{ref}} = \frac{\lambda^2}{4\pi} \left\| \iint_{4\pi} \mathbf{\Gamma}(\Omega', \Omega)\ \mathsf{P}(\Omega', \Omega)\ d\Omega' d\Omega \right\|_{\text{F}}, \tag{4.4}$$

where subscript F indicates the Frobenius norm.

At this point, let us spend a few moments and look upon the presented procedure from a different standpoint. We have attained the average received power by our reference antenna for uncorrelated (4.2) and correlated (4.4) multipath environments by averaging the received power over different AoAs. Nevertheless, we could have achieved them far simpler by virtue of the multiport effective area provided in (3.24). Recall that the incoming EM waves in this multipath are zero-mean complex Gaussian random variables. Therefore, the average received power can be given as a product of the average available radiation power density in the multipath and the multiport effective area of the reference antenna. To find the multiport effective area matrix for this ideal isotropic reference

[2] The symbol δ denotes the Dirac delta function.

antenna, replace $\mathbf{D}_r$ and $\mathbf{e}_{\text{tot}}$ in (3.24) by $\mathbf{I}_{2\times2}$ to arrive at

$$\mathbf{A}_e(\Omega) = \frac{\lambda^2}{4\pi} \cdot \mathbf{I}_{2\times2} \qquad \text{(Ideal Reference Antenna)} \ . \tag{4.5}$$

Using (4.5), the total received power by this reference antenna is the same as in (4.4). For this reason, in this thesis the received power by our ideal reference antenna is also referred to as available power from the multipath environment.

4.2 Open-Circuit Covariance Matrix

Perhaps, one of the most significant parameters in a multiport antenna system is the *open-circuit covariance matrix*. To describe how we evaluate this parameter, let us first remind ourselves that we are restricted to zero-mean complex Gaussian random incoming EM waves. Recall also that the open-circuit received voltage vector at the ports of a multiport antenna in a multipath scenario has been signified by $\bar{v}_\circ$ in Section 3.2. The open-circuit covariance matrix denoted by $\mathbf{C}_\circ$ in volts square is obtained through

$$\mathbf{C}_\circ = \mathbb{E}[\bar{v}_\circ \bar{v}_\circ^\dagger] \ . \tag{4.6}$$

The foregoing covariance matrix plays a significant role for the rest of this chapter and deserves a proper regard. In what follows, we derive some expressions for the normalised open-circuit covariance matrix in isotropic, uncorrelated and correlated multipath environments.

4.2.1 Covariance in Isotropic Multipath Environments

Up until now, the reader should be familiar with the properties of an isotropic multipath environment. In brevity, in this particular environment, we have $\mathsf{P} = \frac{1}{4\pi}$ and $\chi = 0$ dB. The open-circuit voltage has been treated in Section 3.4, for which we can write

$$\bar{v}_\circ = \oint_{4\pi} \mathbf{L}(\Omega) \cdot \bar{E}(\Omega)\ \mathsf{P}(\Omega)\ d\Omega \ , \tag{4.7}$$

which is only credible in uncorrelated multipath scenarios. Inserting the foregoing parameters in (4.7) and using the polarisation matrix concept, we arrive at the open-circuit covariance matrix in volts square as

$$\mathbf{C}_\circ = \frac{2\eta}{4\pi}\ \Gamma_{\psi\psi} \oint_{4\pi} \mathbf{L}(\Omega) \cdot \mathbf{L}^\dagger(\Omega)\ d\Omega \ . \tag{4.8}$$

To normalise the above expression we need to use the total average received power at the ports of our ideal reference antenna in the same multipath environment. This has already been treated in Section 4.1.2. Using the corresponding expression in (4.4), we can normalise (4.8) to reach to

$$\mathbf{C}_{\circ_n} = \frac{\eta}{\lambda^2} \oint_{4\pi} \mathbf{L}(\Omega) \cdot \mathbf{L}^\dagger(\Omega)\ d\Omega \qquad \text{(Isotropic Multipath)} \ , \tag{4.9}$$

in which the subindex n indicates the normalised open-circuit covariance matrix in ohms. Note that this subscript solely signifies the normalised parameters and may not be confused with the number of ports which is shown by the same notation.

4.2.2 Covariance in Uncorrelated Multipath Environments

In a tantamount way to the previous section, we can derive an expression for the open-circuit covariance matrix in a general uncorrelated multipath environment. Recall that in uncorrelated multipath environments, the polarisation matrix is diagonal. To find this normalised matrix, we use the expressions in (4.7) and the reference power in (4.2). After some manipulations, we arrive at

$$\mathbf{C}_{\circ_n} = \frac{2\eta}{P_{\text{ref}}} \oint_{4\pi} \mathbf{L}(\Omega) \cdot \mathbf{\Gamma}(\Omega) \cdot \mathbf{L}^{\dagger}(\Omega)\ \mathsf{P}(\Omega)\ d\Omega \qquad \text{(Uncorrelated Multipath)}\ , \tag{4.10}$$

which is generally valid in uncorrelated multipath environments. In case the power density of the incoming waves in both polarisations is independent of the angular direction, we can further simplify the above expression as follows:

$$\mathbf{C}_{\circ_n} = 4\pi\ \frac{2\eta}{\lambda^2} \oint_{4\pi} \mathbf{L}(\Omega) \cdot \begin{bmatrix} \frac{\chi}{1+\chi} & 0 \\ 0 & \frac{1}{1+\chi} \end{bmatrix} \cdot \mathbf{L}^{\dagger}(\Omega)\ \mathsf{P}(\Omega)\ d\Omega\ . \tag{4.11}$$

4.2.3 Covariance in Correlated Multipath Environments

The points used for calculation of the average received power in Section 4.1.2 can be equally applied for the current purpose. The expression used in calculation of the open-circuit covariance matrix in (4.8), which is credible for uncorrelated multipath environments, can be readily extended to hold for correlated multipath environments. Doing so, we can write

$$\mathbf{C}_{\circ} = 2\eta \iint_{4\pi} \mathbf{L}(\Omega') \cdot \mathbf{\Gamma}(\Omega', \Omega) \cdot \mathbf{L}^{\dagger}(\Omega)\ \mathsf{P}(\Omega', \Omega)\ d\Omega' d\Omega \qquad \text{(Correlated Multipath)}\ . \tag{4.12}$$

We have already the necessary ingredient in access to properly normalise the above covariance matrix. Using the general average received power by our ideal reference antenna in (4.4), the expression in (4.12) is normalised to yield

$$\mathbf{C}_{\circ_n} = 4\pi\ \frac{2\eta}{\lambda^2}\ \frac{\displaystyle\iint_{4\pi} \mathbf{L}(\Omega') \cdot \mathbf{\Gamma}(\Omega', \Omega) \cdot \mathbf{L}^{\dagger}(\Omega)\ \mathsf{P}(\Omega', \Omega)\ d\Omega' d\Omega}{\left\| \displaystyle\iint_{4\pi} \mathbf{\Gamma}(\Omega', \Omega)\ \mathsf{P}(\Omega', \Omega)\ d\Omega' d\Omega \right\|_{\text{F}}} \qquad \text{(Correlated Multipath)}\ . \tag{4.13}$$

The above expression is a general expression and can reduce to its counterparts in uncorrelated multipath environments (4.10) and isotropic multipath environments (4.9). We shall soon show that this expression is a central source for different important performance metrics.

4.3 Terminated Covariance Matrix

Consider the received voltage vector at the terminated ports of a multiport antenna in a multipath scenario, denoted by $\bar{v}_r$. Again, limiting ourselves to zero-mean complex Gaussian random incoming waves, the covariance of the received voltage signals averaged over sufficient number of realisations or time can be obtained by $\mathbb{E}[\bar{v}_r \bar{v}_r^{\dagger}]$.

Since the covariance matrix is going to be normalised by the received power of the ideal reference antenna in the same environment, it is most reasonable to express it in watts. Recall that in the preceding section, we could not express the open-circuit covariance matrix in watts since in the open-circuit circumstance, no power can be received. Nevertheless, that is not the case here. To presumably give the covariance matrix a power nature, let us define the *terminated covariance matrix* in watts, $\mathbf{C}_r$, as

$$\mathbf{C}_r = \frac{1}{2}\, \Re[\mathbf{Z}_r]^{-\frac{1}{2}} \cdot \mathbb{E}[\bar{v}_r \bar{v}_r^{\dagger}] \cdot \Re[\mathbf{Z}_r]^{-\frac{1}{2}} \ , \tag{4.14}$$

where $\Re$ returns the resistive part of its argument. When normalised, the above expression yields a dimensionless normalised terminated covariance matrix.

4.3.1 Terminated versus Open-circuit Covariance Matrices

To find a link between the terminated covariance matrix and its open-circuit counterpart, we can use Equation (3.9). Doing so, we readily reach to

$$\mathbf{C}_r = \frac{1}{2}\, \Re[\mathbf{Z}_r]^{-\frac{1}{2}}\ \mathbf{Z}_r(\mathbf{Z}+\mathbf{Z}_r)^{-1}\ \mathbf{C}_{\circ}\ (\mathbf{Z}+\mathbf{Z}_r)^{-1^{\dagger}} \mathbf{Z}_r^{\dagger}\ \Re[\mathbf{Z}_r]^{-\frac{1}{2}}\ . \tag{4.15}$$

This is a general relation between these two important covariance matrices. As evident in this relation, the open-circuit covariance matrix is the core of the terminated covariance matrix. To find the normalised terminated covariance matrix, it is sufficient to replace $\mathbf{C}_{\circ}$ in (4.15) with the desired normalised open-circuit covariance. For instance, in isotropic and uncorrelated multipath environments, $\mathbf{C}_{\circ_n}$ in (4.9) and (4.10) should respectively substitute for $\mathbf{C}_{\circ}$ in (4.15). And, of course, the most general expression for the normalised terminated covariance matrix, $\mathbf{C}_{r_n}$, is obtained through

$$\mathbf{C}_{r_n} = \frac{1}{2}\, \Re[\mathbf{Z}_r]^{-\frac{1}{2}}\ \mathbf{Z}_r(\mathbf{Z}+\mathbf{Z}_r)^{-1}\ \mathbf{C}_{\circ_n}\ (\mathbf{Z}+\mathbf{Z}_r)^{-1^{\dagger}} \mathbf{Z}_r^{\dagger}\ \Re[\mathbf{Z}_r]^{-\frac{1}{2}}\ , \tag{4.16}$$

with $\mathbf{C}_{\circ_n}$ provided in (4.13). We stress that $\mathbf{C}_{r_n}$ is dimensionless. This is a central expression which is frequently referred to in the following sections.

4.4 Mean Effective Gain

In link budget calculation the received SNR is a key parameter, which is normally used for signals in baseband domain, *i.e.*, after detection.[3] A more precise term from an RF engineer standpoint is carrier-to-noise ratio. Nevertheless, to be in harmony with the literature, let us stick to the term SNR. Regarding the noise in the receiver, it is assumed that the antenna noise is negligible compared to the receiver noise. By this presumption, the receiver SNR becomes directly proportional to the average received power at the ports of the antenna system. Hence, it is more comfortable for further analysis. Basically, the ability of an antenna system to catch available EM power in a multipath environment is

[3] The Signal to Interference plus Noise Ratio (SINR) is also of interest which is not addressed here.

quantified by MEG. This parameter has long played a significant role in characterisation of antennas in multipath environments and is thus one of the major concerns of this chapter.

The notion of using average received power at the port of a terminal in a multipath environment for its characterisation dates back to 1977 [41]. The authors in this paper proposed an experimental method for evaluating the performance efficiency of antennas in a multipath environment. In this method, the mean received power of both an unknown antenna and a reference antenna were obtained over ideally similar multipath scenarios. The ratio between these average received powers formed what has henceforth been universally referred to as MEG.

Later, T. Taga analytically generalised the aforementioned concept and formulated the MEG as a function of AoA distribution and antenna radiation patterns [34]. A major advantage affiliated with this formulation was that it alleviated the burden of measurements for MEG in certain multipath environments. The basis of Taga's closed-form expression for MEG resides on the study performed by Yeh [3, pages 133-140]. In his study, Yeh looked upon the foregoing case from a time-domain standpoint and started with voltage across the terminating impedance and presumably approximated it with a zero-mean complex Gaussian random variable. Subsequently, by virtue of the autocorrelation function of this voltage signal, the associated average power was evaluated. Under certain constraints, for instance, independent incoming EM waves of different polarisations and spatially independent EM waves of similar polarisations[4], the corresponding expression was cast to embody the role of power gain pattern of the antenna.

The main shortcoming concerning the aforementioned formulation is that it does not properly take into account the matching efficiency as well as radiation efficiency of the antennas. In particular, the constraint imposed by [3, Equation (3.1-23)][5] creates an ambiguity on the correct use of *power gain pattern* as an academic term.[6] This issue has also leaked to MEG formulation by Taga [34, Equation (6)] and thus stands a concern which shall be clarified in a moment. Furthermore, the available formulation belongs to single-port antennas. However, based on the analysis presented so far, we have all the necessary tools for reformulation of MEGs for a multiport antenna system. In particular, since the basis of our approach presented in the preceding sections is different from that of Yeh [3, Chapter 3], it bestows considerable insight into the concept of MEG and in general radiation performance of multiport antennas in multipath environments.

4.4.1 Formulation of Mean Effective Gain

MEG, as mentioned, is the ratio between the received powers across different ports of a multiport antenna and that of an ideal isotropic dual-port dual-polarised reference antenna in ideally similar multipath environments. Associated with each port, there comes an MEG. Therefore, in a multiport antenna system, the MEGs can be collectively represented by a diagonal MEG matrix, denoted by $\mathbf{M}_{\mathrm{G}}$. Recall that the diagonal entries in the terminated covariance matrix is the average received power at the corresponding ports in a multipath environment. According to the foregoing definition, when normalised

[4] Recall the properties of an uncorrelated multipath environment from Section 3.8.3 on page 26.
[5] Also, check [34, Equation (4)].
[6] Find more about power gain pattern and radiation intensity in [30, Section 2.4].

properly, these entries yield the MEGs. Hence, the MEGs are simply obtained by

$$\mathbf{M}_{\text{G}} = \text{diag}\left[\mathbf{C}_{r_n}\right] \ , \tag{4.17}$$

wherein $\mathbf{C}_{r_n}$ is provided in (4.16). As a point of caution, it should be evident that MEG is undefined for the open-circuit multiport system.

Thus far, we have formulated the covariance matrices and consequently MEGs based on the multiport effective length matrix. However, from a pedagogical standpoint, it might be also advantageous to provide alternative expressions in terms of the embedded element far-field patterns. This is done in the following short subsections. Bear in mind that these formulas render the same results as that of (4.17) and are just some alternative representations of it.

4.4.2 MEGs in Isotropic Environments

Using the expressions in (4.9), (4.16), (4.17), and further applying (3.6)-(3.8), we can recast the MEG matrix in isotropic environments in terms of the embedded far-field pattern. For the time being, without loss of generality, let us limit ourselves to matched terminated impedances, *i.e.*, $\mathbf{Z}_r = \mathbf{Z}_\circ$. The result is as follows

$$\mathbf{M}_{\text{G}} = \frac{2Z_\circ}{\eta} \ \text{diag}\left[\oint_{4\pi} \mathbf{G}_r^T \cdot \mathbf{G}_r^* \ d\Omega\right] \ . \tag{4.18}$$

Remembering the materials provided in Section 2.3, the above expression seems quite familiar. Identifying the similar terms from (2.14) in the above expression leads to a simple equivalence as follows:

$$\mathbf{M}_{\text{G}} = \frac{1}{2} \ \mathbf{e}_{\text{tot}} \ , \tag{4.19}$$

which is already known. The above equivalence was anticipated in [42] and subsequently demonstrated in [43]. Table 1 in [44] indirectly shows the links between MEGs and the total embedded element efficiencies with regards to the selected reference antenna.

4.4.3 MEGs in Uncorrelated Multipath Environments

We reiterate that MEGs in an uncorrelated multipath environment can be achieved from (4.16) with $\mathbf{C}_{\circ_n}$ given in (4.10). Nevertheless, to provide a similar expression to the one offered by Taga in [34, Equation (6)], let us further assume that the XPR is independent of the AoAs. Pursuing the same path as before, after some manipulations, we arrive at

$$\mathbf{M}_{\text{G}} = \frac{16\pi}{\eta} \ \Re[\mathbf{Z}_r]^{-1} \ \text{diag}\left[\mathbf{Z}_r \oint_{4\pi} \mathbf{G}_r^T \cdot \begin{bmatrix} \frac{\chi}{1+\chi} & 0 \\ 0 & \frac{1}{1+\chi} \end{bmatrix} \cdot \mathbf{G}_r^* \ \mathsf{P} \ d\Omega \ \mathbf{Z}_r^\dagger\right] \ . \tag{4.20}$$

4.4.4 MEGs in Correlated Multipath Environments

In a much similar way, we can rewrite an alternative expression for MEG in correlated environments in terms of the embedded far-field pattern matrix. Let us again restrict ourselves to the case of $\mathbf{Z}_r = \mathbf{Z}_\circ$. Without spending more time, the expression is directly given as

$$\mathbf{M}_{\text{G}} = \frac{4Z_\circ\lambda^2}{\eta\ P_{\text{ref}}}\ \text{diag}\left[\iint_{4\pi} \mathbf{G}_r^T(\Omega')\mathbf{\Gamma}(\Omega',\Omega)\mathbf{G}_r^*(\Omega)\ \mathsf{P}(\Omega,\Omega')\ d\Omega' d\Omega\right]\ , \tag{4.21}$$

wherein P_{ref} is provided in (4.4). To the best of our knowledge, this is the first time that MEG is formulated for general cases of correlated multipath environments.

4.5 Mean Effective Directivity

It is of significance to remember that the normalised terminated covariance matrix and hence the different performance metrics extracted from it contain valuable information. For instance, information about the multipath environments, shapes of the embedded patterns as well as the total radiation efficiencies of the multiport antennas are inherent in a terminated covariance matrix. To better understand the performance mechanism of a multiport antenna design, it could be a privilege for engineers to further separate out the impact of radiation efficiencies of antennas. The latter created a trend in engineers coining the notion of MED. To derive some expression for MEDs we refer to the results presented in Section 4.4.1. First let us specify a few properties of the multiport embedded directivity matrix, $\mathbf{D}_r$, which is a $2 \times n$ matrix associated with an n-port antenna system. The multiport embedded directivity matrix is a function of angular direction and proportional to the embedded far-field pattern matrix. Moreover, it is subject to (3.23) for its normalisation.

For the sake of simplicity in appearance, in what follows we choose $\mathbf{Z}_r = \mathbf{Z}_\circ$ in purpose. A note of caution must be injected here. Bear in mind that the relation between the multiport directivity and embedded pattern matrices are different from the link between directivity and power gain pattern shown in [30, Section 2.7]. Thus, identical notations for those of [30] and the ones introduced here should not be a source of confusion.

4.5.1 MEDs in Uncorrelated Multipath Environments

Consider the expression in (4.20). We can recast this expression in terms of the embedded directivity matrix, $\mathbf{D}_r$. Doing so, under the constraint imposed by (3.23) and after some algebra, we come to

$$\mathbf{M}_{\text{G}} = \mathbf{e}_{\text{tot}} \cdot \text{diag}\left[\oint_{4\pi} \mathbf{D}_r^T \cdot \begin{bmatrix} \frac{\chi}{1+\chi} & 0 \\ 0 & \frac{1}{1+\chi} \end{bmatrix} \cdot \mathbf{D}_r^*\ \mathsf{P}\ d\Omega\right]\ . \tag{4.22}$$

whence the diagonal MED matrix, $\mathbf{M}_{\text{D}}$, can be identified as

$$\mathbf{M}_{\text{D}} = \text{diag}\left[\oint_{4\pi} \mathbf{D}_r^T \cdot \begin{bmatrix} \frac{\chi}{1+\chi} & 0 \\ 0 & \frac{1}{1+\chi} \end{bmatrix} \cdot \mathbf{D}_r^* \; \mathsf{P} \; d\Omega\right] \; . \tag{4.23}$$

As long as there is coupling among the radiation elements in a multiport antenna system, the multiport MED matrix depends on the terminating impedances too. This corresponds to a non-diagonal $\mathbf{Z}$ matrix for a multiport radiation system. However, the impact of total embedded radiation efficiencies are excluded from $\mathbf{M}_{\text{D}}$. Recall also that the total embedded element efficiency at each antenna port contains information about the multiport matching efficiency and the associated embedded ohmic loss.[7]

4.5.2 MEDs in Correlated Multipath Environments

Consider Equation (4.21). Recasting the embedded far-field patterns in terms of the corresponding multiport directivity matrix yields a possibility to factor out the total embedded element efficiency matrix. Doing so, and after some manipulations, we derive a general expression for $\mathbf{M}_{\text{D}}$ in correlated multipath environments as follows:

$$\mathbf{M}_{\text{D}} = \text{diag}\left[\frac{\oint_{4\pi} \mathbf{D}_r^T(\Omega') \cdot \mathbf{\Gamma}(\Omega', \Omega) \cdot \mathbf{D}_r^*(\Omega) \; \mathsf{P}(\Omega', \Omega) \; d\Omega' d\Omega}{\left\| \iint_{4\pi} \mathbf{\Gamma}(\Omega', \Omega) \; \mathsf{P}(\Omega', \Omega) \; d\Omega' d\Omega \right\|_{\text{F}}}\right] \; . \tag{4.24}$$

To the extent of our knowledge, this is the first time a compact expression for calculation of MED in correlated environments is derived. We further can show that there is a straightforward relation between the MEG and MED matrices. Regardless of properties of the multipath environments, the two forgoing metrics are linked through

$$\mathbf{M}_{\text{G}} = \mathbf{e}_{\text{tot}} \cdot \mathbf{M}_{\text{D}} \; . \tag{4.25}$$

This clearly demonstrates that MED has precisely the same functional dependence on polarisation matrix as MEG.

4.6 Spatial Correlations

Thus far, we have been solely concerned with the diagonal entries of the normalised terminated covariance matrix. The reason is we have been only interested in the average received power at each port. This gives rise to a question as what the off-diagonal entries would associate with. This question is of particular interest within the frame of the current section wherein we investigate the spatial correlation.

Spatial correlation is a measure to quantify the amount of similarities between signals at the ports of a multiport antenna in a multipath environment. In the modern wireless

[7] This has been clarified in Section 2.3.3 on page 14.

communication systems, where the spatial signature of the signals across ports are used for an efficient communication, the spatial correlation plays a substantial role. In this respect, the less the spatial correlation, the better the system performance. For instance, in a diversity multiport antenna, if the fading properties of signals across different ports are dissimilar, the probability that signals available at different ports fall in fade simultaneously is negligible. Therefore, an intelligent combination of signals at different ports will conquer the fading problem to a considerable extent.

With this foreword, let us now turn our attention to the covariance matrix. The off-diagonal entries in the terminated covariance matrix is indeed a measure of similarities between the received signals at different ports. When normalised properly, they represent the complex correlation coefficients. Normally, the phases of the foregoing coefficients are insignificant in comparison with their amplitude. Therefore, the absolute values of complex correlation coefficients are mostly regarded, which are henceforth referred to as *correlations* denoted by ρ.

Consider the ith and jth ports of an n-port antenna system. The normalised terminated covariance of this system has already been investigated and shown by $\mathbf{C}_{r_n}$. Let us denote the ith-jth entry of this matrix by c_{ij}. Thus, the correlation between the received signals at these two ports is obtained by [27, Equation (2.5)]

$$\rho_{ij} = \frac{|c_{ij}|}{\sqrt{c_{ii} \cdot c_{jj}}} \ . \tag{4.26}$$

We dedicated a sufficient time for study of the normalised terminated covariance matrix which plays a central role in the calculation of correlations. In addition to the above analysis, we derived the normalised terminated covariance matrix based on the open-circuit embedded far-field pattern matrix in [45]. The two analyses as a whole are remarkably similar yet complementary to each other. Furthermore, in [Paper B] we offer a more general compact formula for calculation of correlations including the influence of excitation schemes.

4.7 Covariance in Terms of Network Parameters

Throughout the preceding sections, we have convinced ourselves about how significant the role of the covariance matrix is in performance evaluation of a multiport antenna system. When the separation between the radiation elements –in terms of the operating wavelength– becomes considerable, the off-diagonal entries of the covariance matrix vanishes. In this condition, the bulk of overall performance is achieved through the diagonal entries which are indicators of the corresponding MEGs. In contrast, as soon as the distances between radiation elements shrink, *e.g.*, in compact array antennas, the role of off-diagonal entries becomes appreciable. Remember that the covariance matrix in a multiport antenna system to some extent also indicates the amount of *pattern diversity* between its radiating elements. Since the embedded pattern matrix, in the presence of coupling, depends on the terminating impedances at other ports too, many studies have been performed to simplify the evaluation of the covariance matrix without resorting to embedded far-field pattern measurements. The latter is fairly costly and in principle a

tedious task. Another useful way to alleviate the burden is via the input network parameters. Limited to lossless structures in isotropic multipath environments, researchers have presented some remarkably useful formulas rendering, for instance, correlations in terms of the input network parameters [46]-[48]. In this section, we clarify some points on usage limitation of the aforementioned formulas. The pattern overlap matrix of the terminal, which shall be defined in a moment, plays a central role in this part. We dedicate a sufficient regard to clarify the link between the pattern overlap matrix and the input network parameters. Within this frame, an overview of an important class of multiport antennas known as *minimum scattering antennas* is provided.

4.7.1 Antenna Pattern Overlap Matrix

Consider a lossless multiport antenna which is excited by some arbitrary voltage sources. We can find the total radiated power by this structure in two ways. Firstly, by virtue of its input network parameters and the associated electric currents across its ports, $\overline{i}$. And, secondly, through the embedded far-field patterns similar to what we used in Section 2.3.3. Using the first approach, under the reciprocity constraint, *i.e.*, $\mathbf{Z} = \mathbf{Z}^T$, the radiated power becomes

$$P_{\text{rad}} = \frac{1}{2}\, \overline{i}^{\dagger} \cdot \Re[Z] \cdot \overline{i}\ . \tag{4.27}$$

On the other hand, we can alternatively use the embedded far-field pattern matrix to obtain[8]

$$P_{\text{rad}} = \frac{1}{2}\, \overline{i}^{\dagger} \cdot \left(\frac{1}{\eta} \oint_{4\pi} \mathbf{G}^T \cdot \mathbf{G}^* \ d\Omega \right) \cdot \overline{i}\ . \tag{4.28}$$

The expression within the parentheses in (4.28) is referred to as *pattern overlap matrix* denoted by $\mathbf{C}$ [26],[49].[9] The symmetrical forms of equations (4.27) and (4.28) can misleadingly result in the apparent equivalence of $\Re[\mathbf{Z}]$ and $\mathbf{C}$, which is solely credible under certain conditions. Indeed, if and only if the pattern overlap matrix is a real matrix, the equivalence in (4.27) and (4.28) leads to the equivalence of $\Re[\mathbf{Z}]$ and $\mathbf{C}$, which is not always necessarily the case. Hence, having lossless structure is, in effect, a necessary constraint for the aforementioned equivalence, but not sufficient. This fact was not dedicated the proper regard in the original work on this subject [46]. To the best of our knowledge, as of yet the nature of the sufficient condition for the foregoing equivalence is not precisely known. Nevertheless, as stressed in [40], for a class of multiport antennas known as minimum scattering antennas, the resistive part of the input impedance matrix approximates the pattern overlap matrix [50], [51].[10]

4.8 Minimum Scattering Antennas

In general, different antennas might be considered as equivalent so long as they present an identical far-field pattern. However, antennas with identical amplitude and phase patterns can differ in a manner and extent to which they respond to an incident wave, *i.e.*, the way

[8] Refer to Equation (2.13) to see how we have come to this expression.
[9] This definition belongs to [Paper B], which is slightly different from its original definition.
[10] Refer to [Paper B, Equation (8)].

they scatter. In this section, we are concerned about a group of antennas with certain scattering property. A mulitport *minimum scattering antenna* is defined in principle by the property that such an antenna becomes *invisible* when its ports are open-circuited [50].

From scattering point of view, for a large class of antennas the scattered power is usually greater than the absorbed power. However, in minimum scattering antennas the scattered and the absorbed powers are equal. To elaborate it more, for a multiport minimum scattering antenna, the power which reaches to its open-circuited ports will be reflected back into the antenna and reradiated in a manner which approximates the reflection that would have occurred in the absence of any antenna.

Let us have a closer look from a circuit point of view. Consider the Thevenin equivalent circuit of an antenna. Under lossless constraint, the radiation resistance can be used to find the total radiated power of the antenna. The same holds for the case of a multiport antenna. In contrast, in receive-mode, the power dissipated on the radiation resistance is normally attributed to the scattered power by the antenna [30, page 76]. As an important point, the latter is solely credible under presumption of a minimum scattering antenna or those types of antennas which approximate them to a considerable extent. Therefore, if the total power scattered by an antenna system in receive-mode can be represented by the power dissipated on the radiation resistance, then this antenna system approximates minimum scattering antennas.

Now a question arises as how one can determine the total scattered power by an antenna system having the equivalent circuit model of it. This was answered by the author in [52]. In short, the total scattered power by an antenna is generally its open-circuit scattered power plus the terminated scattered power which is dissipated on its radiation resistance by the induced electric current over it. This similarly holds for the case of multiport antennas.

Based on [53, page 223] and [54], many lossless single-mode antennas approximate the minimum scattering antennas. To give some examples of antennas which approximate minimum scattering antennas, we use two lossless antennas. First, two cross-dipoles with an angle of α between them. Secondly, two parallel horizontal dipoles at certain height above a perfect electric conductor (PEC). These two-port antennas are single-mode. The equivalence of $\Re[\mathbf{Z}]$ and $\mathbf{C}$ is demonstrated in Figs. 4.1(a) and 4.1(b) where the method of moments has been used to obtain the embedded far-field pattern and the input network parameters [30, Section 8.4]. Note that due to some numerical inaccuracy, $\mathbf{C}$ is not precisely a real matrix. Thus, its entries denoted by c_{ij} are the corresponding amplitudes. We acknowledge that the imaginary components of entries in $\mathbf{C}$ are relatively negligible compared to the corresponding real parts. The agreement between the two sets of results are brilliant in both cases. An interesting example of non-minimum scattering antennas for which the stated equivalence does hold is an array of normal mode helices shown by [55]. This was anticipated previously in [54].

Let us concentrate again on isotropic multipath environments. For multiport antennas which comply with [Paper B, Equation (8)], the normalised terminated covariance matrix can be alternatively given by

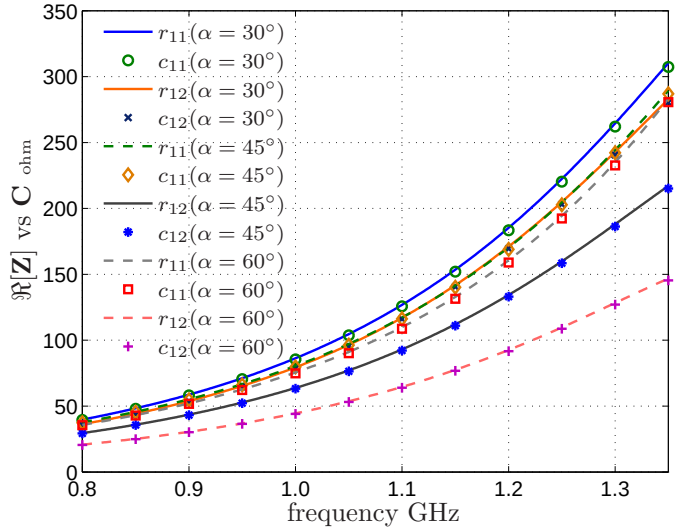

(a)

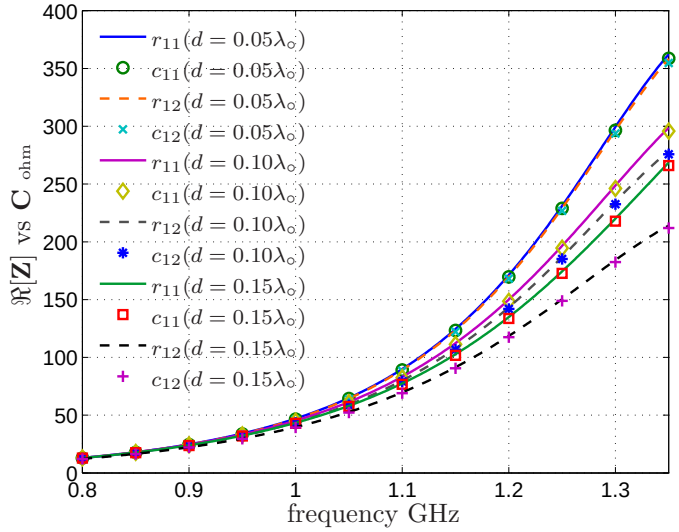

(b)

Figure 4.1: Comparison between $\Re[\mathbf{Z}]$ and $\mathbf{C}$ for (a) two lossless cross dipoles with an angle of α between them, and (b) two horizontal parallel dipoles above a PEC plane at $h = 0.15\lambda_\circ$ height, with element separation d. ($\lambda_\circ = 0.3$ m)

$$\mathbf{C}_{r_n} = 2\ \Re[\mathrm{Z}_r]^{-\frac{1}{2}}\ \mathbf{Z}_r(\mathbf{Z}+\mathbf{Z}_r)^{-1}\ \Re[\mathbf{Z}]\ (\mathbf{Z}+\mathbf{Z}_r)^{-1^\dagger}\mathbf{Z}_r^\dagger\ \Re[\mathrm{Z}_r]^{-\frac{1}{2}}\ . \tag{4.29}$$

Note that the above expression depends only upon the input network parameters.[11] It is rewarding since the measurement of input network parameters is far easier than the associated embedded far-field patterns. Indeed, this expression is central for our analyses in [Paper B].

4.9 Summary

The main concern of this chapter has been to provide analytical expressions for some crucial gauges in multiport antenna systems. These performance metrics are the MEGs, MEDs, and the spatial correlations between signals at different ports. The origin of these parameters is the received signal covariance matrix. Thus, this chapter for the most part has discussed the covariance matrix in different multipath environments. The open-circuit covariance matrix plays an essential role in this discussion. For the first time, two closed-form expressions for the MEG and MED in correlated multipath environments have been derived. We clearly show that both of these metrics have precisely the same functional dependency upon the polarisation matrix. The spatial correlation has also been shortly treated. We highlight the conditions upon which the covariance matrix as a whole can be expressed in terms of the input network parameters. As noted earlier, these compact formulas are most likely solely valid in a rich isotropic multipath environments.[12] Later in Chapter 6, we will discuss about how one can simulate the spatial correlation in non-rich multipath environments.

[11] This expression can be compared with that of (4.16) in isotropic multipath environments.

[12] To read more about rich multipath environments, refer to Section 6.5 on page 64.

Chapter 5

Multiport Antennas in a Cascaded RF Chain

Up to now, we have shown the significance of total embedded element efficiencies in overall performance of multiport antennas. It has also been cleared that the total embedded element efficiency has a persistent and effectual role in MEGs, and in this way directly affects the received SNRs in a wireless receiver system. In addition, recall that based on the discussion presented in Chapter 2, in the absence of ohmic losses the multiport matching efficiency equals the total embedded element efficiency. The salient feature of multiport matching efficiency is that it can be calculated solely through the input network parameters. This property makes its measurement practically more convenient. That aside, in modern multiport wireless systems, rarely can one find a multiport antenna connected directly to the receiver ports. Instead, antennas are integrated with the receiver through a chain of RF cascaded networks. For instance, dependent on applications, a cascaded network can be an uncoupled matching network, or a Butler network which is used for beamforming purposes. Therefore, it is a privilege to be able to calculate the multiport matching efficiencies in the presence of an arbitrary number of cascaded networks. In this chapter, we limit ourselves to multiport matching efficiencies associated with single-port excitation schemes.[1] We first present a brief overview of the case in which we have one cascaded network and then elaborate how we can extend it to the case of an arbitrary number of cascaded networks.

5.1 Radiation Efficiency at a Cascaded Network

Multiport matching efficiency has been introduced in [Paper A] wherein a compact formula for its evaluation is provided. Later, in [Paper C], a compact formula for the aforementioned parameter in the presence of a cascaded network has been presented. In this section, we quickly review the procedure followed in this reference and try to recast the multiport matching efficiency based on the notations used in the frame of our thesis.

Figure 5.1 shows the circuit model of a multiport antenna system, connected to the receiver through an arbitrary cascaded network. The precise description of the submatrices in $\mathbf{S}_{\text{ant}}$ is given in [Paper C]. Even so, in brevity, $\mathbf{S}_b$, $\mathbf{S}_c$ and $\mathbf{S}_d$ are associated with the *radiation ports* and are functions of the angular direction.[2] Conversely, $\mathbf{S}_a$ is the

[1] To know more about this limitation refer to [56].

[2] To read more about these submatrices also refer to [57] and [58].

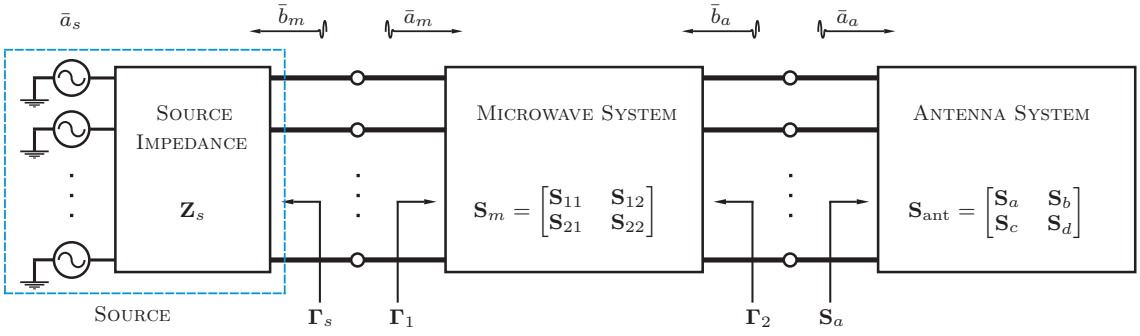

Figure 5.1: Microwave circuit model of a multiport antenna system connected to the receiver through an arbitrary cascaded network.

input port scattering matrix of the multiport antenna system independent of the angular direction. Moreover, $\mathbf{S}_m$ contains four $n \times n$ submatrices as reflection and transmission matrices at its both sides.

The *source transmission* matrix, $\mathbf{T}_s$, relates the voltage vectors at the source to the incident waves at the input of the cascaded network as

$$\bar{a}_m = \mathbf{T}_s \cdot \bar{a}_s \ . \tag{5.1}$$

Similarly, the cascaded network's transmission matrix, $\mathbf{T}_c$, is given by

$$\bar{a}_a = \mathbf{T}_c \cdot \bar{a}_m \ . \tag{5.2}$$

The reflection matrices $\mathbf{\Gamma}_s$, $\mathbf{\Gamma}_1$ and $\mathbf{\Gamma}_2$ shown in Fig. 5.1 are calculated through [Paper C, Equation (6)]:

$$\begin{aligned} \mathbf{\Gamma}_s &= (\mathbf{Z}_s + \mathbf{Z}_\circ)^{-1}(\mathbf{Z}_s - \mathbf{Z}_\circ) \ , \\ \mathbf{\Gamma}_1 &= \mathbf{S}_{11} + \mathbf{S}_{12}\mathbf{S}_a(\mathbf{I} - \mathbf{S}_{22}\mathbf{S}_a)^{-1}\mathbf{S}_{21} \ , \\ \mathbf{\Gamma}_2 &= \mathbf{S}_{22} + \mathbf{S}_{21}\mathbf{\Gamma}_s(\mathbf{I} - \mathbf{S}_{11}\mathbf{\Gamma}_s)^{-1}\mathbf{S}_{12} \ . \end{aligned} \tag{5.3}$$

The input power to the cascaded network, P_{in}, and the antenna system, P_{acc}, can be respectively achieved by

$$\begin{aligned} P_{\text{in}} &= \bar{a}_m^\dagger \ \left(\mathbf{I} - \mathbf{\Gamma}_1{}^\dagger\mathbf{\Gamma}_1\right) \ \bar{a}_m \ , \\ P_{\text{acc}} &= \bar{a}_a^\dagger \ \left(\mathbf{I} - \mathbf{S}_a{}^\dagger\mathbf{S}_a\right) \ \bar{a}_a \ . \end{aligned}$$

The source transmission matrix, $\mathbf{T}_s$, has been provided in [Paper C, Equations (3)-(4)]. By some network theory manipulations, we can obtain the cascaded network's transmission matrix to be

$$\mathbf{T}_c = (\mathbf{I} - \mathbf{S}_{22}\mathbf{S}_a)^{-1} \ \mathbf{S}_{21} \ . \tag{5.4}$$

The *total transmission matrix*, $\mathbf{T}_t$, relating the incident waves at the antenna ports to the source voltages is

$$\mathbf{T}_t = \mathbf{T}_c \cdot \mathbf{T}_s \ . \tag{5.5}$$

The maximum available power from the sources equals the input power to the cascaded network under matched conjugate condition, *i.e.*, $\mathbf{\Gamma}_1 = \mathbf{\Gamma}_s^\dagger$.[3] The source transmission matrix associated with the maximum power transfer is denoted by $\mathbf{T}_m$ which has been provided in [Paper C, Equations (3)-(4)]. Now, we have all primary ingredients in access to establish an analytical expression for the multiport matching efficiency. For this purpose, let us limit ourselves to single-port excitation schemes, which can be stack in a matrix form, say, an identity matrix, $\mathbf{I}_{n\times n}$. Upon this presumption, for the diagonal multiport matching efficiency matrix, $\mathbf{e}_{\rm mp}$, we have

$$\mathbf{e}_{\rm mp} = \mathrm{diag}\left[\mathbf{T}_m{}^\dagger \left(\mathbf{I} - \mathbf{\Gamma}_s \mathbf{\Gamma}_s{}^\dagger\right) \mathbf{T}_m\right]^{-1} \cdot \ \mathrm{diag}\left[\mathbf{T}_t{}^\dagger \left(\mathbf{I} - \mathbf{S}_a{}^\dagger \mathbf{S}_a\right) \mathbf{T}_t\right] \ . \tag{5.6}$$

The entries of the above diagonal matrix are the corresponding multiport matching efficiencies at the ports. It is rewarding to note that the first part of the above expression is solely dependent on the source impedance matrix. On the other hand, the only term in (5.6) which is affected by the properties of the cascaded network is $\mathbf{T}_t$. Consequently, whether we have one or several cascaded networks, as long as the corresponding total transmission matrix is available, we can find the multiport matching efficiency matrix.

5.2 An Analysis for Cascaded Networks

In the preceding section, it has been clarified that the total transmission matrix inherently contains the influence of the cascaded networks upon multiport matching efficiency. In the current section, our main concern is to achieve the total scattering matrix of an arbitrary number of known cascaded multiport networks. Let us assume that we have N arbitrary cascaded n-port networks. A cut of three subsequent units of them is shown in Fig. 5.2. The networks are labelled from left to right as $(l-1)$, l, and $(l+1)$. Let us define the transmission matrix over the lth cascaded network by $\mathbf{T}_l$. That is,

$$\bar{a}_{l+1} = \mathbf{T}_l \ \bar{a}_l \ . \tag{5.7}$$

By virtue of the network theory, it is quite straightforward to show that this transmission matrix reads

$$\mathbf{T}_l = \left(\mathbf{I} - \mathbf{S}_{22}^l \mathbf{\Gamma}_{l+1}\right)^{-1} \mathbf{S}_{21}^l \qquad (l = N, N-1, \ldots, 1) \ , \tag{5.8}$$

in which submatrices associated with the lth network are designated by superscript l. The expression in (5.8) clearly shows that the transmission matrix, as defined in (5.7) over each network, depends only on its scattering parameters as well as the reflection matrix at the input ports of the next cascaded network [59]. This is quite general.

To achieve the total transmission matrix, we start from the Nth cascaded network which is connected to the multiport antenna system with a known reflection matrix as $\mathbf{S}_a$. Then, use the associated expression in (5.8) to obtain $\mathbf{T}_N$. At this moment, in order to achieve $\mathbf{T}_{N-1}$, one needs the reflection matrix $\mathbf{\Gamma}_N$. To find a recursive analytical

[3] For more information on maximum available power from a source, refer to Section 2.1 on page 9.

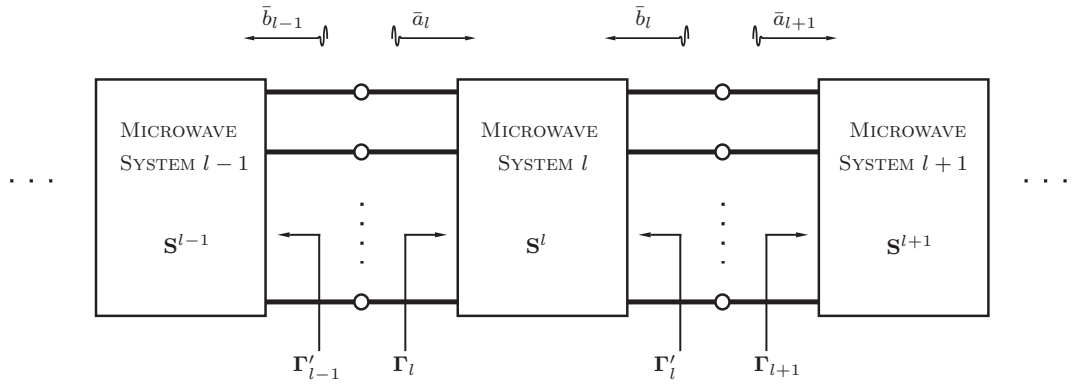

Figure 5.2: Microwave circuit model of three consecutive cascaded networks.

expression for evaluation of the reflection matrix, we pursue a tantamount path as we have gone through for $\mathbf{T}_l$ to arrive at

$$\boldsymbol{\Gamma}_l = \mathbf{S}^l_{11} + \mathbf{S}^l_{12}\ \boldsymbol{\Gamma}_{l+1}\ \mathbf{T}_l \qquad (l = N, N-1, \ldots, 1)\ . \tag{5.9}$$

Recall that $\boldsymbol{\Gamma}_{N+1} = \mathbf{S}_a$. This process of evaluating the transmission and reflection matrices continues to eventually yield the first cascaded network's transmission matrix. Now, the *total transmission matrix* of the whole system becomes

$$\mathbf{T}_t = \mathbf{T}_N\ \cdots\ \mathbf{T}_2\ \mathbf{T}_1\ \mathbf{T}_s \tag{5.10}$$

with $\mathbf{T}_s$ as given in [Paper C, Equations (3)-(4)]. Inserting the above $\mathbf{T}_t$ in (5.6) yields the corresponding multiport matching efficiency matrix in the presence of N cascaded microwave networks.

5.3 Scattering Matrix of Cascaded Networks

Calculation of the total network parameters for some cascaded networks is an important discipline in almost all microwave engineering books [59], [60]. Indeed, introduction of the ABCD matrix[4] has been more due to the convenience it renders for the aforementioned issue [60]. That is, the ABCD matrix of a cascaded connection of different networks can be easily found by multiplying their individual ABCD matrices. For cases of two-port networks a table of conversion between network parameters is available *e.g.*, see [60, Table 4.2]. When it comes to cascaded networks, engineers are recommended to first convert the available parameters to ABCD ones, and then evaluate their total ABCD matrix. Thereafter, the ABCD matrix can be converted to any desired network parameters like S-matrix. Nevertheless, things might be more troublesome when the number of ports exceeds two. In this section, we seek an approach whereby we can calculate the total S-matrix of a chain of cascaded networks for an arbitrarily large number of ports, n.

[4] It is also known as Transmission Matrix [60, page 183]. This terminology has a different use here.

To this end, we must recall that any n-port network can be described by its S-matrix, $\mathbf{S}$, containing four submatrices

$$\mathbf{S}_{2n\times 2n} = \begin{bmatrix} \mathbf{R}_{11\ (n\times n)} & \mathbf{T}_{12\ (n\times n)} \\ \mathbf{T}_{21\ (n\times n)} & \mathbf{R}_{22\ (n\times n)} \end{bmatrix} . \tag{5.11}$$

The reflection matrices at both sides of this network are designated by $\mathbf{R}_{11}$ and $\mathbf{R}_{22}$, while the transmission matrices are shown by $\mathbf{T}_{12}$ and $\mathbf{T}_{21}$. Based on the discussion in Section 5.2, the two submatrices $\mathbf{R}_{11}$ and $\mathbf{T}_{21}$ can be obtained by starting from the second side of the cascaded network ($l = N$) and calculating reflections and transmissions step-by-step towards the first side of the cascaded networks ($l = 1$). One should recall that the S-matrix is defined based on the matched terminated networks. That means, $\mathbf{\Gamma}_{N+1}$ in (5.9) is a zero submatrix, *i.e.*, $\mathbf{\Gamma}_{N+1} = \mathbf{0}$. By virtue of (5.8) and (5.9) and pursuing the same recursive procedure as described before, we achieve $\mathbf{T}_N$, $\mathbf{\Gamma}_N$, $\mathbf{T}_{N-1}$, $\mathbf{\Gamma}_{N-1}$, $\ldots$, $\mathbf{T}_1$, and finally $\mathbf{\Gamma}_1$. Equating the corresponding terms from (5.11), we arrive at

$$\begin{aligned} \mathbf{R}_{11} &= \mathbf{\Gamma}_1 , \\ \mathbf{T}_{21} &= \mathbf{T}_N \cdots \mathbf{T}_2\, \mathbf{T}_1 . \end{aligned} \tag{5.12}$$

To achieve two further submatrices, we have to follow the same way as we derived (5.8) and (5.9). For this time, we need to start from the first side ($l = 1$) and step-by-step calculate the single-block transmission and reflection matrices towards the second side ($l = N$). To distinguish between these submatrices from the previous ones, we use a prime superscript. The corresponding reflection matrices are shown in Fig. 5.2. For transmission matrices in this case, we have

$$\bar{a}_{l-1} = \mathbf{T}'_l\, \bar{a}_l \qquad (l = 1, 2, \ldots, N) . \tag{5.13}$$

Similar to what we saw earlier, for ($l = 1$), the definition of the S-parameters requires the initial reflection matrix to be $\mathbf{\Gamma}_\circ = \mathbf{0}$. To obtain other desired matrices we make use of

$$\mathbf{T}'_l = (\mathbf{I} - \mathbf{S}^l_{11}\mathbf{\Gamma}'_{l-1})^{-1}\, \mathbf{S}^l_{12} \qquad (l = 1, 2, \ldots, N) , \tag{5.14}$$

and also,

$$\mathbf{\Gamma}'_l = \mathbf{S}^l_{22} + \mathbf{S}^l_{21}\, \mathbf{\Gamma}_{l-1}\, \mathbf{T}'_l \qquad (l = 1, 2, \ldots, N) . \tag{5.15}$$

When all desired matrices are known, equating the corresponding terms from (5.11) will lead to

$$\begin{aligned} \mathbf{R}_{22} &= \mathbf{\Gamma}'_N , \\ \mathbf{T}_{12} &= \mathbf{T}'_1 \cdots \mathbf{T}'_{N-1}\, \mathbf{T}'_N . \end{aligned} \tag{5.16}$$

Therefore, in case there are two or more cascaded n-port networks between the multiport antenna and the receiver system, the above procedure can be used to find the total S-matrix of the whole cascaded chain. Now, if the multiport matching efficiencies of the complete system are desired, the expression in (5.6) or equivalently in [Paper C, Equation (13)] should be used. The next section is dedicated to highlighting the effects of cascaded networks over the received signals' covariance matrix.

5.4 Covariance in a Cascaded RF Chain

The effects of a cascaded microwave network upon the received covariance matrix has been studied first in [47]. In [Paper D], we have dealt with a similar concept slightly differently. However, based on the discussion presented in Section 5.3, we are able to extend the available formulations for cases of an arbitrary number of cascaded networks. For the sake of completeness, we ought to briefly review the derivations.

For this purpose, a receiver multiport antenna system in the presence of a cascaded network is shown in Fig. 5.3. The voltage vector at the antenna ports is denoted by $\bar{v}_r$. In contrast, at the receiver ports it is shown by $\bar{v}_l$. In Chapter 3, we studied the received voltage signals extensively. In particular, analytical expressions have been provided in this chapter for received signals in multipath environments of zero-mean complex Gaussian incoming EM waves. Our primary concern here is to relate $\bar{v}_r$ and $\bar{v}_l$. The details of the derivation have been provided to a point of satisfaction in [Paper D, Section 3], and is beyond our patience in the present chapter. However, the outcome is as follows [Paper D, Equation (16)-(17)]

$$\bar{v}_l = \mathbf{Q}\ \bar{v}_r\ , \tag{5.17}$$

in which

$$\mathbf{Q} = (\mathbf{I} + \mathbf{S}_l)\ (\mathbf{I} - \mathbf{S}_{22}\mathbf{S}_l)^{-1}\ \mathbf{S}_{21}\ (\mathbf{I} + \mathbf{R}_{\text{in}})^{-1}\ , \tag{5.18}$$

and for $\mathbf{R}_{\text{in}}$,

$$\mathbf{R}_{\text{in}} = \mathbf{S}_{11} + \mathbf{S}_{21}\ \mathbf{S}_l\ (\mathbf{I} - \mathbf{S}_{22}\mathbf{S}_l)^{-1}\ \mathbf{S}_{21}\ . \tag{5.19}$$

The covariance matrix in volts square for the received voltage at the receiver is

$$\mathbb{E}[\bar{v}_l\bar{v}_l^{\dagger}] = \mathbf{Q}\ \mathbb{E}[\bar{v}_r\bar{v}_r^{\dagger}]\ \mathbf{Q}^{\dagger}\ . \tag{5.20}$$

The term $\mathbb{E}[\bar{v}_r\bar{v}_r^{\dagger}]$ has been examined thoroughly in Section 4.3. It is important to stress that the covariance matrix at the ports of a multiport antenna can depend on the terminating impedances seen at its ports. This highlights a need for calculation of the corresponding impedance matrix through the available known parameters. This is most conveniently given by $\mathbf{R}_{\text{in}}$ in (5.19) through [Paper D, Equation(18)]

$$\mathbf{Z}_r = \mathbf{Z}_{\circ}\ (\mathbf{I} - \mathbf{R}_{\text{in}})^{-1}(\mathbf{I} + \mathbf{R}_{\text{in}})\ . \tag{5.21}$$

Now, if the MEGs at the ports of the receiver are desired, the diagonal entries in (5.20) should be normalised by the suitable reference power. For instance, for a general case of correlated multipath environments, one can use (4.4) as the reference power. It is worthwhile noting that in the presence of N cascaded networks, we can pursue the evaluation of the total covariance matrix as follows. First, we calculate the total S-matrix whose calculation was detailed in the preceding section. Then, we use equations (5.17) - (5.20) and the further useful expressions from Section 4.3. This suggests that we might consider the whole chain of cascaded networks and the multiport antenna –all together– the multiport antenna system. This consideration makes things far more favourable to treat. The interested reader can compare the formulas presented in this chapter to their original counterparts in [47, Section IV].

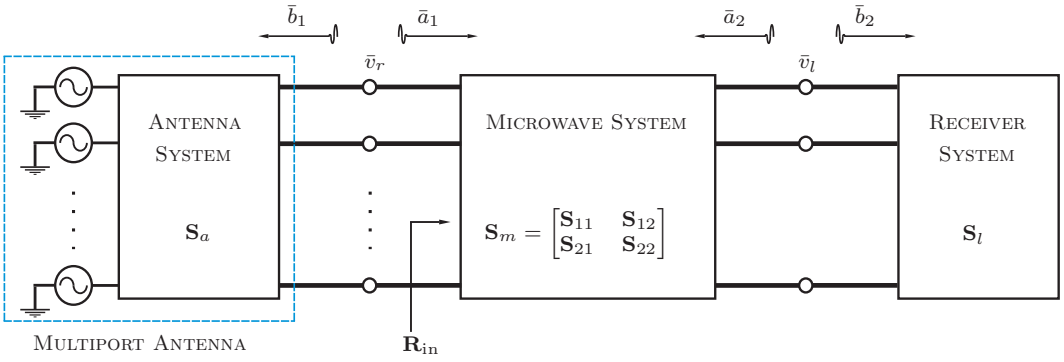

Figure 5.3: Receiver system's circuit model in the presence of a middle cascaded microwave network.

5.5 A Practical Example of Beamforming

As an example of a cascaded network, let us use an ideal Butler network whose network parameters are well documented [61]. A case of such an example is provided in [Paper C]. In this paper, correlations and total embedded element efficiencies at the ports of four lossless monopoles above a PEC plane are calculated. Likewise, let us examine similar results for a case of four horizontal lossless dipoles (4HD) at certain height above a PEC plane in the presence of a cascaded Butler network. Fig. 5.4 illustrates the schematic of this multiport antenna, wherein $h = 0.15\lambda_\circ$ ($\lambda_\circ \approx 0.3$m). The network parameters of this structure have been achieved by the moment method [30, Section 8.4]. The S-parameters of the ideal Butler network are also known as given by [Paper C, Equation (14)]. For simplicity, let us restrict ourselves to isotropic multipath environments and a single-port ideal reference antenna. Using the expressions provided in the preceding section, the normalised received signals' covariance matrix at the ports of the Butler network becomes [Paper C, Equation (16)]

$$\mathbf{C}_{r_n} = \mathbf{I} - \mathbf{\Gamma}_m^\dagger \mathbf{\Gamma}_m \ , \tag{5.22}$$

in which[5]

$$\mathbf{\Gamma}_m = \mathbf{T}\ \mathbf{S}_a\ \mathbf{T}^T \ . \tag{5.23}$$

It is interesting to derive the same expression from some independent formulas provided in [47, Section IV]. To this end, we shall slightly modify the notation utilised by [47] in the current section to be in harmony with those chosen in this thesis.[6] Based on [47, Equation (19)-(20)], if we denote the normalised covariance matrix at antenna ports by $\mathbf{C}_{a_n}$, the normalised covariance matrix at receiver ports, $\mathbf{C}_{m_n}$, becomes[7]

$$\mathbf{C}_{m_n} = \mathbf{Q}'\ \mathbf{C}_{a_n}\ \mathbf{Q}'^\dagger \tag{5.24}$$

wherein,

$$\mathbf{Q}' \triangleq (\mathbf{I} + \mathbf{S}_l)(\mathbf{I} - \mathbf{S}_{22}\mathbf{S}_l)^{-1}\mathbf{S}_{21}(\mathbf{I} - \mathbf{S}_a\mathbf{\Gamma}_{\text{in}})^{-1} \tag{5.25}$$

[5] The subindex m indicates the input ports of the middle Butler network, referred to as beam ports.
[6] Note that matrices are denoted by a double-bar sign in the original paper.
[7] Referring to the original text, we have replaced $\mathbf{R}_s$ by $\mathbf{C}_{r_n}$, $\mathbf{\Gamma}_{\text{in}}$ by $\mathbf{R}_{\text{in}}$, $\mathbf{S}_s$ by $\mathbf{S}_a$, and $\mathbf{Q}$ by $\mathbf{Q}'$.

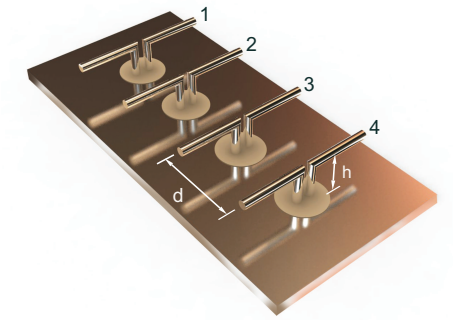

Figure 5.4: Four equidistant horizontal dipoles at a certain height above a PEC plane.

in which the multiport antenna's S-matrix is denoted by $\mathbf{S}_a$ and the receiver's reflection matrix by $\mathbf{S}_l$. The remainders belong to the microwave middle network as shown in Fig. 5.3. Referring to the aforementioned Butler example, the receiver impedances as well as both sides of the Butler network are all assumed to be matched to the transmission line characteristic impedances. That is, $\mathbf{S}_l = \mathbf{S}_{11} = \mathbf{S}_{22} = \mathbf{0}$. Substituting the corresponding terms in [47, Equation (4)], we obtain no reflection at the first side of the Butler network, $\mathbf{R}_{\text{in}} = \mathbf{0}$. In addition to that, substituting the necessary parameters in (5.25) leads to $\mathbf{Q}' = \mathbf{S}_{21}$. Moreover, $\mathbf{C}_{a_n}$ in (5.24) can be replaced by [47, Equation (31)]. Therefore, the covariance matrix at the receiver ports becomes

$$\begin{aligned} \mathbf{C}_{m_n} &= \mathbf{S}_{21}(\mathbf{I} - \mathbf{S}_a\mathbf{S}_a{}^\dagger)\mathbf{S}_{21}{}^\dagger \\ &= \mathbf{I} - \mathbf{S}_{21}\mathbf{S}_a\mathbf{S}_a{}^\dagger\mathbf{S}_{21}{}^\dagger \\ &= \mathbf{I} - \mathbf{S}_{21}\mathbf{S}_a\mathbf{S}_{12}\mathbf{S}_{12}{}^\dagger\mathbf{S}_a{}^\dagger\mathbf{S}_{21}{}^\dagger \\ &= \mathbf{I} - \mathbf{\Gamma}_m\mathbf{\Gamma}_m{}^\dagger \,, \end{aligned} \tag{5.26}$$

where we defined

$$\mathbf{\Gamma}_m \triangleq \mathbf{S}_{21}\mathbf{S}_a\mathbf{S}_{12} \,.$$

Recalling that $\mathbf{S}_{21} = \mathbf{T}$ and $\mathbf{S}_{12} = \mathbf{T}^T$, the expressions in (5.26) and (5.22) become identical demonstrating the equivalence of the corresponding formulas.

Let us now study the total embedded element efficiencies as well as the correlations for this sample multiport antenna. Based on the resultant covariance matrix in (5.26), the total embedded element efficiencies for the 4HD antennas shown in Fig. 5.4 can be obtained. Fig. 5.5 illustrates the total embedded element efficiencies at the antenna and the receiver ports which are connected by the ideal Butler network. Note that the element separation is $d = 0.2\lambda_\circ$ at $\lambda_\circ \approx 0.3$ m. Evidently, the differences between the internal and lateral ports' efficiencies are more considerable at the receiver ports. Furthermore, there are slight discrepancies between the resonance frequencies associated with different ports. But, all in all, the arithmetic mean value of them at the receiver and the antenna ports are similar. In a tantamount way, the corresponding correlations[8] between different ports can be achieved which are shown in Fig. 5.6. As mentioned earlier, these correlations are associated with a rich isotropic multipath environment.[9] In addition to the results in

[8] Recall that 'correlation' here refers to the absolute value of complex correlation.

[9] For more information on properties of this multipath environment, refer to Section 3.8.2 on page 25.

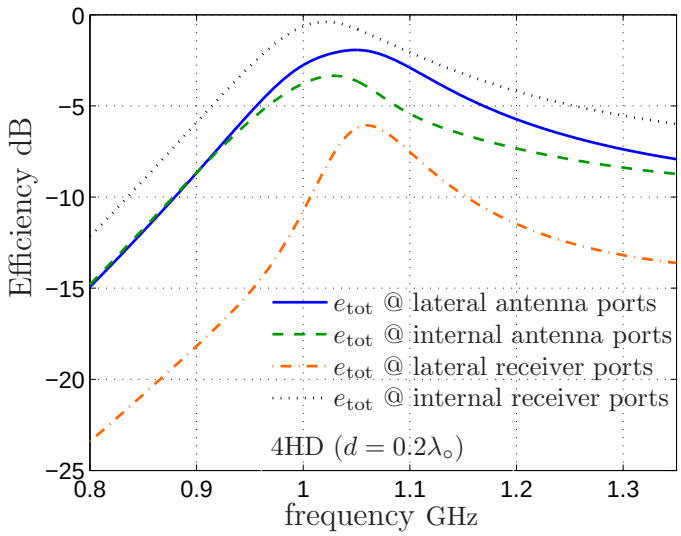

Figure 5.5: Total embedded element radiation efficiencies versus frequency at the antenna and receiver ports for four horizontal dipoles above a PEC plane.

[Paper C], once more it is observed that the corresponding correlations are different at the receiver and the antenna ports.

5.6 Summary

This chapter deals with a closed-form formula for the multiport matching efficiency in the presence of an arbitrary large number of cascaded networks. The closed-form formula presented here is a complementary to that of [Paper C, Equation (13)]. We have described an algorithm for calculation of total S-matrix of any arbitrary number of cascaded networks. Later, we show how one can incorporate the foregoing materials to find the total covariance matrix in the presence of these arbitrary cascaded networks. The latter is an alternative method to the one prevalent in the literature for calculation of the total covariance matrix. An example has been provided for better illustration of the matter. This example is in harmony with the one presented in [Paper C, Section 3].

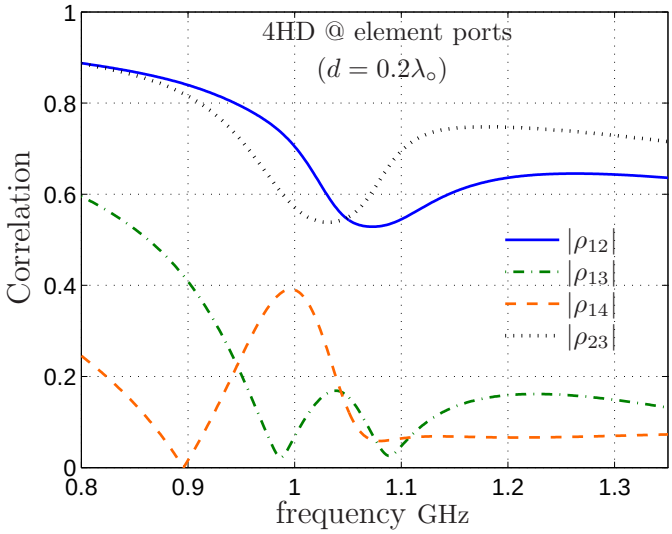

(a) Correlations at the element ports.

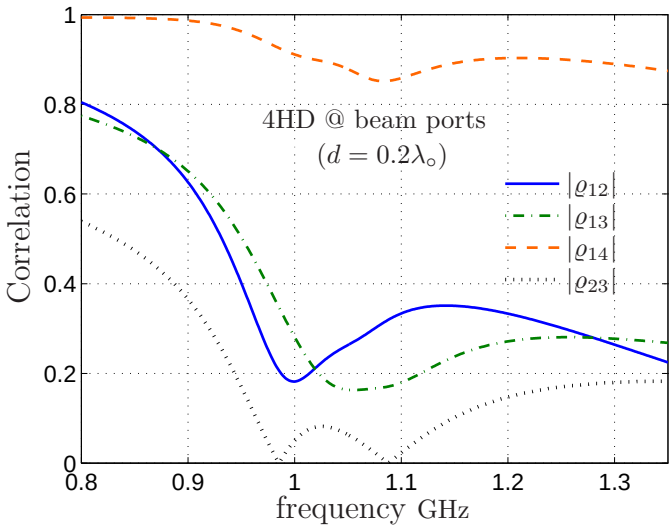

(b) Correlations at the beam ports.

Figure 5.6: Magnitude of the complex correlations for four horizontal dipoles above a PEC plane.

Chapter 6

Simulation of Multipath Environments

The current chapter is dedicated to the description of the way we simulate the received signals at the ports of a multiport antenna in a multipath environment. Based on the formulas developed in the preceding chapters, the received signal depends on the EM characteristics of the antenna structure, *e.g.*, input impedance matrix, terminating impedances, embedded element patterns *etc.*, and the incoming EM waves' properties. Therefore, in order to simulate the received signals, one first needs to emulate a multipath scenario in which random incoming waves of different polarisations are incident on an antenna structure. The latter is one of the primary aims of this chapter where we elaborate how to emulate a multipath environment. Upon simulating the random received signals at different antenna ports, we can further calculate different performance metrics introduced in Chapter 4. This helps to study the convergence of covariance matrix which was not addressed in the former chapters. Likewise, diversity gain is another major concern of this chapter. To describe more, in a multipath environment, the received random signals at the antenna ports can be combined by any arbitrary combining scheme. Under the presumed circumstance, by virtue of the received signals' cumulative probability density functions (CDFs)[1] and that of the combined one, the diversity gain of the multiport antenna can be calculated. A brief review of different ways for calculation of diversity gain is also provided.

6.1 Emulation of a Multipath Scenario

In order to realise a multipath scenario, one needs to first determine the direction of arrival of the incoming EM waves. This has been already referred to as AoA and denoted by solid angle Ω. Recall that in the spherical coordinate system, which serves our purpose best, Ω is represented by its latitude θ and longitude ψ angles, respectively. In Section 3.8.1 on page 24, some prevalent models were introduced for θ coordinate. With a slight modification, similar models can be applied equally to ψ coordinate too. This shall be cleared soon. Now the question is upon presumption of a distribution function, how one can realise random samples of this distribution. Let us start for a simple case of uniform multipath environment.

[1] This is also referred to as probability distribution function in contrast to probability density function.

6.1.1 Realisation of Uniform AoA

For the uniform distribution of AoA over the far-field sphere, it can be shown that the joint probability density function (PDF) of random variables θ and ψ is sinusoidal [39, Problem 4.6.1]. If the two random variables are presumably independent, a uniform distribution of $\psi \in [0, 2\pi]$, *i.e.*, $\mathsf{P}_\psi = 1/2\pi$, necessitates a sinusoidal distribution of $\theta \in [0, \pi]$. In general, if the CDF of a variable denoted by F is an invertible function, the inverse transform technique will be an efficient choice [39, Section 4-11]. In this method, first a uniform random variable is produced within the interval $[0, 1]$, and then these random samples are exposed to the inverse distribution function F^{-1}. The resultant random samples when scaled for the required range will have the desired distribution function within the preferred domain. In the frame of this thesis, to realise uniform random samples of AoA, we first create samples for ψ uniformly over the range $[0, 2\pi]$. Later, using the inverse transform technique as described, we create random samples for θ having a sinusoidal PDF function in the interval $[0, \pi]$. By these components, the distribution of $\Omega(\theta, \psi)$ becomes uniform over the far-field sphere.

6.1.2 Realisation of Nonuniform AoA

The probability density function for the two constituents of random Ω is known for a uniform distribution. However, when it comes to nonuniform AoA distribution over the far-field sphere, things may not be as simple as before. The probability density functions of some renowned nonuniform multipath environments have been provided in Section 3.8.1. It is worth mentioning that the inverse transform technique described above is conceptually an easy technique, but from a practical standpoint it has some drawbacks. For instance, for the continuous functions, as is the case here, it is required to know or calculate the inverse distribution function F^{-1}, which is not always a simple task. This problem forces us to seek an alternative method for sample realisation from the aforementioned functions given in Section 3.8.1. For this purpose, a suitable choice for us could be the *rejection method* [39, page 123]. In this method, in order to realise a sample from a given density function, we need an independent pair of samples from a uniform and a known density function. Within the frame of this thesis, we have used the sinusoidal density function achieved from the inverse technique as our secondary density function. In this case, there must exist a coefficient $a \in \mathbb{R}$ such that $\mathsf{P}(\theta) \leq a \sin(\theta)$.[2] If the created pair of random samples satisfy a certain condition[3], the corresponding sample from sinusoidal function has the required density function P and is thus accepted. If the stated condition is not met, the selected pair of random samples should be discarded. And, the process is iterated until the desired condition is satisfied. This technique has been used to create results in [Paper B, Figure 3].[4]

[2] $\mathbb{R}$ denotes the real numbers.

[3] This condition is provided in [39, page 124]. Assume that samples (U, θ) are the independent pair of samples from uniform and sinusoidal density functions. Now if the condition $a\, U \sin(\theta) \leq \mathsf{P}(\theta)$ holds, then θ has the density function P.

[4] Also, the same technique was used for simulations in [44, Figure 4].

6.1.3 Realisation of Random EM Waves

In Section 3.8.2, a fair description has been provided in which we reasoned that using complex Gaussian random incoming EM waves is presumably a suitable option. We have used a Marsaglia's Ziggurat algorithm, which is a rejection sampling algorithm available in MATLAB, to realise random samples.

Bear in mind that for both polarisations, *i.e.*, θ and ψ polarisations, we need to realise random samples. If the random incoming waves from the two polarisations are uncorrelated, we simply create two independent sets of samples commonly with identical variances. If we wish to create correlated samples for the two polarisations, we can follow the same approach as described in [Paper E].[5] Furthermore, if the incoming waves should comply with certain XPR, it is sufficient to weight the realised sets of random samples according to this parameter.

6.2 Random Received Signals

Antennas in multipath environments are exposed to several incoming EM plane waves of certain polarisation. These incident waves give rise to voltage signals at different ports of the antennas which may vary fast with respect to frequency, space and time. It is of importance to note that the time dependency meant here is irrelevant to time harmonic nature of the incoming EM waves. The latter is already accounted for by postulation of time-harmonic regime and virtue of phasor notation [28, Section 7.2].

Let us assume that there are K number of scatterers, presumably located in the far-field region of the terminal, with certain distribution, moving around continuously. Originating from each of these scatterers there comes an incident EM wave contributing upon the voltage signal at the port of each radiation element. At a particular moment, we take samples of the voltage signals available at different ports, which make the entries in the first output voltage vectors, $\bar{v}_r$. To avoid any possible confusion between time and space domains let us preferably attribute each sample of the voltage signals to a *scenario*.

Now in the second scenario, the same number of scatterers but with different positions -of still the same distribution- are responsible for the new sets of EM waves which, in turn, create our second set of voltage samples at the corresponding ports. This process of realisations continues to eventually result in sufficient number of voltage samples at the ports of a multiport antenna.

In Section 6.1, we described how we realise a multipath scenario. That is, first, we randomly select the AoAs from which the random incoming EM waves are incident. Then, we assign a random EM plane wave to each of these AoAs. It is evident that for each polarisation, there is a random incoming EM wave. In parallel, the analysis developed in Chapter 3 and in particular Equation (3.26) can be utilised which uses superposition concept to hold for this particular purpose. Doing so, we can derive the equation governing the relation between the K multiple incident waves and the received voltage sample at each port as

$$\bar{v}_r^{\text{sc}} = \frac{2\lambda}{j\eta}\, \mathbf{Z}_r \sum_{k=1}^{K} \mathbf{G}_r^T(\Omega_k) \cdot \bar{E}^{\text{sc}}(\Omega_k)\ . \tag{6.1}$$

[5] For this purpose, just use two independent sets of samples exposed to [Paper E, Equation (2)].

In (6.1), the superscript 'sc' stands as an identity tag to show to which scenario the ports' sample voltage vector belongs. All parameters in (6.1) have been defined in Chapter 3. For instance in an uncorrelated multipath environment, each incident wave presumably comes from a certain scatterer, say k, from direction Ω_k totally independent from those of other scatterers in the same scenario. Should we denote the total number of scenarios by N_{sc}, the results of simulations become N_{sc} number of entries in each port's voltage vector. The voltage vectors stand as samples of the received signals in the emulated multipath environment. They are the major source of different gauges for performance assessment of the affiliated multiport antenna. In what follows, we detail how to derive these criteria from the voltage vectors. Yet, before moving towards them, we shall clarify the way we normalise the received voltage vectors.

6.2.1 Normalisation of the Received Signals

Dependent on the number of the incident waves and their strength, the received power can vary significantly. Thus, the average received power alone does not matter unless it is properly normalised. To see how the multiport antenna under test performs against an ideal antenna, we can again choose a dual-polarised dual-port isotropic ideal antenna, as we did in Chapter 4 on page 29. This dual-port reference antenna is exposed to the same scenarios and afterwards its received average power is used for normalisation purposes. Despite the fact that in the simulation domain, we are able to conveniently choose any arbitrary reference antenna as we wish, in practice, it is not possible. We stress that in a particular case of a rich isotropic scattering environment, the shape of the pattern of a radiation element is irrelevant to its performance [3, page 139], [62]. Therefore, as long as it is compensated for the known total radiation efficiency of any antenna, it can be used as a reference antenna.[6] However, validity of the latter is strictly limited to rich isotropic environments and should not be generalised to nonuniform cases.

6.3 Performance Metrics from Received Signals

In this short section, we briefly describe how we derive the desired performance metrics from the received signal vectors. Let us first start with MEGs.

Note that choosing a dual-polarised dual-port ideal isotropic reference antenna is quite useful for calculation of MEGs. We solely need to calculate the average received power from the voltage signals over different scenarios. The ratio between the received average power at each port and that of the reference antenna in the same multipath scenarios yields the corresponding MEGs. For further description on this matter, the interested reader may refer to Chapter 4.

In the foregoing chapter we also showed how one can calculate the correlation coefficient from the random received voltage vectors. Nevertheless, concerning the spatial correlation, we shall inject an important point. That is, one can also form the covariance matrix from the associated received average power signals. From measurement point of

[6] For different polarisations, we can use different antennas. But in an isotropic environment, like a multipath scenario created in a reverberation chamber, a known single-polarised antenna is sufficient to stand as a reference.

view, the latter might be of more interest compared to the received voltage covariance matrix. This is because measurement of the received average power is easier than the received voltage signal. In this particular case, the amplitude of correlations between different average power signals is referred to as *envelope correlation*, ρ^{e}. It is known that in a *rich* Rayleigh fading environment, the link between the correlation and the associated envelope correlation is as[7] [40]

$$\rho^{\mathrm{e}}_{ij} \approx |\rho_{ij}|^2 \ . \tag{6.2}$$

In [63, Figure 1], it is shown that the relative error in this approximation does not exceed 3%. The above approach has been used for calculation of the correlation in [Paper C]-[Paper D], and partly in [Paper B].

6.4 Calculation of Diversity Gain

Thanks to a rich literature in this field (*e.g.*, [3], [40]), the concept of diversity gain is already well established. Thus far, we have described how to simulate the received signals across ports of a multiport antenna in a multipath environment. These signals can be combined in a way to render a more desirable signal of significantly enhanced fading properties.[8] The combining can be realised in several ways having different levels of complexity and performance [4, Section 7.2]. Among all available combining schemes, we focus on selection combining (SC) and maximum ratio combining (MRC) ones. The former is well-known for its simplicity in simulation whereas the latter is appealing mostly due to its optimum performance.[9]

An important point concerning the diversity gain is that it lacks a unanimous definition among different research societies worldwide. For instance, while communication engineers refer to the slope of bit error rate curves versus SNR as diversity gain, antenna experts define different diversity gains based on the received signals' CDF curves as well as the diversity's one. Of course, the former definition resides within the baseband frame whereas the latter within the RF domain. In this thesis, we restrict ourselves to RF domain and look upon the diversity gain concept in this framework, wherein the array gain is inherent.[10]

From antenna engineers' point of view, *apparent diversity gain* (ADG) is specified as the ratio between strengths of the diversity signal and the best received signal at a certain level of their CDF curves [3], [40]. In the frame of this thesis, let us opt for 1% of CDF curves for diversity gain calculation. To clarify the selected definition, we illustrate it in Fig. 6.2 which goes for an arbitrary two-port antennas in an isotropic environment. The maximum MEG of the two radiation elements, $M_{\mathrm{G}} = -4$ dB, is shown in the figure. The correlation between the two radiation elements is $\rho = 0.5$. To realise the diversity combining signal, the MRC scheme has been used. To attain the *effective diversity gain* (EDG) in isotropic multipath environments we use [44][11]

$$\mathrm{EDG} = M_{\mathrm{G}} \cdot \mathrm{ADG} \ , \tag{6.3}$$

[7] To read more about it, please refer to [27, Chapter 2].

[8] More information on fading signals can be found in [6, Chapter 2] and [4, Chapter 3].

[9] From a practical standpoint, the equal-gain combining scheme seems to be the simplest.

[10] The array gain was illustrated in Fig. 1.1 on page 5.

[11] This definition is a modified version of its original counterpart in [64].

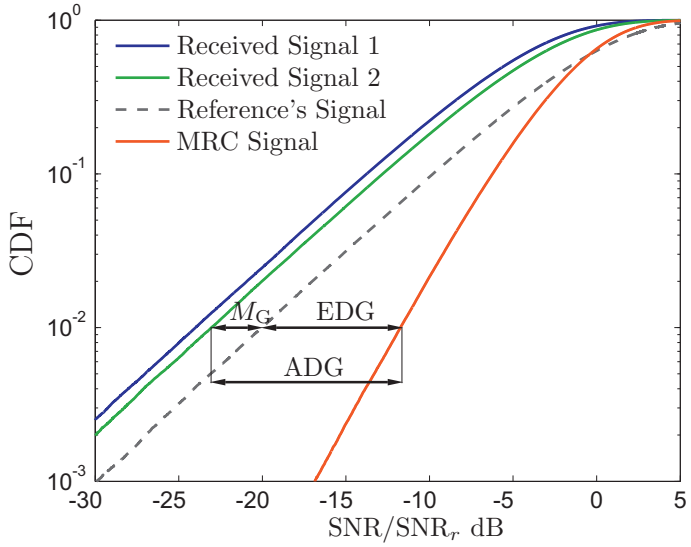

Figure 6.1: Definitions of ADG and EDG based on the received signals' CDF curves. The symbol M_{G} denotes the MEG of the best branch. SNR_r stands for averaged received SNR by the ideal dual-port reference antenna.

which is also valid in more general cases of nonuniform multipath environments compared to the definition in [64]. Upon choosing a definition for ADG, the first question that comes to mind is as, in an ideal circumstance, how much diversity gain can be achieved by utilising multiport antennas. This curiosity has been already addressed. For the MRC scheme, the answer has been shown in [65, Figure 7]. For both MRC and SC, the maximum ADG have been given in [27, Table 1].

The main concern regarding the definition of the ADG at 1% level of the CDF curves is its precise measurement. Due to inherent statistical nature of the received signals in multipath environments, the corresponding CDF curves deviate from their converged counterparts at 1% level. This necessitates a high number of measured samples, which is unacceptably cumbersome if not impossible.

To find the sufficient number of realisation, N_{sc}, for this simulation approach, one has to refer to [Paper E, Table I]. For instance, based on this table, in order to reach an accuracy better than 0.25 dB, the number of realisations should exceed ten thousands ($N_{\mathrm{sc}} > 10^4$). In [Paper A] and [Paper C], the number of realisations used to calculate EDGs exceeds $N_{\mathrm{sc}} > 10^6$. Despite requiring a bulky burden of computation, this number of realisations yields an accuracy better than 0.01 dB.

Having elaborated the simulation approach whereby diversity gain can be obtained, we shall dedicate a few lines presenting a comparative study of a number of prevalent ways for diversity gain calculation. To simplify this study, let us limit ourselves to two-port antennas and the MRC scheme. Of course, the conclusions derived can be directly generalised to any number of ports.

6.4.1 Diversity Gain by Eigenvalue Method

It is already known that diversity gain of a multiport antenna in a *rich* multipath environment depends on the spatial correlation as well as the MEGs of the antenna elements [Paper E]. These two crucial parameters have been analysed in Chapter 4. The normalised covariance matrix of the received signals can be also recast as[12]

$$\mathbf{C}_r = P_{\text{ref}} \cdot \begin{bmatrix} M_{\text{G}_1} & \sqrt{M_{\text{G}_1} \cdot M_{\text{G}_2}} \cdot \rho \\ \sqrt{M_{\text{G}_1} \cdot M_{\text{G}_2}} \cdot \rho & M_{\text{G}_2} \end{bmatrix} \tag{6.4}$$

in which $M_{\text{G}_{1,2}}$ are the MEGs of the two radiation elements. Observe the symmetrical nature of $\mathbf{C}_r$, which shows the possibility to make an eigenvalue decomposition of it. That is, $\mathbf{C}_r = \mathbf{Q}\Lambda\mathbf{Q}^{\mathbf{T}}$ in which $\mathbf{Q}$ is presumably an orthonormal matrix whereas Λ is a diagonal matrix whose entries are the eigenvalues of $\mathbf{C}_r$.[13] There is a brilliant interpretation for the above decomposition. Since different columns of $\mathbf{Q}$ are orthogonal, indeed, the eigenvalue decomposition represents an alternative multiport system with no correlation between them but normalised mean received powers of ξ_1 and ξ_2, the corresponding eigenvalues. The foregoing equivalent system with no correlation renders the same diversity gain as the original system [65]. The eigenvalues of $\mathbf{C}_r$ are simply given by

$$\begin{aligned} \xi_1 &= \frac{1}{2} P_{\text{ref}} \left(M_{\text{G}_1} + M_{\text{G}_2} + \sqrt{(M_{\text{G}_1} - M_{\text{G}_2})^2 - 4\rho^2} \right) \\ \xi_2 &= \frac{1}{2} P_{\text{ref}} \left(M_{\text{G}_1} + M_{\text{G}_2} - \sqrt{(M_{\text{G}_1} - M_{\text{G}_2})^2 - 4\rho^2} \right) \ . \end{aligned} \tag{6.5}$$

Now assume a two-port diversity system in a Rayleigh multipath environment, with no correlation between them. The well-known Rayleigh PDF of each branch with the corresponding mean received power is given by [4, Equation (7.5)]

$$\mathsf{P}_m(\gamma) = \frac{1}{\xi_m} \exp(-\frac{\gamma}{\xi_m}) \qquad (m = 1, 2) \ . \tag{6.6}$$

The moment generating function associated with the above PDF can be obtained as [4, Equation (6.62)]

$$\mathcal{M}_m(\upsilon) = \int_0^\infty p_m(\gamma) \exp(j\gamma\upsilon) \ d\gamma = \frac{1}{1 - j\xi_m\upsilon} \ . \tag{6.7}$$

To achieve the PDF of the MRC combined signal we take the product of the two exponential moment generating functions [4, page 214]:

$$\begin{aligned} \mathcal{M}_\Sigma(\upsilon) &= \mathcal{M}_1(\upsilon) \cdot \mathcal{M}_2(\upsilon) \\ &= \frac{1}{1 - j\xi_1\upsilon} \frac{1}{1 - j\xi_2\upsilon} \\ &= \frac{1}{\xi_1 - \xi_2} \left(\frac{\xi_1}{1 - j\xi_1\upsilon} - \frac{\xi_2}{1 - j\xi_2\upsilon} \right) \ . \end{aligned} \tag{6.8}$$

[12] The index for correlation, ρ, is dropped for simplicity in appearance.

[13] Distinguish between the $\mathbf{Q}$ defined here and that of the preceding chapter.

Thus, the PDF of the MRC diversity signal, P_Σ, becomes

$$\begin{aligned}\mathsf{P}_\Sigma(\gamma) &= \frac{1}{2\pi}\int_0^\infty \mathcal{M}_\Sigma(\upsilon)\exp(-j\gamma\upsilon)\,d\upsilon \\ &= \frac{1}{\xi_1-\xi_2}\left(\exp(-\frac{\gamma}{\xi_1})-\exp(-\frac{\gamma}{\xi_2})\right)\ .\end{aligned} \tag{6.9}$$

Obtaining the corresponding CDF, F_Σ, requires a simple integration:

$$\begin{aligned}\mathsf{F}_\Sigma(\gamma<x) &= \int_0^x \mathsf{P}_\Sigma(\gamma)\,d\gamma \\ &= \frac{1}{\xi_1-\xi_2}\left[\xi_1\left(1-\exp(-\frac{x}{\xi_1})\right)-\xi_2\left(1-\exp(-\frac{x}{\xi_2})\right)\right]\ .\end{aligned} \tag{6.10}$$

The above expression is a two-port equivalence of a more general formula provided by [65, Equation (33)]. Having the CDFs, we can numerically solve the point upon which they reach their 1% level. Subsequently, the same point for either the best branch's CDF (for calculation of ADG) or the theoretical one (for EDG calculations) can be achieved. The ratio of the former and the latter points yields the desired diversity metric. This method is an elegant one which is computationally preferable with respect to the simulation approach described earlier. However, bear in mind that in this approach the covariance matrix of the multiport system is needed. Quite interestingly, in [56], it has been shown that the available analytical formulas in the literature for calculation of the covariance matrix are probably only credible in a *rich* multipath environment.[14] This issue exerts some limitations in usage of the above method for a general multipath case. As a final point, it is worth mentioning that in [Paper F] we showed how one can measure the antenna pattern overlap matrix. As demonstrated in [45], this metric plays an essential role in terminated covariance matrix of the antenna and can be used for its calculation. Having the covariance matrix, based on the above discussion, we can calculate the diversity gain accordingly. In this way, one can considerably bypass the inaccuracy in the diversity gain measurements due to the lack of sufficient number of independent samples in a reverberation chamber.

6.4.2 Diversity Gain by Principal Component Analysis

This numerical approach is based on the realisation of sufficient number of Rayleigh random samples satisfying the required conditions. The principal component analysis (PCA) can be used to create the desired random signals of the given correlations and appropriate normalisations. The average weight of a random signal indicates its port's associated MEG. The correlations between a received signal and those at the other ports present in turn its conjunction with them. Therefore, as long as the numerically created random signals have Rayleigh distribution and present the same covariance matrix as the original fading signals, they can represent them brilliantly. Depending on the computation resources, the corresponding CDFs can be achieved to the desired preciseness.

[14] As an example, see Equation (4.16) with $\mathbf{C}_{\circ_n}$ provided in (4.13).

As an initial step toward creating the Rayleigh random variables, we need to create independent samples of complex Gaussian random variables of zero mean and standard deviation of unity. By now, this problem should be familiar which has been briefly yet satisfactorily addressed in Section 6.1.3. After realising the required independent sets of random samples, we can convert them to a new set of random samples complying with the desired covariance matrix. To that end, two methods are more prevalent: the PCA method and the Cholesky's decomposition method. The former is a more stable one whereas the latter can break down pretty easily depending on how stable the covariance matrix is.[15]

The PCA method is based on the eigenvalue decomposition concept. Recall that the covariance matrix can be recast as $\mathbf{C}_r = \mathbf{Q}\mathbf{\Lambda}\mathbf{Q}^{\mathbf{T}}$, an $n \times n$ matrix. On the other hand, presume a matrix $\mathbf{B}_{n\times N_{\rm sc}}$, whose rows are independent zero-mean complex Gaussian random samples. Recall that index n stands for the number of the ports involved and $N_{\rm sc}$ indicates the number of realised samples. Now the rows of matrix $\mathbf{X}_{n\times N_{\rm sc}}$, defined as

$$\mathbf{X} = \mathbf{Q}\ \sqrt{\mathbf{\Lambda}}\ \mathbf{B}\ , \tag{6.11}$$

renders the n random vectors associated with the corresponding ports. Afterward, one may use any arbitrary combining scheme to realise the diversity signal and later draw the CDF curves in order to extract the corresponding diversity gains.

The above approach is highly beneficial for the cases wherein we have more radiation elements. It is to some extent rigorous, easy to implement, and fairly fast. The accuracy is likely dependent only on the computation resources and the time. As a reminder, in [Paper E, Table 1], the relative errors for different numbers of samples are provided. In principle, $N_{\rm sc} > 10^5$ bestows sufficient accuracy.

Therefore, this approach is highly recommended for diversity gain measurements in a reverberation chamber. Being restricted to isotropic environments, a reverberation chamber is the fastest way to measure antenna efficiencies as well as correlations. As said earlier, this measurement tool is limited to a finite number of independent samples making it inefficient in accurate diversity gain measurements. Despite that, the reverberation chamber presents quite acceptable accuracy in measurement of efficiency as well as correlation compared to the diversity gain. Therefore, the current approach is advantageous in calculation of diversity gain based on the covariance matrix obtained by these measurement tools.

The main drawback with this scheme is that it requires further computation resources compared to Eigenvalue method. Moreover, there might be some occasions in which PCA method also breaks down. Under these circumstances, the calculated diversity gains are not accurate.

6.4.3 Compact Formulas for Diversity Gain

To overcome the problem of calculation of diversity gain for two-port antennas, we have devised a couple of compact formulas associated with SC and MRC combining schemes [Paper E]. Among all the introduced methods, these compact formulas offer the fastest ones. They are plainly simple and use the least computation resources. Of course, there is

[15] *http://www.risklatte.com/Articles*, Principal Component Analysis and the Cholesky Decomposition.

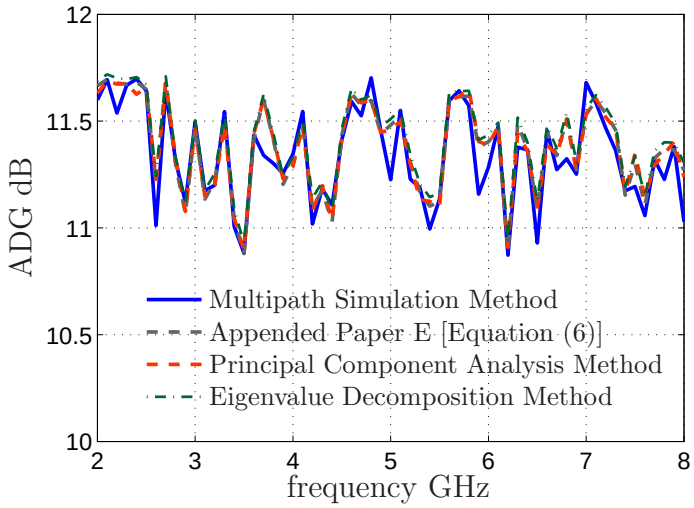

Figure 6.2: Apparent diversity gains of an Eleven antenna achieved by four different methods.

certain inaccuracy inherent in both these formulas. Furthermore, they are only available for SC and MRC combining schemes.

To show a comparative study for calculation of diversity gain by these methods we use an example. In this example, diversity gain of an Eleven antenna is studied. To read more about the Eleven antenna, one can refer to [27, Section 4.3.1] or [66]. In brief, it is a two-port wideband antenna which has been developed for use as a feed in future radio telescopes. The embedded far-field patterns of this antenna were measured in Technical University of Denmark with angular resolution of $1^\circ \times 1^\circ$ in both θ and ψ. The diversity gain of this multiport antenna in an isotropic multipath environment has been obtained by all four presented methods. Fig. 6.2 illustrates the results. To achieve the associated results, the number of incoming waves in each realisation and the total number of scenarios were $K = 200$ and $N_{\text{sc}} = 10^5$, respectively. The outcomes are in agreement not only with each other, but also with the reverberation chamber measurements provided in [27, Figure 4.2].

In general, for two-port antennas in a rich multipath environment, the compact formulas present the best method for calculation of diversity gain. If the number of ports in a multiport system exceeds two, the eigenvalue decomposition method is the most elegant one. In this circumstance, the PCA method can also be used. This latter method might be utilised with a proper caution though. However, the multipath simulation approach elaborated earlier in this chapter is useful for circumstances in which we are concerned about the number of incident waves in each scenario. No other method can be used for this specific case, which is treated in the next section.

6.5 Antennas in Non-rich Multipath Environments

For several decades, the main concern of the multiport antenna engineers has been to design antennas of negligible correlations. The common criterion upon which they eval-

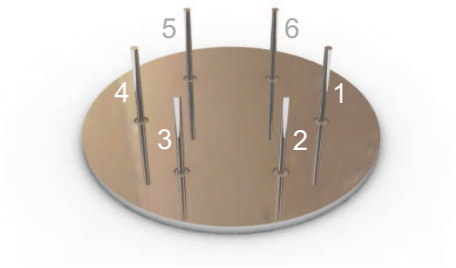

Figure 6.3: Configuration of six monopoles above an ideally large PEC plane.

uated their design has been the embedded pattern covariance matrix.[16] If the multipath environment has nonuniform AoA distribution and certain known polarisation matrix, the expressions provided in Chapter 4 are useful to yield the corresponding correlations.

However, those expressions are most likely only credible in *rich* multipath environments. In general, the *rich* multipath is referred to those multipath environments wherein the joint probability density function of the random received signals across the antenna ports converges to its asymptotic state. It is a question of interest to know how many number of independent incident waves are required to yield a converged covariance matrix. In [67], we illustrate that this number, in principle, depends to a certain extent on the properties of the multiport antennas. The foregoing concern created a trend in us to look into the case further and possibly parameterise it as a new criterion. The expended effort on this subject has led to the notion of *richness threshold* which was first coined in [44].

Convergence in joint distribution function depends on convergence in the covariance as well as the distribution of the received signals at the antenna ports. To simplify our analysis, and more importantly to confine the richness threshold's definition in the antenna engineering area, we should presumably alleviate the dependency of convergence upon distribution. For this purpose, we assume complex Gaussian random incoming EM waves in each realisation. Under this constraint, convergence in joint probability density function –and thus the threshold richness– only depends on convergence in covariance matrix.

To parameterise how many independent random incoming waves are required to have a converged covariance matrix, we need to rely on a single metric containing an overall information about the covariance matrix. In this thesis, we preferred the diversity gain, as perhaps the simplest performance metric. By this choice, the richness threshold is the minimum number of independent incoming waves required to realise a converged diversity gain. For further simplicity in determining the threshold at which we have convergence, let us set the threshold level at the point wherein 90% (-0.5 dB) of the asymptotic diversity gain value is realised.

To envision the concept of richness threshold, we make use of an example. In this example we show how the richness parameter can be used as a further performance metric to evaluate a multiport antenna. For this purpose, consider a case of six equidistant lossless monopoles (6MP) in a hexagonal configuration over an infinite PEC plane. The

[16] They may also use the pattern overlap matrix discussed in Section 4.7.1 on page 40, or in [45].

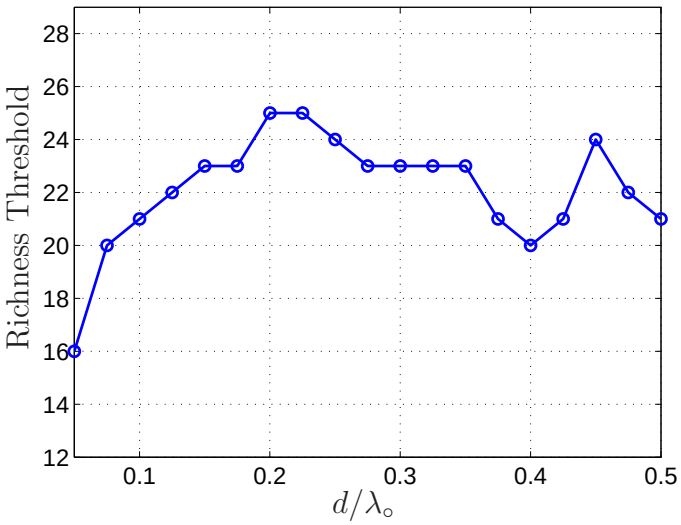

Figure 6.4: Richness threshold at -0.5 dB versus element separation for six monopoles above a PEC plane. (After [56])

terminations at the ports of these radiation elements are all 50 ohm. Like before, the element separation is denoted by d. Due to the structural symmetry in this multiport antenna, its S-matrix is circulant. It equivalently means that the covariance matrix of this antenna can in general be represented by four independent parameters. We use this fact to our advantage in illustration of the results. Figure 6.3 shows the configuration of the structure under study in which the resonance frequency of each antenna element is slightly more than $f_\circ = 1$ GHz. We used the simulation approach described earlier in this chapter to obtain the SC diversity gain versus the number of incident waves in each realisation, K. We repeated the simulation for different element separations. For sufficient accuracy in our simulations, a realisation number of $N_{\text{sc}} = 10^6$ was used. The results of richness threshold values versus element separations in isotropic environment are plotted in Fig. 6.4. These richness thresholds were calculated at -0.5 dB level from the diversity gains' asymptotic values. Based on this figure, for $d \geqslant 0.1\lambda_\circ$ ($\lambda_\circ = 0.3$ m), the minimum number of independent incident waves required to achieve 90% of the ultimate diversity performance is 20 waves at the element separation $d = 0.4\lambda_\circ$. As mentioned earlier, at the risk of oversimplifying the problem, the distribution of the incoming EM waves was assumed to be complex Gaussian. Therefore, regardless of the number of incident waves, the distribution of the random received signals across antenna ports is complex Gaussian. Hence, the convergence in diversity gain appears as a result of convergence in covariance matrix. Also, remember that in SC combining scheme, the signals with more average power will be directly connected to the combiners' output. Thus, the envelope correlation plays a substantial role. To gain better insight into this problem and for the sake of clarity, the square roots of different envelope correlations have been plotted in Fig. 6.5. As pointed out, due to the symmetry in the structure, there are only four independent correlations to be plotted. Further examples of richness threshold for a couple of four-port antennas are provided in [Paper C]. In this paper, we have described the richness threshold to a considerable extent. Moreover, it is shown numerically how the richness threshold in

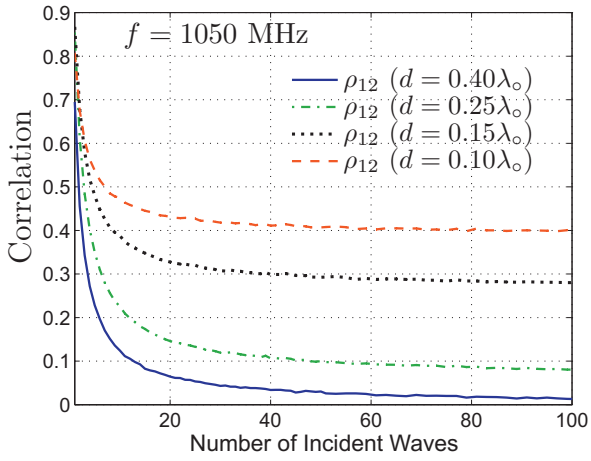

(a) ρ_{12}

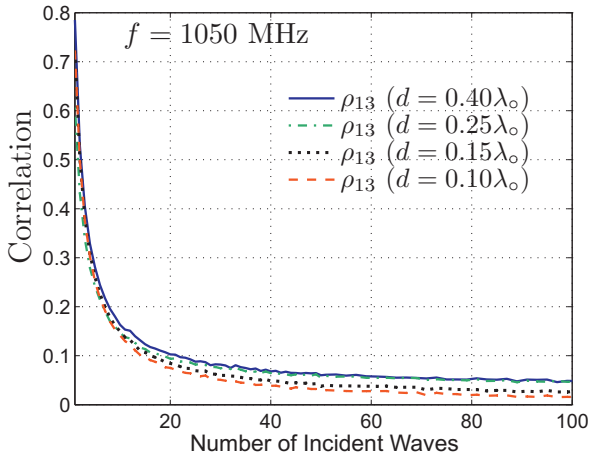

(b) ρ_{13}

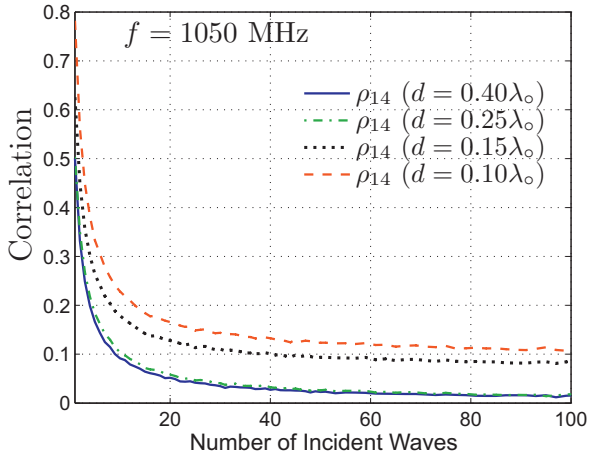

(c) ρ_{14}

Figure 6.5: Convergence in correlation versus the number of incident waves for six monopoles above a PEC plane. (After [56])

a multiport antenna system can be significantly modified by virtue of a Butler network.

6.6 Summary

The major part of this chapter has been dedicated to the simulation approach used in much of the studies carried out in the frame of this thesis. We have described how we emulate a multipath environment and simulate the received random signals at the antenna ports. In addition, we have briefly explained a few different ways for calculation of diversity gain based on these received signals. A comparative study of the foregoing approaches has been presented. We describe why –despite a computationally bulky method– the introduced numerical approach is important for behavioural study of antennas in non-rich multipath environments. The richness threshold as a further performance metric has been elaborated for its better comprehension. The example provided at the end of this chapter goes pretty well as a complementary to those of [Paper C] and is thus of an equal significance.

Chapter 7

Contributions and Future Outlook

The current chapter is dedicated to a brief overview of the contributions made within the frame of this thesis during the last few years. We look upon these contributions from four independent standpoints. First, we discuss about those dealing with the performance metrics in the areas of multiport and diversity antennas. Later, we treat the characterisation of antennas in non-rich multipath environments. Accordingly, we speak of the predictor antenna systems and how they can be made use of in the modern moving relay systems. A portion of our effort has been devoted to measurements of the multiport antennas in multipath environments. In particular, our earlier works were limited to measurements in reverberation chambers. We briefly glance through our contribution in this field. Finally, we slightly talk about few works which we have done in designing some multiport antennas to be used by mobile users. In this part, we also have a quick look upon our supplementary publications which were not included in this thesis.

7.1 Performance Metrics

Multiport antennas in mobile communication applications have been under study for many years. During this time, different performance metrics were coined to meet engineers' expectation as fair assessment criteria. In addition to the performance metrics treated in this thesis, the parameters such as Total Active Reflection Coefficients (TARC), multiplexing efficiencies of MIMO antennas, active matching efficiencies *etc.* are further metrics which are also typically used in the literature. In general, due to the multidisciplinary nature of this realm of science, it suffers from inconsistent nomenclature. Thus, in an attempt to unify the definitions of the influential performance metrics, we have dedicated a portion of the thesis to this issue.

7.1.1 Paper A

In this paper, the multiport matching efficiency is introduced. A compact formula for its evaluation is derived. This paper also describes some features of different radiation metrics like decoupling efficiency and TARC. It stresses that the multiport matching efficiency is superior compared to the total embedded radiation efficiency more due to the convenience in its formulation and measurement. We further, define the mean matching efficiency

for diversity performance evaluation of lossless structures. We clearly describe how an estimate of diversity gain can be achieved by this metric. Besides, although it has not been mentioned explicitly in this paper, we acknowledge that the mean matching efficiency in a multiport antenna system can also be used for a quick estimation of its bandwidth as an alternative metric to what has been proposed in [32]. In this respect, it can perform a role similar to what matching efficiency does in a single-port antenna case. As a quick reminder, bear in mind that diversity antennas are presumably narrowband. Therefore, it is important to monitor the bandwidth of a diversity antenna in its early design phase continuously. In this paper, the first author is the major contributor and responsible for motivation, terminology, analysis, simulation, discussion, and eventually writing of the paper.

7.1.2 Paper B

Spatial correlation is perhaps the most regarded performance metric in the area of MIMO wireless communication systems. Much effort has been expended to formulate this metric. Initially, the correlation due to antenna characteristics was formulated in terms of the embedded element far-field patterns [40]. Soon, the time-consuming and costly process of the embedded far-field pattern measurements made it necessary to seek an alternative approach. This ultimately led to the formulation of spatial correlation in isotropic environments by virtue of the input network parameters [46]. Since then, engineers have had this privilege to assess their design right away by a quick measurement of its scattering parameters. One should note that the forgoing advantage has been limited to lossless multiport structures. In this paper, we first point out that being lossless is a necessary but not a sufficient condition for expressing the spatial correlation in terms of the input network parameters. We emphasise that the design should also be a single-mode structure for the latter possibility to be valid. Moreover, we recast the formulas in terms of the input electric currents across the antenna ports and show its advantages compared to the available formulas in the literature. We further extend the revised compact formula to hold also in the cases of correlated multipath environments. Consequently, by use of an example, we reason that if the isolated embedded pattern of different radiation elements can be estimated, the spatial correlation can be comfortably achieved in terms of the input network parameters. The humble author of the current thesis is the major contributor in this article in particular for motivation, analysis, simulation, and writing.

7.1.3 Related Contributions

The roots of almost all performance metrics can be found in one important parameter. This critical parameter is nothing except the normalised covariance matrix of the received signals, which is the main concern of our research in [45]. In this paper, we firstly distinguish between correlated, uncorrelated and isotropic multipath environments. The core of the normalised covariance matrix is the pattern overlap matrix which is known for long time [26]-[49, Section 6.4]. This paper extends the pattern overlap matrix definition to correlated multipath environments and refer to it as correlated pattern overlap matrix. We also provide a compact formula for evaluation of the foregoing matrix. This critical

metric plays a key role in many performance metrics in correlated multipath environments.

Moreover, in paper [68], we provide a compact formula which presents the multiport matching efficiency in the presence of an arbitrary number of cascaded networks. The approach used in this paper is somewhat different from what we use in this thesis in Chapter 5. Nevertheless, the way along which this paper is evolved made it possible to provide also formulas rendering decoupling efficiency in the presence of an arbitrary number of cascaded networks. Additionally, in this paper for the first time we show that the multiport matching efficiency reduces to decoupling efficiency under a certain condition. We further stress that the multiport matching efficiency matrix equals the total embedded element efficiency matrix in cases of lossless structures. Also, through the multiport matching efficiency matrix, we are able to comfortably calculate the mean matching efficiency.

7.2 Antennas in Non-rich Multipath Environments

Perhaps one of the major contributions of the current thesis is associated with evaluation of antennas in multipath environments of finite richness. Until recently, designs and prototypes have been evaluated only in rich multipath environments. Recall that a rich multipath environment refers to those environments wherein the covariance matrix of the received signals across antenna ports converges to its asymptotic state. Conversely, when the number of random uncorrelated incoming waves is insufficient, the received signals' covariance matrix does not converge. Under this circumstance, the diversity and multiplexing performance of antennas can be quite different. Indeed, all closed-form formulas presented in this thesis and in the literature are likely only credible under rich multipath scenarios. The importance of this concern becomes more known if one realises that in actual multipath environments the number of incoming waves are quite limited and rarely exceeds ten.[1]

7.2.1 Paper C

The main goal in this paper is to show how a static RF Butler network can help to improve the performance of a multiport antenna in real multipath environments. For normalisation of the embedded pattern in the presence of a Butler network, the multiport matching efficiency with a cascaded network is derived. Indeed, the material presented in [68] for more of the cascaded networks is the continuation of this analysis. Later, for an arbitrary four-port antenna, the spatial correlations and total embedded element efficiencies in the presence and absence of a Butler network are shown. It is stressed that in a rich isotropic environment a Butler network does not prove beneficial. In addition, by numerical study of the matter, it is shown that in non-rich multipath environments the diversity gain in the presence of a Butler network is likely improved. Limiting ourselves to random circular complex Gaussian incoming waves in an uncorrelated uniform environment, we associate the reason for this improvement to the convergence in correlations. At the end, we conclude that the diversity gain achieved by pattern diversity is superior compared

[1] A list of references for this claim is provided in [Paper C] as well as [44].

to that obtained only by element separation. To quantify the improvements, we use the richness threshold as a performance metric. Concerning the contributions, the first author is the main contributor in this research article. The respectable co-authors played a substantial role in trimming the final structure of this paper.

7.2.2 Related Contributions

The dependency of the diversity gain on the number of uncorrelated random incoming EM waves was first revealed in paper [67]. In this paper, we were concerned with how directivities of the elements would affect their overall performance in multipath environments. We chose four ideal antennas with similar embedded patterns at half a wavelength separation from each other. All these antennas were pointing towards the same direction in space. It was shown that the more directive the elements were, the higher number of independent incident EM waves was required for their optimum performance. Subsequently, in paper [44], we showed that the reason for the preceding achievement was most likely the convergence in joint probability density function. We also demonstrated that in case of a nonuniform multipath, the convergence was still a concern. We presented the advantage of a Butler network as a preliminary result in this paper. For a fair comparison, we further introduced the notion of richness threshold in this paper. Up until this time, it has been shown by the foregoing papers that the number of incident waves plays a crucial role in its ultimate diversity performance. At this point, the question is, in a multiport system, how the coupling among the radiation elements affects the convergence. This is also assessed through richness threshold. In [56], we dedicate a detailed numerical study to the foregoing issue. Our conclusion is that coupling would in general improve the convergence in joint probability distribution of the received signals likely by increasing the pattern diversity. In this paper, we specify a range for the spatial correlation in a multiport antenna system compared to a single value for it, which has been prevalent in the literature. We stress that, from one standpoint, within a certain multipath circumstance, two factors cause the spatial correlation: the pattern diversity and element separation. We conclude that the spatial correlation as caused by pattern diversity is to a considerable extent independent of the number of uncorrelated incoming waves which is presumably more than one.

7.3 Predictor Antennas in Moving Relays

Concerning the importance of this contribution, it suffices to say that we owe the title of this thesis almost entirely to it. The channel state information is crucial in the overall performance of modern wireless communication systems [4]. One of the main tools for prediction of the channel is through the renowned Kalman filter. Nevertheless, the limitation inherent in prediction of the channel by a Kalman filter for longer horizon ranges has made it necessary to use a predictor antenna system. The latter is essential for moving relays in vehicular velocities [69]. Since a predictor antenna system includes some in-line antennas at relatively close proximity, it can be considered as a multiport antenna system. Thus, all the tools presented in the frame of this thesis can be utilised to design a desirable predictor antenna system. For instance, as soon as a vehicle reduces its speed, due to a

shorter prediction horizon range, the separation between the predictor and the receiver antennas in this system should shrink. As element separation between the two nearby radiating structures reduces, the coupling between them rises. This, in turn, deforms the shapes of the embedded patterns of these elements. Since antennas see the profile of the incoming waves through the filter of their far-field patterns, any dissimilarity between the far-field patterns of the predictor and the receiver antennas deteriorates prediction capability of the system. This concern has been addressed in [Paper D].

7.3.1 Paper D

This paper in the first step derives an analytical expression for extracting the received signals' open-circuit covariance from arbitrary terminated received signals. Although the aforementioned relation is already known[2], a different approach used for its derivation in this paper provides considerable insight into it. We later reason that in lossless single-mode multiport antennas, the open-circuit received voltage can be thought of as the received signal at each port in the absence of other nearby radiating elements. Thus, it inherently excludes the impact of coupling among the elements. Upon this achievement, we devise a simulation tool, whose bases have already been created in [Paper C]. Using this simulation tool, for the first time, we are able to quantify the relative enhancement achievable by the foregoing relation in a predictor antenna system. We stress that the terminated to open-circuit covariance conversion can be fulfilled both in baseband and passband domains, even though the former is far easier for implementation purposes. Moreover, from a practical standpoint, it is rare to find antennas directly connected to the receiver ports. Instead, they are connected through a chain of one or more cascaded networks. This paper also provides an expression for the desired conversion in the presence of an arbitrary cascaded network. Examples are presented supporting the ideas provided in this framework. Here, the humble author of this thesis is again the major contributor for problem definition, solution proposal, analysis, simulation, discussion, and writing. The respectable co-authors provided valuable suggestions and trimming specifically for Section 4.2 in this article.

7.4 Measurements in Multipath Environments

Since the advent of wireless communications in urban areas, there has been a challenge for real scenario measurements. In this respect, besides being costly and time-consuming, there is one important issue being referred to as repeatability. By repeatability, we mean how invariant the results of a measurement scenario are with respect to the repetition of their measurement. In early 2000, an application of reverberation chambers was introduced for quick measurements of small antennas in a multipath scenario. The literature is rich in this respect and shows that a reverberation chamber provides a rich isotropic multipath environment with acceptable accuracy. However, there is a primary concern for these new measurement tools. This issue is associated with the number of independent samples which has been partially addressed in our papers on this subject.

[2] It was spoken of in [40] and subsequently presented in [70].

7.4.1 Paper E

In this paper, we devise two compact formulas rendering the diversity gain in a rich Rayleigh multipath environment. As it has been pointed out in Section 6.4 on page 59, the definition of diversity gains in RF domain relies on the received signals' CDF curves. Because the values of the curves at their 1% level are desired, their accuracy are highly important. Dependent on the required accuracy, this demands at least a certain number of independent measured samples, *e.g.*, 10^4. Table I in this paper lists the necessary number of independent samples for certain required accuracy. To bypass this difficulty, there are several ways, some of which are brought in Chapter 6 on page 55. Yet, for case of two-port antennas, as mentioned before, the formulas presented in this paper offer the simplest way for diversity gain calculation. The application of these formulas is not limited to isotropic environments and can be applied to other types of Rayleigh fading environments as long as the corresponding spatial correlation and MEGs are available. In this article, the first author is the main contributor. He is responsible for motivation, numerical simulation, verification, and writing. The respectable co-authors helped considerably in devising the first compact formula for SC scheme.

7.4.2 Paper F

For an identical level of accuracy, it is known that measurements of correlation and embedded radiation efficiency in a reverberation chamber require fewer independent samples compared to measurement of diversity gain [66]. To achieve the covariance matrix in an isotropic environment for any arbitrary complex terminations, as pointed out in Section 4.3.1 on page 34, one needs to achieve the pattern overlap matrix. Formerly in [Paper B], we recommended to achieve this important metric by measuring the covariance matrix for two independent sets of terminating impedances and post-processing of the results. Nevertheless, in this paper, we show how one can achieve the pattern overlap matrix by a single round of measurement in a reverberation chamber. To the best of our knowledge, so far this is the fastest way for measurement of the aforementioned metric. In this article, the author of this thesis is the major contributor for motivation, analysis, simulation, calculation, and writing.

7.4.3 Paper G

The main concern in this paper is to reveal whether there is any difference among rectangular, cylindrical, or spherical reverberation chambers of the same volume. Since they have the same volume, the total number of EM resonance modes in each cavity should be the same. However, the total number of the modes is not our concern here. This is because for having sufficient number of independent samples, uniformity in the density of the modes over the required frequency range is of foremost importance. We show that in this regard a rectangular reverberation chamber is superior. Incidentally, from manufacturing point of view, this is also the best choice. Moreover, while the symmetrical chambers produce more degenerate modes, we conclude that the more unsymmetrical the shape of the chamber, the more uniform the density of its modes, and thus the better its performance. Regarding the contributions, the second and the third co-authors in this

paper are independently responsible for all associated simulations.

7.4.4 Related Contributions

There are few papers which are associated with measurement of multiport antennas in a reverberation chamber for their characterisation. For instance, in paper [71] few multiport antennas are measured and evaluated in the presence of head phantom for their evaluation. In [72] for the first time, we implement an ideal Butler network in the signal processing part of the reverberation chamber measurements. The outcome shows that a Butler network does not affect the diversity gain measured in a reverberation chamber. This verifies the simulation results implied in [Paper C]. However, the interesting part of this contribution is the influence of the cascaded Butler network in the measured embedded radiation efficiencies. The results obtained in this paper, which are associated with the case of four monopoles above an almost PEC plane, are used later to verify our simulation outcomes in some subsequent papers including [Paper C] for a rich multipath environment.

7.5 Multiport Antenna Design

In the frame of the current thesis, the stress has been more on the basic performance metrics and criteria for evaluation of multiport antennas. Therefore, less attention has been paid to design antennas which meet certain specifications. Nevertheless, there have been few contributions with other colleagues in Aalto University in Finland and Universidad Politécnica de Madrid in Spain, which could be classified as antenna design contributions.

7.5.1 Paper H

In this paper, some state-of-the-art low-profile multiport antennas for mobile application have been studied. The selected antenna designs also differ in the number of elements and their configurations on the chassis. We evaluate and measure these antennas in different practical scenarios. Simulations used for evaluation of these results are relatively similar to those used in [Paper C]. The three scenarios considered are in the absence and presence of user's hand in both browse grip and data grip configurations. We show that our novel antenna design outperforms others in all the aforementioned scenarios. Concerning contributions, the humble author of this thesis is responsible for multipath performance calculations carried out in the frame of this paper. He has also contributed in its writing.

7.5.2 Related Contributions

In paper [73], a two-element diversity antenna which has a strong coupling with the chassis is designed, evaluated, and measured in an anechoic and a reverberation chamber. In this design, two L-shape thin copper plate antennas are optimally positioned along the two corners of the chassis. The shape of the radiation patterns of the antenna elements are quite identical but pointing towards different directions. It is shown that this simple design performs quite well in isotropic multipath environments. This author is responsible for measurements conducted in this research article. In paper [74], we use a circuit network to optimise the overall performance of PIFA antennas over a mobile chassis.

7.6 Future Outlook

The materials presented in the frame of this thesis is in principle limited to multipath environments of Rayleigh distribution. Although it is almost globally accepted as a standard model for designing terminal antennas suitable for multipath environments, there are also some other types of environments which are common among the communication system society. Therefore, there is room to study whether choosing other types of distribution for the received signals would change the current design criteria. In addition, we shall acknowledge that due to the generic nature of our research, in many of our studies a uniform AoA served our purpose sufficiently. However, other types of AoA distributions can also be of interests for further investigation.

The literature is pretty rich about how to evaluate the antenna designs in Rayleigh fading multipath scenarios. An overview of it may lead to the conclusion that future belongs to small antenna designs which show orthogonal embedded patterns in a small space. There are certain designs available which are interesting. However, they are not considered as low-profile antennas. Therefore, designing highly efficient compact multiport antennas with considerable pattern diversity remains still a challenge for antenna engineers. In this respect, the microwave circuits cascaded to the antennas will be a helpful tool to get closer to these ultimate design goals.

In the frame of the current thesis, we have formulated the effects of terminating impedances in the covariance matrix in a general sense. Devising a rigorous algorithm for finding the proper set of terminating impedances rendering an optimum performance is of foremost interests. Moreover, our discussions throughout this report -for the most part- were restricted to calculation of diversity gain. Nevertheless, the ingredients provided in this framework suffice for further study on capacity too. It is true that the literature is fairly rich on this subject. Yet, there is more space to look into the convergence in capacity for non-rich multipath environment case.

Furthermore, in the area of vehicular antenna technology, the challenge for intelligent transportation systems remains as a discipline of its own in the next few years. The typical attenuation for wireless communication with a person inside a vehicle is around $7-9$ dB. However, as car industries require shielding inside of the car from severe heat or cold, it simultaneously affects the aforementioned EM attenuation deteriorating it up to 19 dB. This alone requires a use of relays on the roof of the vehicle. The effects of roof curvature, the attenuating impact of sunroofs, and the blind spot for the front communications are still certain challenging issues which require effective multiport antenna designs.

Bibliography

[1] D. Aronsson, *Channel Estimation and Prediction for MIMO OFDM Systems: Key Design and Performance Aspects of Kalman-based Algorithms.* Uppsala University, March 2011.

[2] A. F. Molisch, *Wireless Communications.* John Wiley & Sons, 2007.

[3] W. C. Jakes, *Microwave Mobile Communications.* John Wiley & Sons, 1974.

[4] A. Goldsmith, *Wireless Communications.* Cambridge University Press, 2005.

[5] R. G. Vaughan and J. B. Andersen, *Channels, Propagation and Antennas for Mobile Communication.* Instituation for Electrical Engineers, IET, 2003.

[6] A. Paulraj, R. Nabar, and D. Gore, *Introduction to Space-Time Wireless Communications.* Cambridge University Press, 2006.

[7] G. Foschini and M. Gans, "On limits of wireless communications in a fading environment when using multiple antennas," *Wireless Personal Communications*, vol. 6, pp. 311–335, March 1998.

[8] H. Wheeler, "Fundamental limitations of small antennas," *Proceedings of the IRE*, vol. 35, no. 12, December 1947.

[9] D. M. Pozar, "Microstrip antennas," *Proceedings of the IEEE*, vol. 80, no. 1, January 1992.

[10] J. Johnson and Y. Rahmat-Samii, "The tab monopole," *IEEE Transactions on Antennas and Propagation*, vol. 45, no. 1, pp. 187–188, January 1997.

[11] C. Rowell and R. Murch, "A capacitively loaded PIFA for compact mobile telephone handsets," *IEEE Transactions on Antennas and Propagation*, vol. 45, no. 5, pp. 837–842, May 1997.

[12] B. Quist and M. Jensen, "Optimal antenna radiation characteristics for diversity and MIMO systems," *IEEE Transactions on Antennas and Propagation*, vol. 57, no. 11, pp. 3474–3481, November 2009.

[13] M. Martínez-Vázquez, R. Serrano, J. Carlsson, and A. K. Skrivervik, "Terminal antennas in ACE2," *Radioengineering*, vol. 17, no. 2, pp. 8–12, June 2008.

[14] K. Karlsson and J. Carlsson, "Circuit based optimization of radiation characteristics of single and multiport antennas," *Radioengineering*, vol. 18, no. 4, pp. 438–444, December 2009.

[15] A. Diallo, C. Luxey, P. Le Thuc, R. Staraj, and G. Kossiavas, "Study and reduction of the mutual coupling between two mobile phone PIFAs operating in the DCS1800 and UMTS bands," *IEEE Transactions on Antennas and Propagation*, vol. 54, no. 11, pp. 3063–3074, November 2006.

[16] J. W. Wallace and M. A. Jensen, "Mutual coupling in MIMO wireless systems: A rigorous network theory analysis," *IEEE Transactions on Wireless Communications*, vol. 3, no. 4, pp. 1317–1325, July 2004.

[17] M. Morris and M. Jensen, "Improved network analysis of coupled antenna diversity performance," *IEEE Transactions on Wireless Communications*, vol. 4, no. 4, pp. 1928–1934, July 2005.

[18] A. Derneryd and G. Kristensson, "Antenna signal correlation and its relation to the impedance matrix," *Electronics Letters*, vol. 40, no. 7, pp. 401–402, April 2004.

[19] V. Plicanic, B. K. Lau, A. Derneryd, and Z. Ying, "Actual diversity performance of a multiband diversity antenna with hand and head effects," *IEEE Transactions on Antennas and Propagation*, vol. 57, no. 5, pp. 1547–1556, May 2009.

[20] A. Sibille, C. Oestges, and A. Zanella, Eds., *MIMO: From Theory to Implementation*. Academic Press, November 2010.

[21] M. A. Jensen and J. W. Wallace, "A review of antennas and propagation for MIMO wireless communications," *IEEE Transactions on Antennas and Propagation*, vol. 52, no. 11, pp. 2810–2824, November 2004.

[22] K. Rosengren and P.-S. Kildal, "Radiation efficiency, correlation, diversity gain and capacity of six monopole antenna array for a MIMO system: Theory, simulation and measurement in reverberation chamber," *Proceedings IEE, Microwaves Antennas and Propagation*, vol. 152, no. 1, pp. 7–16, 2005, see also Erratum published in August 2006.

[23] K. Karlsson, J. Carlsson, and P.-S. Kildal, "Reverberation chamber for antenna measurements: Modeling using method of moments, spectral domain techniques, and asymptote extraction," *IEEE Transactions on Antennas and Propagation*, vol. 54, no. 11, pp. 3106–3113, November 2006.

[24] J. Yun and R. Vaughan, "Impact of total efficiency of multiple element antennas on diversity and capacity," in *Proceedings of the Sixth European Conference on Antennas and Propagation*, March 2012.

[25] M. Ivashina, M. Kehn, P.-S. Kildal, and R. Maaskant, "Decoupling efficiency of a wideband vivaldi focal plane array feeding a reflector antenna," *IEEE Transactions on Antennas and Propagation*, vol. 57, no. 2, pp. 373–382, February 2009.

[26] S. Stein, "On cross coupling in multiple-beam antennas," *IRE Transactions on Antennas and Propagation*, vol. 10, no. 5, pp. 548–557, September 1962.

[27] N. Jamaly, "Spatial Characterization of Multi-element Antennas," Chalmers University of Technology, Sweden, Tech. Rep. R002/2011, February 2011. [Online]. Available: http://publications.lib.chalmers.se/records/fulltext/137635.pdf

[28] D. K. Cheng, *Field and Wave Electromagnetics, 2nd Edition.* Addison-Wesley, 1989.

[29] R. E. Collin, *Antennas and Radiowave Propagation.* McGraw-Hill, 1985.

[30] C. A. Balanis, *Antenna Theory: Analysis and Design, 2nd Edition.* John Wiley & Sons, 1997.

[31] P.-S. Kildal, "Equivalent circuits of receive antenna in signal processing array," *Microwave and Optical Technology Letters*, vol. 21, no. 4, May 1999.

[32] B. K. Lau, J. Andersen, G. Kristensson, and A. Molisch, "Impact of matching network on bandwidth of compact antenna arrays," *IEEE Transactions on Antennas and Propagation*, vol. 54, no. 11, pp. 3225–3238, November 2006.

[33] M. Jensen and B. K. Lau, "Uncoupled matching for active and passive impedances of coupled arrays in MIMO systems," *IEEE Transactions on Antennas and Propagation*, vol. 58, no. 10, pp. 3336–3343, October 2010.

[34] T. Taga, "Analysis for mean effective gain of mobile antennas in land mobile radio environments," *IEEE Transactions on Vehicular Technology*, vol. 39, no. 2, pp. 117–131, 1990.

[35] K. Kalliola, K. Sulonen, H. Laitinen, O. Kivekas, J. Krogerus, and P. Vainikainen, "Angular power distribution and mean effective gain of mobile antenna in different propagation environments," *IEEE Transactions on Vehicular Technology*, vol. 51, no. 5, pp. 823–838, September 2002.

[36] M. K. Ozdemir, E. Arvas, and H. Arslan, "Dynamics of spatial correlation and implications on MIMO systems," *IEEE Communications Magazine*, vol. 42, no. 6, pp. 14–19, 2004.

[37] R. G. Vaughan, "Signals in mobile communications, a review," *IEEE Transactions on Vehicular Technologies*, vol. 35, no. 4, pp. 133–145, 1986.

[38] T. Aulin, "A modifed model for fading signal at the mobile radio channel," *IEEE Transactions on Vehicular Technologies*, vol. 28, no. 3, pp. 182–203, August 1979.

[39] G. Grimmett and D. Stirzaker, *Probability and Random Processes*, 3rd ed. Oxford, 2001.

[40] R. Vaughan and J. Andersen, "Antenna diversity in mobile communications," *IEEE Transactions on Vehicular Technology*, vol. 36, no. 4, pp. 149–172, November 1987.

[41] J. B. Andersen and F. Hansen, "Antennas for VHF/UHF personal radio: A theoretical and experimental study of characteristics and performance," *IEEE Transactions on Vehicular Technology*, vol. 26, no. 4, pp. 349–357, 1977.

[42] P.-S. Kildal and K. Rosengren, "Correlation and capacity of MIMO systems and mutual coupling, radiation efficiency, and diversity gain of their antennas: simulations and measurements in a reverberation chamber," *IEEE Communications Magazine*, vol. 42, no. 12, pp. 104–112, December 2004.

[43] A. Alayon Glazunov, A. Molisch, and F. Tufvesson, "Mean effective gain of antennas in a wireless channel," *IET Microwaves, Antennas & Propagation*, vol. 3, no. 2, pp. 214–227, March 2009.

[44] N. Jamaly, M. Iftikhar, and Y. Rahmat-Samii, "Performance evaluation of diversity antennas in multipath environments of finite richness," in *Proceedings of the Sixth European Conference on Antennas and Propagation*, March 2012.

[45] N. Jamaly, A. Derneryd, and T. Svensson, "Analysis of antenna pattern overlap matrix in correlated nonuniform multipath environments," in *Proceedings of the Seventh European Conference on Antennas and Propagation*, April 2013.

[46] S. Blanch, J. Romeu, and I. Corbella, "Exact representation of antenna system diversity performance from input parameter description," *Electronics Letters*, vol. 39, no. 9, pp. 705–707, May 2003.

[47] J. W. Wallace and M. A. Jensen, "Termination-dependent diversity performance of coupled antennas: Network theory analysis," *IEEE Transactions on Antennas and Propagation*, vol. 52, no. 1, pp. 98–105, January 2004.

[48] A. Stjernman, "Relationship between radiation pattern correlation and scattering matrix of lossless and lossy antennas," *Electronics Letters*, vol. 41, no. 12, pp. 678–680, June 2005.

[49] K. F. Warnick and M. Jensen, "Antennas and Propagation for Wireless Communications," *course materials in Brigham Young University*, (available online) 2011.

[50] W. Kahn and H. Kurss, "Minimum-scattering antennas," *IEEE Transactions on Antennas and Propagation*, vol. 13, no. 5, pp. 671–675, September 1965.

[51] W. Wasylkiwskyj and W. Kahn, "Theory of mutual coupling among minimum-scattering antennas," *IEEE Transactions on Antennas and Propagation*, vol. 18, no. 2, pp. 204–216, March 1970.

[52] R. Collin, "Limitations of the thevenin and norton equivalent circuits for a receiving antenna," *Antennas and Propagation Magazine, IEEE*, vol. 45, no. 2, pp. 119 – 124, april 2003.

[53] R. C. Hansen, *Phased Array Antennas*, ser. Microwave and Optical Engineering, K. Chang, Ed. John Wiley & Sons, 1998.

[54] J. Andersen, H. Lessow, and H. Schjaer-Jacobsen, "Coupling between minimum scattering antennas," *IEEE Transactions on Antennas and Propagation*, vol. 22, no. 6, pp. 832–835, November 1974.

[55] H. T. Hui, W. Yong, and K. Toh, "Signal correlation between two normal-mode helical antennas for diversity reception in a multipath environment," *IEEE Transactions on Antennas and Propagation*, vol. 52, no. 2, pp. 572–577, February 2004.

[56] N. Jamaly and A. Derneryd, "Coupling effects on richness threshold of multi-port antennas in multipath environments," in *15th International Symposium of Antenna Technology and Applied Electromagnetics*, June 2012.

[57] W. Wiesbeck and E. Heidrich, "Wide-band multiport antenna characterization by polarimetric RCS measurements," *IEEE Transactions on Antennas and Propagation*, vol. 46, no. 3, pp. 341–350, March 1998.

[58] M. Manteghi and Y. Rahmat-Samii, "Multiport characteristics of a wide-band cavity backed annular patch antenna for multipolarization operations," *IEEE Transactions on Antennas and Propagation*, vol. 53, no. 1, pp. 466–474, January 2005.

[59] R. E. Collin, *Foundations for Microwave Engineering.* Wiley-IEEE Press, 2001.

[60] D. M. Pozar, *Microwave Engineering*, 3rd ed. John Wiley & Sons, 2005.

[61] G. P. Riblet, "Simplified 8-port S-matrix of the general reciprocal lossless matched 4-way divider with output port isolation," *IEEE Microwave and Guided Wave Letters*, vol. 5, no. 11, pp. 365–367, November 1995.

[62] A. Grau, J. Romeu, S. Blanch, L. Jofre, and F. D. Faviis, "Optimization of linear multi-element antennas for selection combining by means of a Butler matrix in different MIMO environments," *IEEE Transactions on Antennas and Propagation*, vol. 54, no. 11, 2006.

[63] R. Ertel and J. Reed, "Generation of two equal power correlated Rayleigh fading envelopes," *IEEE Communications Letters*, vol. 2, no. 10, pp. 276–278, October 1998.

[64] P.-S. Kildal, K. Rosengren, J. Byun, and J. Lee, "Definition of effective diversity gain and how to measure it in a reverberation chamber," *Microwave and Optical Technology Letters*, vol. 34, no. 1, pp. 56–59, July 2002.

[65] O. Norklit, P. Teal, and R. Vaughan, "Measurement and evaluation of multi-antenna handsets in indoor mobile communication," *IEEE Transactions on Antennas and Propagation*, vol. 49, no. 3, pp. 429–437, March 2001.

[66] J. Yang, S. Pivnenko, T. Laitinen, J. Carlsson, and X. Chen, "Measurements of diversity gain and radiation efficiency of the Eleven antenna by using different measurement techniques," in *Proceedings of the Fourth European Conference on Antennas and Propagation*, April 2010.

[67] N. Jamaly, H. Zhu, P.-S. Kildal, and J. Carlsson, "Performance of directive multi-element antennas versus multi-beam arrays in MIMO communication systems," in *Proceedings of the Fourth European Conference on Antennas and Propagation*, April 2010.

[68] N. Jamaly and A. Derneryd, "Multi-port matching efficiency in antenna systems with cascaded networks," in *15th International Symposium of Antenna Technology and Applied Electromagnetics*, June 2012.

[69] M. Sternad, M. Grieger, R. Apelfrojd, T. Svensson, D. Aronsson, and A. Martinez, "Using "predictor antennas" for long-range prediction of fast fading for moving relays," in *IEEE Wireless Communications and Networking Conference Workshops (WCNCW)*, April 2012.

[70] R. Vaughan and N. Scott, "Closely spaced terminated monopoles for vehicular diversity antennas," in *IEEE Antennas and Propagation Society International Symposium*, vol. 2, July 1992.

[71] C. Gomez-Calero, N. Jamaly, L. Gonzalez, and R. Martinez, "Effect of mutual coupling and human body on MIMO performances," in *Proceedings of the Third European Conference on Antennas and Propagation*, March 2009.

[72] N. Jamaly, C. Gomez-Calero, P.-S. Kildal, J. Carlsson, and A. Wolfgang, "Study of excitation on beam ports versus element ports in performance evaluation of diversity and MIMO arrays," in *Proceedings of the Third European Conference on Antennas and Propagation*, March 2009.

[73] A. Azremi, J. Toivanen, T. Laitinen, P. Vainikainen, X. Chen, N. Jamaly, J. Carlsson, P.-S. Kildal, and S. Pivnenko, "On diversity performance of two-element coupling element based antenna structure for mobile terminal," in *Proceedings of the Fourth European Conference on Antennas and Propagation*, April 2010.

[74] J. Carlsson, K. Karlsson, N. Jamaly, and P.-S. Kildal, "Analysis and optimization of multiport antennas by using circuit simulation and embedded element patterns from full-wave simulation," in *COST2010/ASSIST Workshop on Multiple Antenna Systems on Small Terminals*, May 2009.